GREEN RISK 4 ALPS

WP T1 PRONA

Responsibility for Deliverable

Stefan Steger (Eurac)

Contributors

Michaela Teich (BfW), Alice Crespi (Eurac), Georg Kindermann (BfW), Robert Jandl (BfW), Anne Hormes (BFW), Matthias Plörer (BFW), Marcello Petitta (Eurac)

Bozen/Bolzano, March 27, 2020

GreenRisk4ALPs Partnership

BFW - Austrian Research Centre for Forests (AT)
DISAFA - Department of Agricultural, Forest and Food Sciences, University of Turin (ITA)
EURAC - European Academy of Bozen-Bolzano – EURAC Research (ITA)
IRSTEA - National research institute of science and technology for environment and agriculture, Grenoble regional centre, IRSTEA (FRA)
LWF - Bavarian State Institute of Forestry (GER)
MFM - Forestry company Franz-Mayr-Melnhof-Saurau (AT)
SFM - Safe Mountain Foundation (ITA)
UL - University of Ljubljana, Biotechnical Faculty, Department of Forestry and Renewable Resources (SLO)
UGOE - University of Göttingen, Department of Forest and Nature Conservation Policy (GER)
WSL - Swiss Federal Institute for Forest, Snow and Landscape Research (CH)
WLV - Austrian Service for Torrent and Avalanche Control (AT)
SFS - Slovenia Forest Service (SLO)

Table of Contents

Table of Figures

Table of Tables

1 Introduction

The project GreenRisk4ALPs aims to develop and implement innovative ecosystem and forestry-based risk management strategies for alpine natural hazards. In this context, a particular focus is set on frequent damage causing gravitational mass movements, such as landslides, rock falls and snow avalanches. In order to establish efficient and proactive risk reduction measures, it is vital to consider potential implications of current and future developments that determine the natural hazard risk situation (Cutter, 1996; Einhorn et al., 2015; Keiler et al., 2010). Besides changes associated to assets potentially at risk (e.g. people, infrastructure), also current and future trends related to "natural" dynamic factors (e.g. climate, forest) have to be considered.

Figure 1 highlights that mass movements result from an interplay of static predisposing and dynamic preparatory and triggering factors: The margin of stability describes the ability of a hillslope area to withstand (i.e. resist) potential environmental alterations. Predisposing factors, such as hillslope topography, are often considered static in time and responsible for rendering a location more or less prone to a mass movement (static spatial view). Instead, dynamic preparatory factors (e.g. land cover changes, snow melting) decrease the margin of stability without actually initiating a mass movement. Typical mass movement triggers, such as heavy rainfall (e.g. for landslides), seismic shaking (e.g. for rock fall) or intensive snow fall followed by warm temperatures (e.g. for snow avalanches), act over short time periods and usually initiate the downward movement. Stable areas are likely to resist the majority of dynamic stressor, such as triggering events. Slopes that exhibit an unfavorable predisposition (e.g. steep slopes, presence of weak material) are close to a critical state and likely to initiate a mass movement in response to dynamic disturbances.

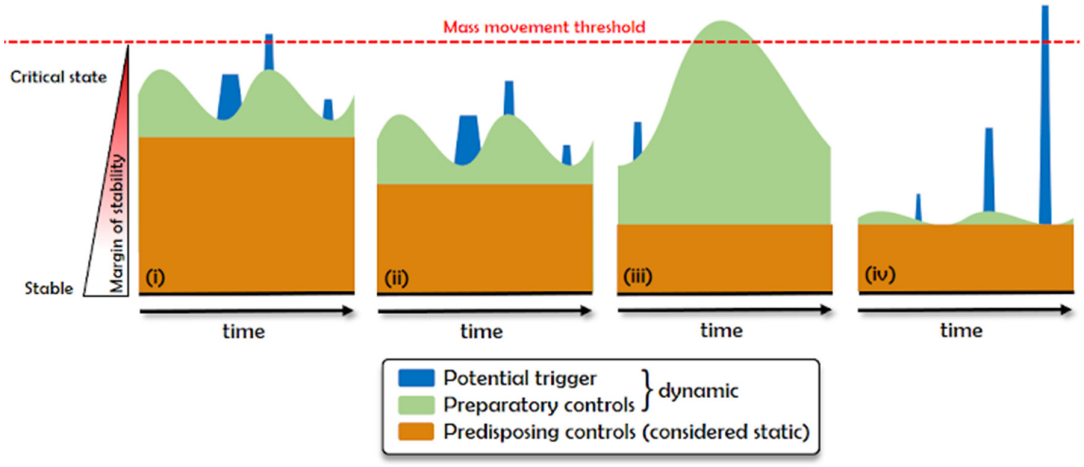

Figure 1 Mass movement occurrence (e.g. landslides, rock falls, snow avalanches) due to an interplay of spatial (location; i – iv) and temporal (time; x-axis) dynamic and static controls. The four locations exhibit different combinations of static and dynamic geo-environmental characteristics that determine the margin of stability (y-axis). During the time period considered (x-axis), locations i and ii feature identical dynamic mass movement controls (e.g. rainfall, snow cover, land cover changes) whereas only location i exceeds the mass movement threshold due to its a-priori higher predisposition (e.g. steeper slope). Although location iii exhibits a comparably low static predisposition, mass movement occurs due to e.g. slowly changing environmental conditions (e.g. prolonged snow melting). Location (iv) is affected by mass movement mainly due to an extraordinary triggering event (e.g. heavy precipitation). The figure follows the concepts presented in Crozier (1989), Steger (2017) and Zimmermann (1997).

Projected changing climatic conditions can be interpreted as potential dynamic stressors for mountainous landscapes that can influence not only mass movement triggering (e.g. heavy precipitation), but also environmental conditions that directly influence the natural hazard process (e.g. forest and its structure). Thus, an improved understanding of past, current and future climatic trends as well as their influence on the forest development represents an important step towards an efficient risk reduction, also due to (i) the known influence of climatic/meteorological dynamics on the occurrence of mass movements, (ii) the dependency of forest structures on climatic conditions and (ii) the manifold effects of forests on gravitational hazards, such as landslides of the slide-type movement (e.g. Rickli et al., 2002; Schmaltz et al., 2019), rock falls (e.g. Berger et al., 2013; Moos et al., 2017) and snow avalanches (e.g. McClung, 2003; Schneebeli and Bebi, 2004; Teich et al., 2012a).

The report "New climate impact scenarios based on CC (climate change) - FC (forest change) - HC (hazard change) links" highlights observed and projected climatic changes in the pilot action regions (PARs) and their potential effects on (some) forest parameters that might influence gravitational mass movements. The report first introduces the methods applied to derive CC scenarios (section 2.2), subsequent FC scenarios (section 2.3) and the linkage to mass movement processes (section 2.4). Section 3 presents the results obtained at pilot action region (PAR) level in terms of climate change scenarios (section 3.1) and changes in some forest parameters (section 3.2). Section 3.3 builds upon the derived CC (and partly FC) scenarios in order to link those environmental changes to well-established natural hazard process knowledge. The deliverable is concluded by the final discussion (section 4).

2 Methods

2.1 General framework

The methodical framework behind this deliverable is summarized in Figure 2. The meteorological time series station data, which was collected for the PARs, represented the basis to downscale and bias-correct EURO-CORDEX climate simulations (temperature, precipitation) for two representative concentration pathways (RCPs), namely the RCP4.5 (greenhouse gas emissions peak at around 2040) and the RCP8.5 (emissions continue to rise in the 21st century). Then, the derived (local) temperature and precipitation scenarios were fed into the tree growth simulator CALDIS to derive information on how climate may affect the development of forest parameters (basal area and total stem volume). Ensuing information on potential climate (and partly forest changes) was then linked with the main mass movement processes considered within GreenRisk4ALPs, namely landslides, rock falls and snow avalanches.

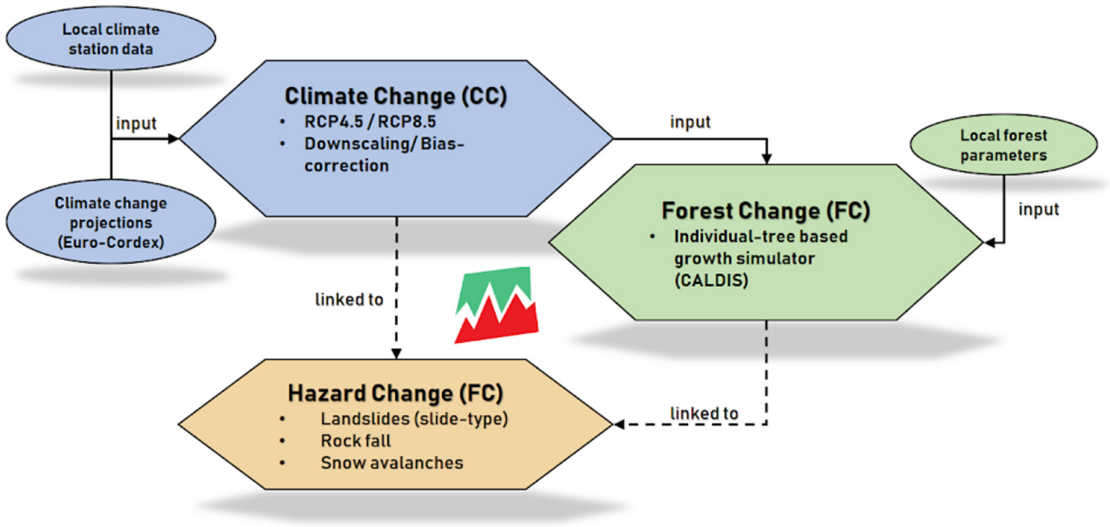

Figure 2 Schematic workflow for the derivation of Climate Change (CC), Forest Change (FC) and Hazard Change (HC) scenarios for the PARs.

2.2 Derivation of climate change (CC) scenarios

Climate model data are nowadays widely applied to assess the impact of expected climate change at regional and local scale. The underlying climate projections for different greenhouse gas emission scenarios (Representative Concentration Pathway, RCP) are commonly computed by global-scale general circulation models (GCMs) with spatial horizontal resolutions in the range of 100-300 km. In order to increase the spatial resolution of climate information (~10-50 km), dynamical downscaling is applied by running physically based regional climate models (RCMs) with boundary conditions provided by a GCM (Zhang et al., 2019).

However, the still rather coarse resolution and associated potential systematic biases prevent the RCM outputs from being directly applicable for local studies (e.g. for assessing climate impacts). To enhance their explanatory power for specific locations, additional statistical downscaling and bias correction is required. In recent decades, several approaches have been developed in order to provide reliable estimators of the local scale climate (see e.g. Maraun et al., 2010). These statistical techniques build upon local observations (i.e. reference data) and aim to achieve site-specific "corrected" climate model simulations. Local bias-corrected scenarios for a certain meteorological variable, such as precipitation or temperature, can be computed by retrieving proper *transfer functions* over a historical calibration period. In simple terms, these approaches seek to "match" the available coarsely-scaled model data (e.g. RCMs) and the in-situ observations (e.g. meteorological station data). The ensuing models can then be applied to elaborate local bias-corrected future climate simulations (Figure 3a). One of the most widely used bias-correction approach is Quantile Mapping (QM), in which the distributions of simulated and observed values are matched by establishing a quantile-dependent correction function that translates simulated quantiles into their observed ones (Figure 3b) (Themeßl et al., 2012; Gudmundsson et al., 2012).

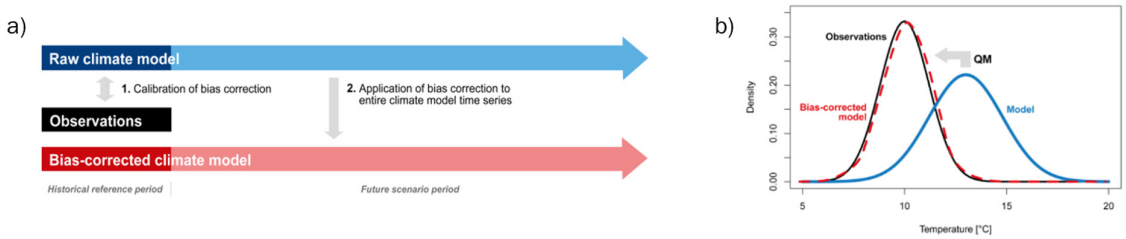

Figure 3 Methodical framework to downscale and bias-correcting raw climate model data. Panel a) describes the general bias correction workflow and panel b) depicts an overview of the quantile mapping concept (from Feigenwinter et al., 2018).

The efficiency of bias-correction procedures is highly dependent on the accuracy of available observational data used as reference for the statistical model calibration. The reference data should cover the model historical period (at least for 20 years) and should not be affected by significant inhomogeneities (e.g. sudden jumps in the series or climate-unrelated gradual trends) in order to assure the reliability of the final local CC scenarios. In addition, the simultaneous consideration of the outputs from different climate models, i.e. climate model ensembles, is recommended in order to account for variabilities and specific features inherent in the several available GCMs and RCMs. Model ensembles allow to gain insights into the variability and uncertainties in CC model simulations (Murphy et al., 2004; Tebaldi et al., 2007).

In the framework of GreenRisk4ALPs, the bias-corrected CC projections were retrieved to get indications on how climate change might alter the development of forests and natural hazards in the different PARs. The available GCM-RCM projections (n=15) provided by the EURO-CORDEX initiative built the basis for the subsequent analyses. The considered temperature and precipitation data cover Europe at a ~12 km spatial resolution (EUR-11) up to the end of the 21st century (Jacob et al. 2014, Kotlarski, et al. 2014). More specifically, daily mean temperature and daily precipitation projections under two emissions scenarios, namely RCP4.5 (emission peak at around 2040) and RCP8.5 (emissions continue to rise), were retrieved for each PAR. Site-specific bias-

correction was performed by means of the QM-based statistical approach employing meteorological records from weather stations as a calibration data. The selected stations are considered representative for the available forest data (i.e. one station per PAR) and were selected on the basis of their proximity to the forest sample locations and data availability. In this context, stations covering at least 20 years over the calibration period 1970 – 2000 were prioritized.

For all PARs, the applied QM implementation took data related to the 31-year historical period 1970 – 2000 to "match" observed station data and simulated data (i.e. climate projections) and to derive a PAR specific correction function that can be transferred to the future CC projections. The correction functions were computed for each month and applied to the relative daily precipitation and temperature values. The QM approach was applied to all 15 available EURO-CORDEX projections and separately for RCP4.5 and RCP8.5 to obtain bias-corrected scenarios for the period 2006 – 2097. Figure 4 exemplarily highlights differences between the original model (i.e. uncorrected data) and bias-corrected annual time series of mean temperature (a) and total precipitation (b) for one of the 15 GCM-RCM combinations and RCP8.5 for the PAR Kranjska Gora (Slovenia). In this case, the original uncorrected model shows a systematic underestimation of the station values of around 3-4 °C for temperature and around 500 mm for precipitation. Such biases are also evident when comparing the mean annual temperature cycle (Figure 5a) and the mean annual frequency of wet days (Figure 5b).

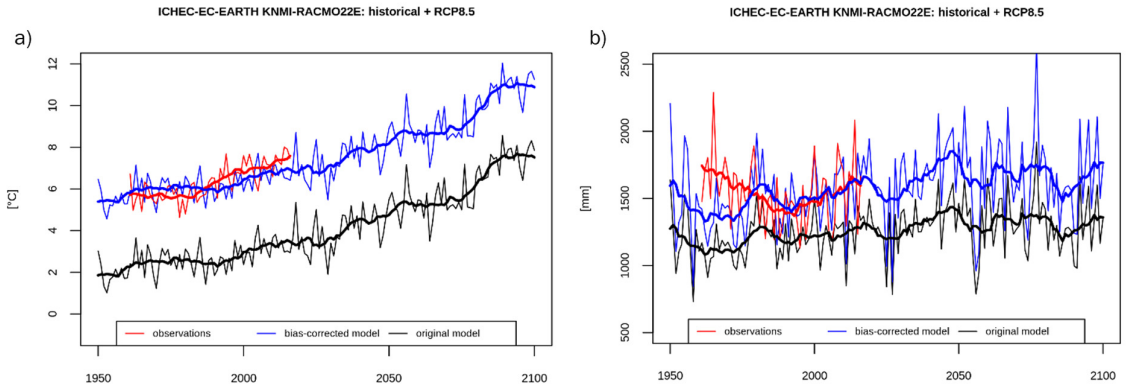

Figure 4 Comparison of observed, bias-corrected and original modeled annual (a) mean temperature and (b) total precipitation values for the Kranjska Gora PAR (Slovenia). A 11-year moving window average is superimposed on the series.

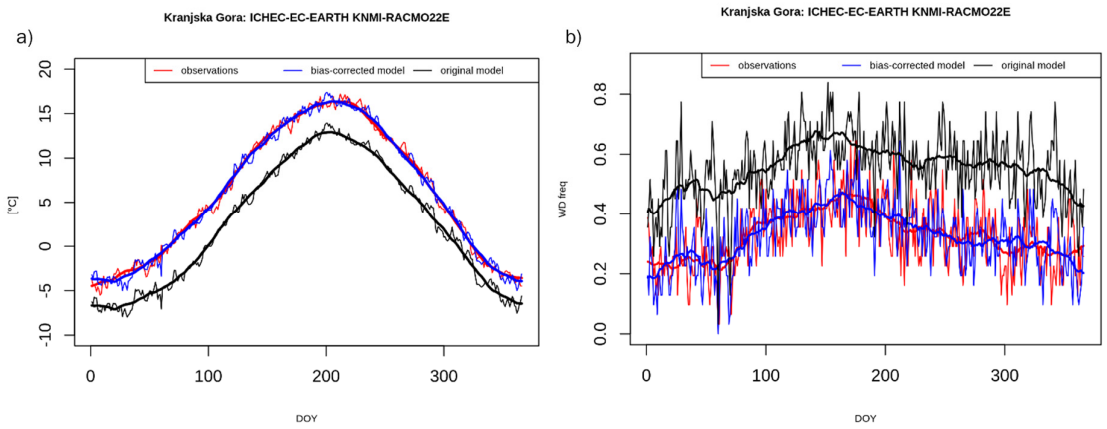

Figure 5 Comparison of observed, bias-corrected and original modeled (a) mean annual temperature cycle and (b) mean annual wet-day frequency cycle for the Kranjska Gora PAR (Slovenia). A 30-day moving window average is superimposed on the series.

2.3 Derivation of forest change (FC) scenarios

The calculation of FC scenarios aimed to highlight future forest growth under projected climate change conditions. The main goal was to elaborate whether changes in temperature and precipitation will affect the protection forests in the PARs. The FC modelling approach was applied to investigate how differences in the greenhouse gas emission scenarios (RCP4.5 vs. RCP8.5) may materialize in terms of forest growth in the Alpine Space. In this context it is important to note that non-climate related disturbances and (changes in) forest management practices were not taken into account. Thus, the obtained results reflect "management-independent" forest scenarios for the selected stands.

In other words, trees were allowed to grow without human intervention. Therefore, differences between forest growth under RCP4.5 and RCP8.5 might be considered as "pure" climate effects (emissions peak at around 2040 vs. emissions continue to rise). The forest growth simulator CALDIS was applied to elaborate changes in the basal area (i.e. the average amount of an area occupied by tree stems) and the total stem volume in response to projected changes in precipitation and temperature (Kindermann, 2010; Ledermann et al., 2017). Thus, besides climate parameters (cf. section 2.2) associated with the RCP scenarios 4.5 and RCP 8.5, also local forest parameters (i.e. single stem parameters), and site conditions have been included to derive FC scenarios. An additional altitude-dependent correction factor was applied for the temperature scenarios (0.6°C per 100 m) to account for differences between the temperature at the forest sample sites and the selected representative climate station.

CALDIS was originally developed for the Austrian National Forest Inventory (ANFI) data and parameterized for different growth regions specific to Austria. In order to reflect the growth conditions related to Slovenia, Germany, and Italy the most suitable (i.e. most similar growth region in Austria) was selected for each PAR and its parameters were adopted. For each PAR, no more than 20 data records that included tree, forest and site parameters were compiled from existing forest inventories or permanent forest plots as well as data that was collected in the field using angle-count sampling or fixed-radius sampling designs. Data records represented forests with a

protective function or with functions that are of particular interest in the respective PAR. A maximum of three main forest types such as subalpine spruce, spruce-fir and/or spruce-fir-beech forests was considered (see Appendix A) for detailed instructions on data collection). To match the minimum input data requirements for FC calculations with CALDIS, each protection forest data record included:

Basic information:

- ID (each record of forest and site parameters has one unique ID that links forest, site and other parameters)
- Sampling date
- Stand size (ha)

Forest parameter for each ID/record:

- Tree species
- Diameter at breast height (dbh) (cm)
- Tree height (m)
- Crown height (height up to the beginning of the living crown) (m)
- Number of stems per ha

Site parameters:

- Slope angle (°)
- Exposition (°)
- Relief: position of the stand on a slope/in the landscape in 8 classes:
    - 1 upper slope/convex slope
    - 2 middle slope
    - 3 lower slope/concave slope
    - 4 trench
    - 5 valley bottom
    - 6 flat
    - 7 depression
    - 8 stream
- Soil type (according to the ANFI)
- Vegetation type (according to the ANFI)
- Elevation (m)
- Position (Lat, Lon)
- Water balance/hydrological regime (estimated in 5 classes):
    - 1 dry
    - 2 moderately fresh
    - 3 fresh
    - 4 very fresh
    - 5 wet
- Soil depth (2 classes):
    - 1, 0-30 cm
    - 2, >30 cm

Appendix B lists the forest and tree parameters, which represent the current state of the selected protection forest stands and the starting point for the CALDIS simulations, and site conditions for

each PAR. The extensive dataset collected at one of the Austrian sites (PAR Vals/Gries) consisted of sampling points that were arranged in a regular 100-m grid over an area of approximately 137 ha (data records are not listed in Appendix B). This dataset was analyzed separately and split into three elevation strata (low, medium, high).

CALDIS was then run for yearly time steps for the time period 2019-2097. From year to year, each tree that was part of a data record and therefore growing in the represented forest stand in 2019 (category "standing stock") can either remain in this category or be assigned to the categories "thinning operation", "final harvest", or "tree mortality". That is, this tree will be either removed from the data record and therefore from the forest strata or taken over to the next year. Since we did not take (changes in) forest management practices into account, trees could only be assigned the categories "standing stock" or "tree mortality". In simplified terms, tree mortality can be caused by high stand density and high competition as well as by specific climatic conditions. The initial CALDIS outputs were dbh, tree height and canopy height of individual trees in yearly timesteps. The stem volume was derived from height and diameter with species-specific shape factors for stems.

2.4 Linkage of CC and FC with natural hazards

After analyzing calculated CC and FC scenarios, potential implications for natural hazard processes were elaborated on the basis of established process knowledge. A particular focus is set on the effects of climate-induced changes on the occurrence of landslides, snow avalanches and rock falls. The related literature review represents the current state of the art related to the topic while the established linkage to the PAR information (climate and forest change) aimed to provide insights into how the projected climate and forest alterations may alter the future hazard situation in the PARs. In this respect, this report puts a stronger focus on CC effects, also because other project activities and deliverables elaborate the forest effect in detail.

3 Results

3.1 CC scenarios for the PARs

The described QM-based approach was performed for the PARs listed in Table 1 to derive bias-corrected daily mean temperature and daily precipitation for the two scenarios RCP4.5 and RCP8.5. Table 1 depicts the reference stations chosen for each PAR together with related information about their geographical location. For the PARs, except Oberammergau, the used temperature and precipitation data relate to the identical station. The rain gauge related to Oberammergau is located in Oberammergau while the thermometer data relates to Bad Kohlgrub (similar elevation and 7 km far from the Oberammergau station). Due to the more relevant CC signal of temperature (see below), the thermometer location was used as reference and the precipitation observations were associated to this site.

Table 1 List of reference sites for each PAR for which the CC projections were computed

PAR	Station	Longitude	Latitude	Elevation [m]
VALS/GRIES	Brenner	11.30	47.00	1445
OBERAMMERGAU	Bad Kohlgrub	11.08	47.67	835
WIPPTAL SOUTH	Brennerbad	11.49	46.98	1330
VAL FERRET	Courmayeur La Villette	6.97	45.80	1220
KRANJSKA GORA	Kranjska Gora	13.71	46.50	846

The QM bias-correction approach was performed for each of the 15 GCM-RCM projections and the final series spans the interval 2006 – 2097. The Figures 6-10 highlight the projections for winter (December – January – February, DJF) and summer (June – July – August, JJA) temperature. Precipitation trends are reported for each PAR together with the model historical period starting in 1950. The average of all 15 models (*ensemble mean*) is reported together with the variability range (10^{th} – 90^{th} percentiles). More details on the calculated CC modelling results are highlighted within D.T1.1.6.

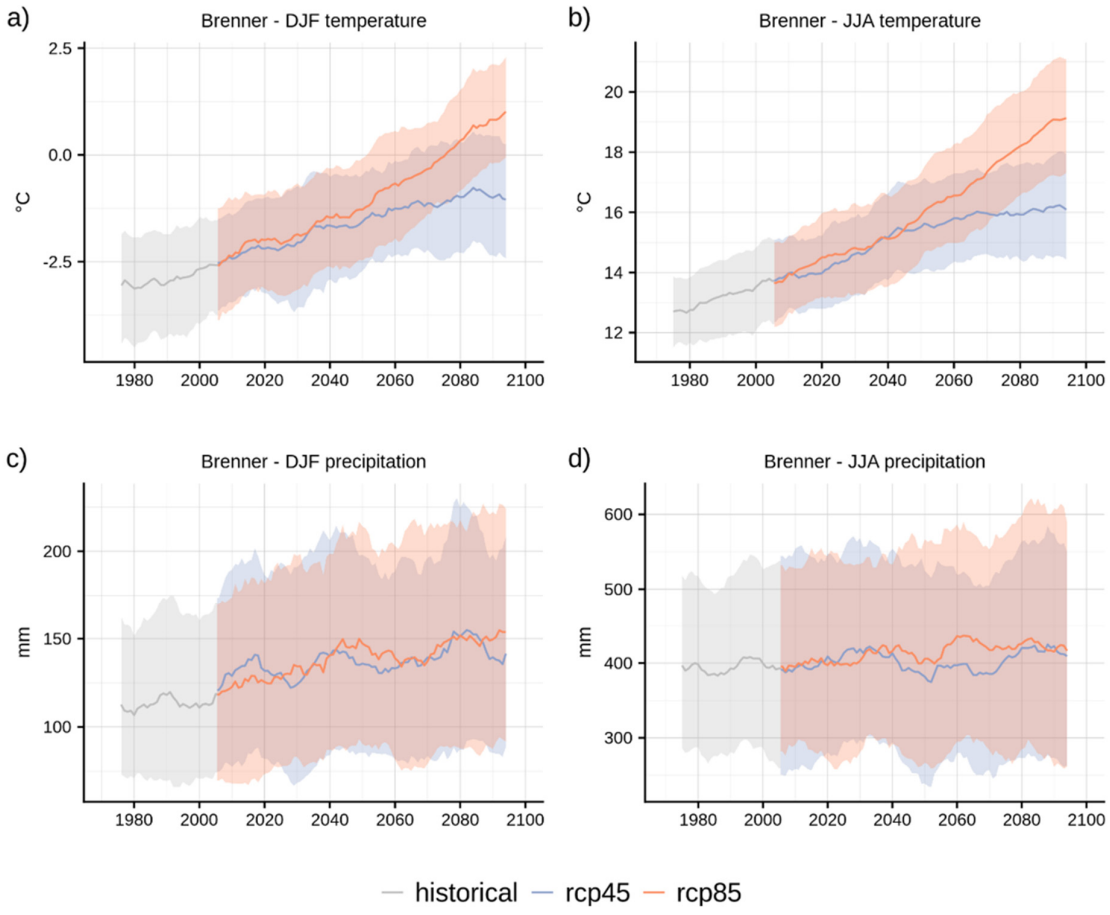

Figure 6 CC projections of winter (DJF) and summer (JJA) mean temperature and total precipitation representative for the PAR Vals/Gries for the two RCP scenarios. All series were filtered by a 11-year moving average and the ensemble mean is reported as solid line, the shaded area represents the range between the 10th and 90th percentile of all available 15 projections. The historical period is reported in grey color.

Besides the large variability of the climate model projections, a positive trend in temperature is clearly depicted by all models and for each PAR. Also, an evident distinction between RCP4.5 and the RCP8.5 emission scenarios can be seen, especially by considering longer-term developments. On the contrary, precipitation projections show a much greater variability and no clear trend (i.e. rising or declining) can be pointed out. Even though the precipitation trends have to be interpreted cautiously (see variabilities in the figures), a closer look at the data could suggest slightly wetter conditions for future winters. These outcomes are in agreement with existing studies focusing on climate changes over Europe and Alpine regions and based on both observations and climate model simulations (see e.g. Schmidli and Frei, 2005; Schmidli et al., 2007; IPCC, 2014; Brönnimann et al., 2018; Isotta et al., 2019).

The ensemble mean allows to interpret the average seasonal behavior among all CC projections. However, averaging all the daily simulations, the resulting series is strongly smoothed, which reduces its meaningful implementation into the CALDIS forest growth model. In order to preserve

the daily signal and to consider the spread of CC projections without running the forest model for each simulation, a cluster analysis was performed on the 15 GCM-RCM projections for each PAR. This procedure allowed to classify the CC projections into a smaller number of groups on the basis of the similar features and to reduce the dimension of data (Wilcke and Bärring, 2016). More specifically, the Partitioning Around Medoids (PAM) was performed (Reynolds et al., 2006) and the CC projections for each PAR were grouped into four clusters on the basis of the seasonal rates of change depicted in temperature and precipitation values over a future 30-year interval (2065 – 2094) in respect with an historical one (1971 – 2000).

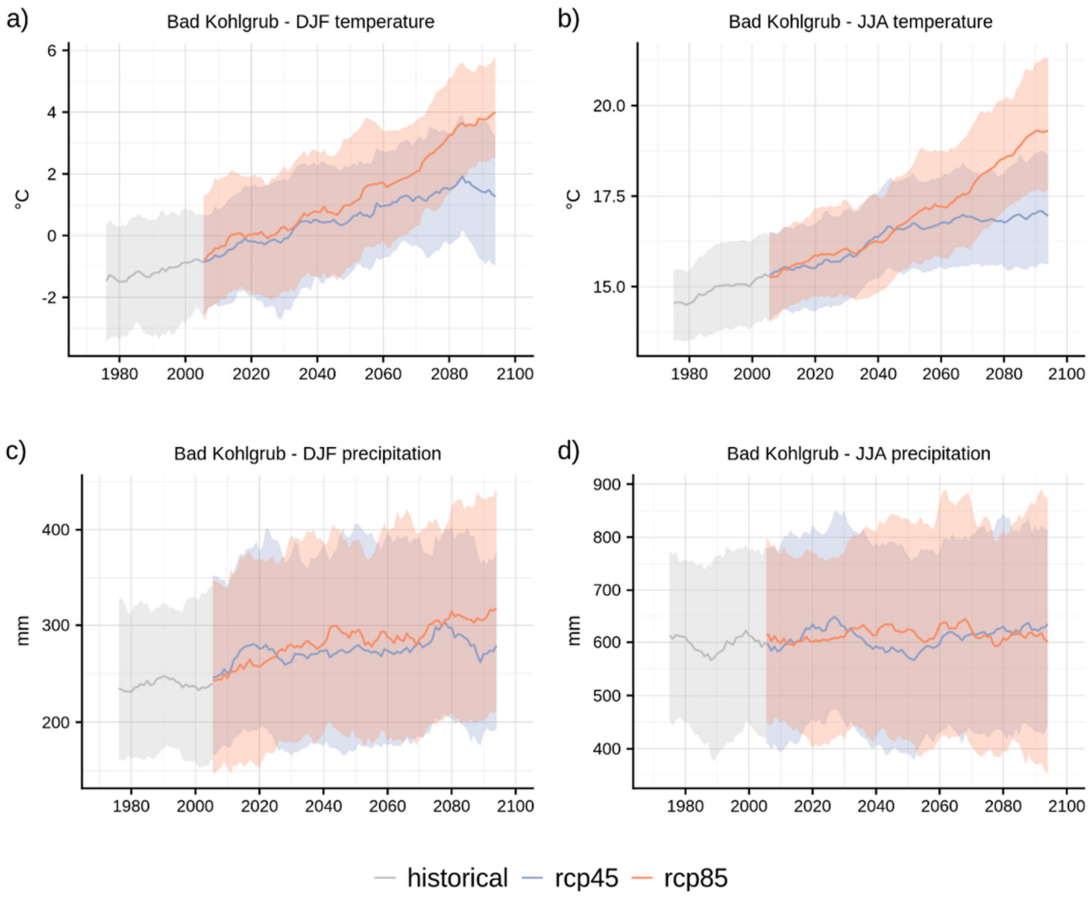

Figure 7 CC projections of winter (DJF) and summer (JJA) mean temperature and total precipitation representative for the PAR Oberammergau for the two RCP scenarios. All series were filtered by a 11-year moving average and the ensemble mean is reported as solid line, the shaded area represents the range between the 10th and 90th percentile of all available 15 projections. The historical period is reported in grey color.

The cluster classification allowed to choose the GCM-RCM combination that shows "most likely" changing rates, i.e. close to the average variations depicted by all projections, for both temperature and precipitation. The data was then selected as an input for the CALDIS forest model. In particular, the projections derived from the GCM ICHEC-EC-EARTH combined with the RCM named "KNMI-

RACMO22E" was selected for both RCP scenarios in all PARs. The choice of the same model assures a better interpretability and inter-comparison of the final forest scenarios among PARs by avoiding possible discrepancies in projections due to specific features of the climate model from which they were derived.

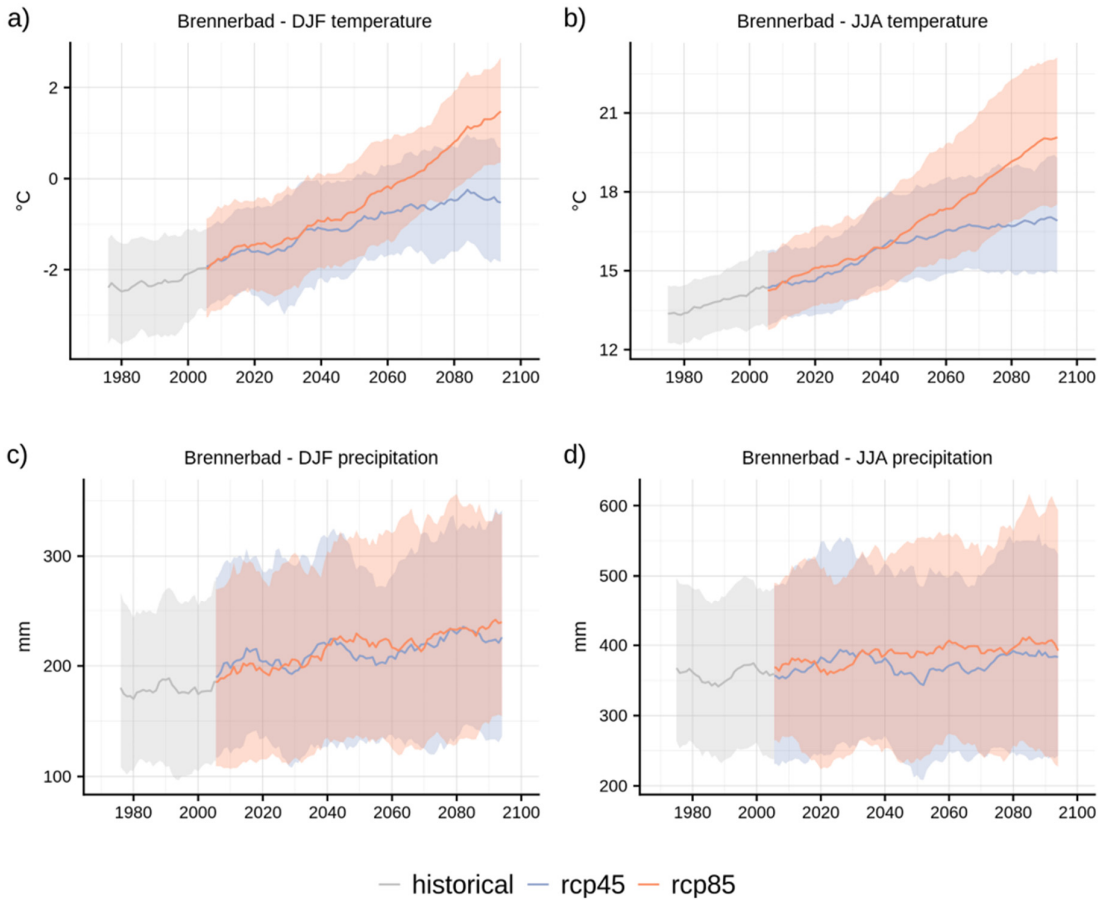

Figure 8 CC projections of winter (DJF) and summer (JJA) mean temperature and total precipitation representative for the PAR Wipptal South for the two RCP scenarios. All series were filtered by a 11-year moving average and the ensemble mean is reported as solid line, the shaded area represents the range between the 10th and 90th percentile of all available 15 projections. The historical period is reported in grey color.

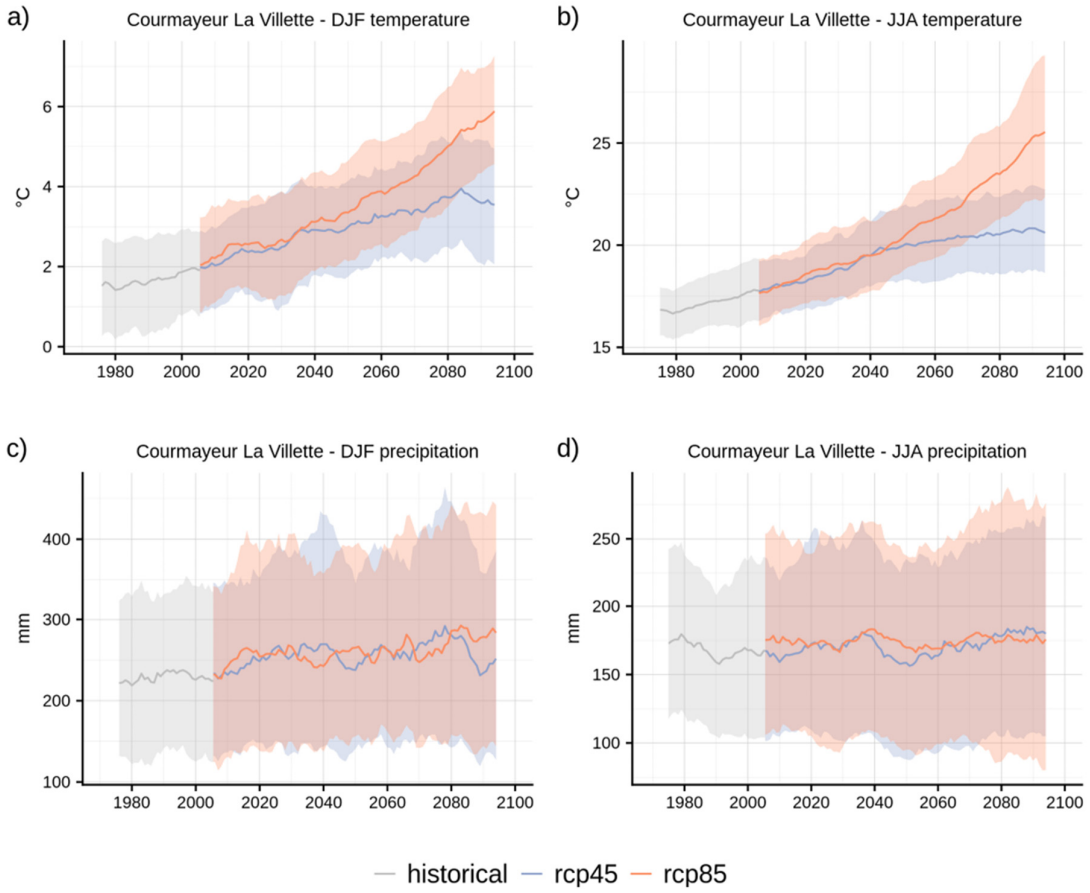

Figure 9 CC projections of winter (DJF) and summer (JJA) mean temperature and total precipitation representative for the PAR Val Ferret for the two RCP scenarios. All series were filtered by a 11-year moving average and the ensemble mean is reported as solid line, the shaded area represents the range between 10th and 90th percentiles of all available 15 projections. The historical period is reported in grey color.

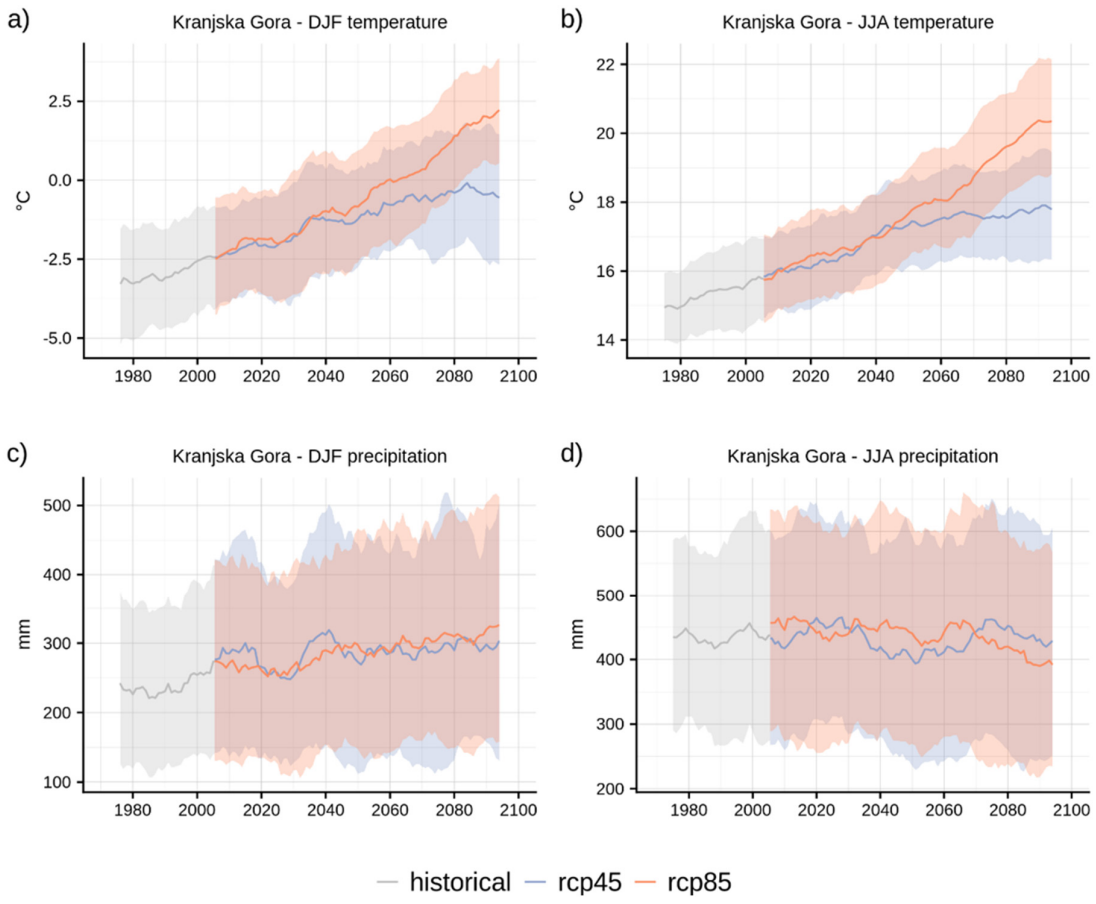

Figure 10 CC projections of winter (DJF) and summer (JJA) mean temperature and total precipitation representative for the PAR Kranjska Gora for the two RCP scenarios. All series were filtered by a 11-year moving average and the ensemble mean is reported as solid line, the shaded area represents the range between 10th and 90th percentiles of all available 15 projections. The historical period is reported in grey color.

A trend analysis in temperature and precipitation was performed for the selected ICHEC-EC-EARTH KNMI-RACMO22E projections for each PAR by applying the Theil-Sen test (Theil, 1950) for trend slope estimation and the Mann Kendall method (Kendall, 1975) for the trend significance evaluation. The trends were computed over the 147-year period spanned by the historical simulations and RCP scenarios at seasonal and annual scales. The results are summarized in Tables 2 and 3. The trend values are reported only if they are statistically significant (p-value < 0.05), otherwise only the sign of trend (+ or -) is specified.

Table 2 Trend in seasonal and annual mean temperature anomalies (reference 1971 – 2000) for the period 1950 – 2097. The values are expressed as °C per century. Interpretation example (in bold): annual mean temperature variation over one century (e.g. 1951 – 2050) is +4°C (+2°C in 25 years).

	Vals/Gries		Oberammergau		Val Ferret		Wipptal South		Kranjska Gora	
	RCP4.5	RCP8.5	RCP4.5	RCP8.5	RCP4.5	RCP8.5	RCP4.5	RCP8.5	RCP4.5	RCP8.5
DJF	+1.8	+3.1	+2.7	+4.9	+2.2	+3.9	+1.7	+2.9	+1.9	+3.7
MAM	+1.6	+3.0	+2.3	+3.6	+1.8	+3.3	+1.5	+2.9	+2.0	+3.4
JJA	+2.5	+4.3	+2.2	+3.7	+2.7	+4.7	+2.2	+3.8	+2.1	+3.7
SON	+2.4	+4.2	+2.2	+3.7	+2.7	+4.7	+2.0	+3.6	+2.3	+3.7
YEAR	+2.1	+3.5	+2.3	+3.9	+2.3	**+4.0**	+1.8	+3.2	+2.0	+3.5

Table 3 Trend in seasonal and annual total precipitation anomalies (reference 1971 – 2000) over the period 1950 – 2097. The values are expressed as % per century. The trend sign (+ or -) is only reported for not significant trends (p-value < 0.05). Interpretation example (in bold): annual total precipitation variation over one century (e.g. 1951 – 2050) is +10% (+2.5% in 25 years).

	Vals/Gries		Oberammergau		Val Ferret		Wipptal South		Kranjska Gora	
	RCP4.5	RCP8.5	RCP4.5	RCP8.5	RCP4.5	RCP8.5	RCP4.5	RCP8.5	RCP4.5	RCP8.5
DJF	+	+25.3	+22.6	+30.0	+	+23.9	+	+26.7	+	+18.3
MAM	+	+	+16.4	+27.0	+	+	+	+	+15.9	+
JJA	+	+	+	+9.1	-	-17.5	+	+15.2	+	+
SON	+	+	+	+	+	-	+11.8	+	+13.4	+17.9
YEAR	+	+10.3	+10.2	+17.2	+	+	+8.1	+14.1	**+10.0**	+15.0

In addition, the future variations in precipitation extremes depicted by the selected CC projections were analyzed. The data is reported within D.T1.1.6. Changes in annual maximum 1-day precipitation (Rx1day) as well as in the total daily precipitation values exceeding the 99th percentile over 1971 – 2000 (R99ptot) were considered.

In summary, a statistically significant increment in the indicators is pointed out for the RCP8.5 scenario for all PARs, except for Val Ferret. For Val Ferret no significant variation was observed. At seasonal scale, the most relevant variation in Rx1day occurs in autumn. The average Rx1day in autumn over 2068 – 2097 is expected to be 30% (Kranjska Gora), 20% (Vals/Gries) and 17% (Oberammergau) greater than the corresponding value in the period 1971 – 2000. In these PARs the total daily precipitation values exceeding the 99th percentile (R99ptot) are almost two times as common for the period 2068 – 2097 compared to 1971 – 2000. In the PAR Wipptal South, no season-related trend of Rx1day is depicted and no significant variation in R99ptot is observed. If the RCP4.5 scenarios are considered, the signal in precipitation extreme indicators is lower and no statistical significance is found in most cases. It is emphasized that the obtained numbers should be interpreted with caution, especially the analysis concerning total precipitation and extremes. The results are valid only for the selected model (see e.g. Nikulin et al., 2011; Rajckaz and Schär, 2017).

3.2 FC scenarios for each PAR

The results of CALDIS are summarized within this section. Figure 11 (left panel) shows the calculated stem volumes for all sampling points in each PAR for the year 2019 in the form of violin

plots (see Appendix B for 2019 mean forest and site parameters). It is shown that the sampled stems in the PAR Vals/Gries exhibit very high stem volumes that are especially present at the area sampled on a regular grid (108 sampling points). Normally, forest stands with these dimensions would be harvested or at least heavily thinned. Apparently, the stand dimensions are not yet considered critical for stand sustainability.

Stem volumes for the PARs Wipptal South, Oberammergau and Val Ferret show lower (mean) values. Particularly low stem volumes were observed for the PAR Kranjska Gora. The main reason for these low values is that forest data was mainly collected in areas that were heavily affected by bark beetle infestation resulting in a high tree mortality. These forests mainly consisted of Norway spruce (*Picea abies*), which was planted in the past. From 2008 to 2018, salvage and sanitation logging following the bark beetle outbreak varied between 10% and 22% of the annual harvest, which made these stands even more vulnerable to other natural disturbances such as windthrow or snow breakage. Currently, the main tree species is European beech (*Fagus sylvatica*) (see Appendix B).

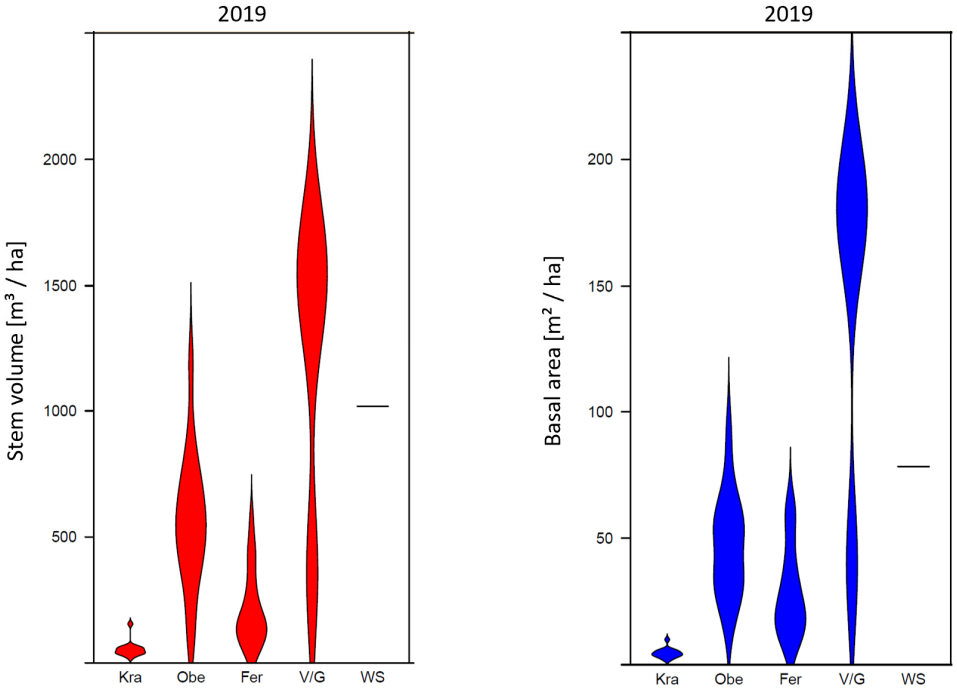

Figure 11 Summary of calculated stem volumes (left) and stem basal areas (right) that were observed in 2019 in the different PARs (Kra: Kranjska Gora, Obe: Oberammergau, Fer: Val Ferret, V/G: Vals/Gries, WS: Wipptal South). The width of the color areas corresponds to data densities (e.g. for V/G, a high portion of observations point to stem volumes around 1500 m³/ha). Due to the limited availability of forest data for the PAR WS, only the mean value is shown.

As expected, the calculated stem basal area (Figure 11, right panel) shows similar trends compared to the calculated stem volume (Figure 11, left panel): very high values for the PAR Vals/Gries, medium values for the PARs Oberammergau, Val Ferret, Wipptal South and low stem basal areas for Kranjska Gora.

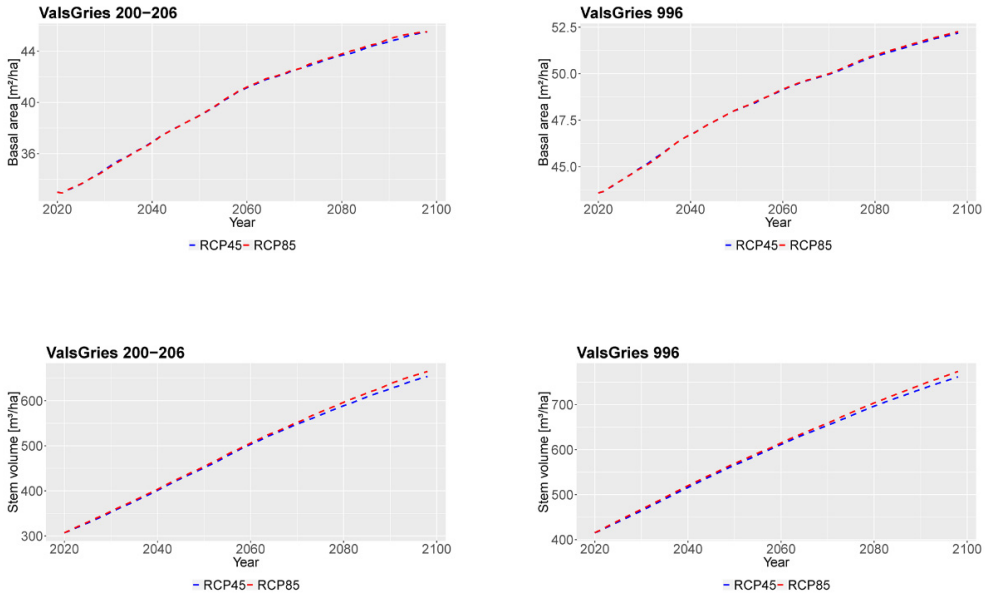

Figure 12 Summary of calculated forest changes for RCP4.5 (blue) and RCP8.5 (red): basal area (top row) and stem volume (bottom row) for the PAR Vals/Gries (2020-2097). The panels "ValsGries 200-206" show mean values that are calculated for six forest stands/sampling points spatially distributed over the PAR. Panels Vals/Gries 996 summarize all sampling points at the low elevation band of the area that was sampled on a regular 100-m grid.

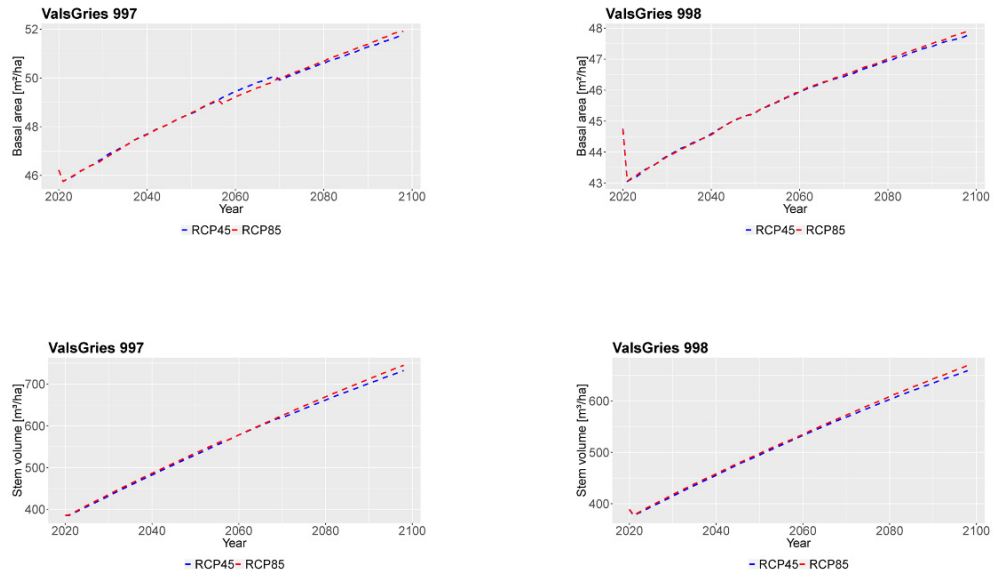

Figure 13 Summary of calculated forest changes for RCP4.5 (blue) and RCP8.5 (red): basal area (top row) and stem volume (bottom row) for the PAR Vals/Gries (2020-2097). Panels Vals/Gries 997 summarize all sampling points at mid elevation and 998 at high elevation bands. The data was collected at the area that was sampled on a regular 100-m grid.

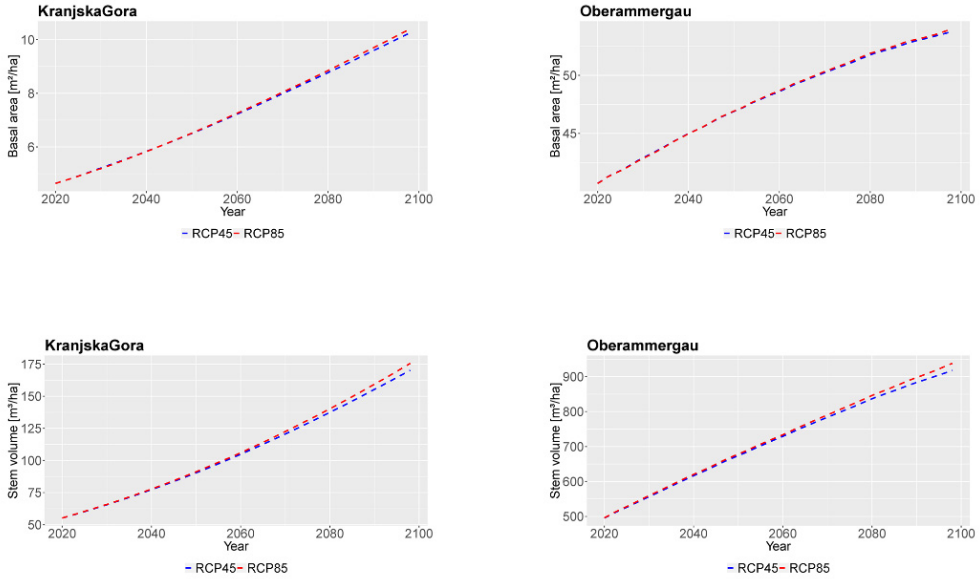

Figure 14 Summary of calculated forest changes for RCP4.5 (blue) and RCP8.5 (red): basal areas (top row) and stem volumes (bottom row) for the PARs Kranjska Gora and Oberammergau (2020-2097).

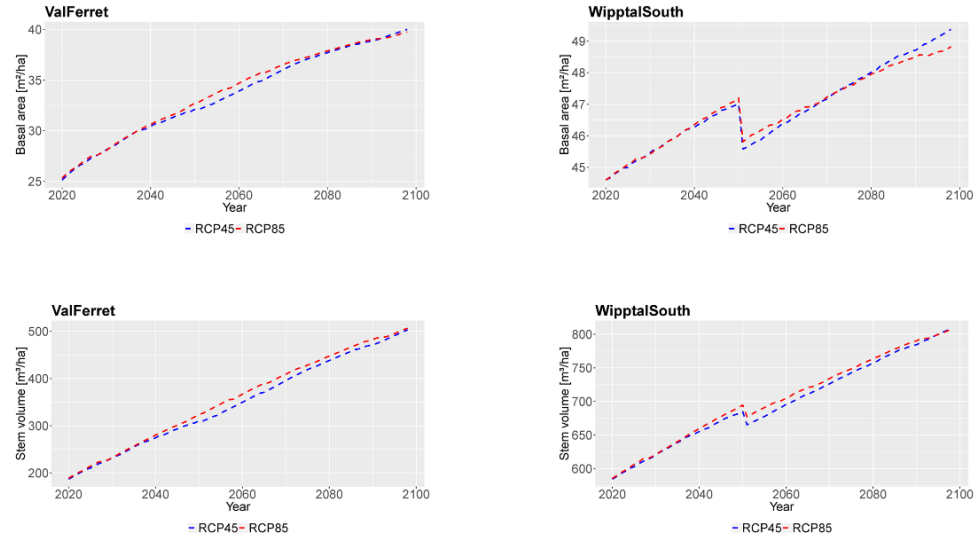

Figure 15 Summary of calculated forest changes for RCP4.5 (blue) and RCP8.5 (red): basal areas (top row) and stem volumes (bottom row) for the PARs Val Ferret and Wipptal South (2020-2097).

Figures 12-15 show the developments of mean stem volume and basal area for each PAR over time and separate for each regional climate projection. For all PARs, modelled mean stem volume and basal area developments are very similar for both RCP scenarios (see also Appendix C). These minor differences between the climate change scenarios indicate that the “pure” effect of divergent

greenhouse gas emissions (RCPs) may not influence forest growth patterns substantially. Associated non-climate disturbances, such as forest management scenarios are known to have a substantial influence on forest growth patterns but were not taken into account within this analysis.

The strong decrease in mean stem volume and basal area for PARs Vals/Gries (sampling locations 996-998) and Wipptal South after 2019 results from the high stem densities that are currently present in these PARs (see Figure 11). That is, the CALDIS model exerts at the beginning of the simulation period a high tree mortality rate (i.e. a high number of trees are categorized as "mortality" and are removed from the forest strata) from one year to the next to decrease stem densities to a more representative level. The model is set up in the way that such immediate/drastic changes are often realized in the very first step, i.e. from the first to the second year. A new maximum stem density is calculated, which again triggers new mortality, if it is exceeded. The exceedance of a certain threshold for stem density is also the cause for the decrease in stem volume and basal area around 2050 for the PAR Wipptal South.

In summary, the results provide indications that, if trees in the sampled forests are allowed to grow without human intervention, an increase in biomass (increase in basal area and stem volume) and, therefore, in the protective effects against landslides, rock falls and avalanches may be generally expected, independent of the greenhouse gas emission scenario. However, our simulation results do neither provide insights into potential shifts in species composition nor estimates of the influence of changing forest disturbance regimes (e.g. windthrow, insect outbreaks or forest fire), which will also affect their future protective capacity (see section 3.3). Moreover, a crucial factor in the development of protection forests in the Alpine Space relates to the partly unforeseeable future management practices. In many cases it can be expected that the applied management practice outweighs the influence posed by climate change. Challenges of FC in the context of natural hazard risk reduction are evident: if future forest management practices (which may be partly driven by CC) lead to a decrease in the protective effect of current forests, alternatives at presumably higher costs have to be considered. Changes in forest management practice and higher investments in technical protection measures are among the most widely discussed implications of a potential reduction in forests' protective effects. Literature exposes divergent opinions on how complex climate changes may affect forests in the Alpine Space:

- The growth of mountain forests is presently constrained by thermal factors. In a warmer world, this growth limiting factor will be less relevant.
- Future forests may be affected by a higher pressure from biotic (simply because warmer conditions allow pests and pathogen to extend their habitats into higher elevations), and abiotic stressors.

3.3 Natural hazard scenarios

This descriptive part on natural hazard scenarios builds upon the calculated changes (CC, FC) and a literature review in order to link the projected alterations to snow avalanches (section 3.3.1), rock falls (section 3.3.2) and landslides of the slide-type movement (section 3.3.3).

3.3.1 Snow avalanche scenarios

Future changes in climate and land-use are likely to have considerable impacts on both avalanche activity and forest cover and composition. However, the protective effects of forests to reduce frequency and magnitude of destructive avalanches could improve or deteriorate dependent on elevation and ecological shifts (Bebi et al., 2009), land-use and forest management practices (Maroschek et al., 2014), feedback loops between forests and avalanches (Zurbriggen et al., 2014) as well as the occurrence of other natural disturbances such as windthrow and bark beetle outbreaks (Wohlgemuth et al., 2017; Teich et al., 2019; Figure 16).

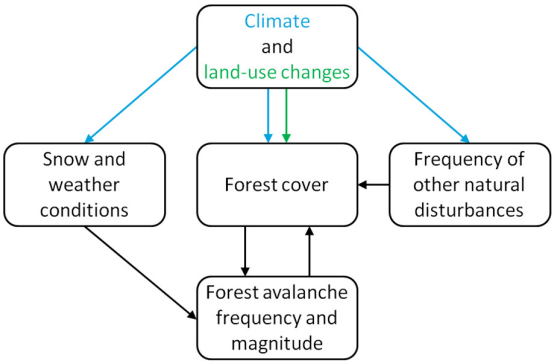

Figure 16 Factors and feedback effects, which influence future avalanche activity in forested terrain and, therefore, the protective effects of forests. (adapted from Teich et al., 2012c)

Climate change and snow avalanches: The effects of climate change on avalanche activity in general are largely unknown but are of great importance for future risk management and inhabitants of alpine areas (Schneebeli et al., 1997; Jomelli et al., 2007). Existing knowledge on avalanche-climate interactions is still insufficient for global and long-term predictions (Beniston et al., 2018). Most studies dealing with interactions between avalanche activity and climate are local and focus only on the past few decades. This is mainly due to relatively scarce long and continuous historical observations, so that studies on avalanche-climate interactions have remained restricted to a few areas in the world, for which long-term data is available (Schläppy et al., 2016). In forested avalanche terrain, dendrogeomorphology can be a powerful tool used to fill gaps in historical records. This technique can be applied to reconstruct avalanches at annual resolutions as well as decadal to centennial scales from their impacts on trees that are preserved in the sequence of tree rings (e.g. Stoffel and Corona, 2014); however, there is a potential for years with avalanche activity to be underestimated by up to 60 % (Corona et al., 2012).

The existing local studies related to the influence of climate change on changes in avalanche activity over the last decades suggest that it has had little impact on avalanche frequency in open unforested terrain (Laternser and Schneebeli, 2002), but that the proportion of wet snow avalanches has increased (Pielmeier et al., 2013), and that the runout elevation of large avalanches has retreated further upslope (Eckert et al., 2010; 2013). In forested terrain, the number of days with favorable snow and weather conditions for forest avalanche release has

decreased (Teich et al., 2012b). The observed changes come as a direct consequence of changes in snow and weather patterns and, therefore, snow cover characteristics (Teich et al., 2012b; Castebrunet et al., 2012; Bellaire et al., 2016); however, linking climate change to avalanche activity remains challenging. For example, the increase in mean winter temperature (that is also predicted for all PARs and both climate scenarios) might stabilize the snow cover, but warmer air can also hold more moisture. This effect might therefore result in larger winter precipitation amounts (which is also shown in the CC scenarios, but mainly for RCP8.5 for all PARs) and thus an increase in avalanche activity (Bellaire et al., 2016). Due to the complex interactions between snow, weather conditions, terrain and land cover, which synergistically influence avalanche release and dynamics (Schweizer et al., 2003; Bartelt et al., 2012), it still remains unclear whether warmer temperatures will lead to fewer avalanches because of decreased snow fall and solid precipitation rates (Marty and Meister, 2012). That is, direct effects of climate change on avalanche frequency, timing, magnitude, and type mainly exist in the form of changes in snow amounts, snowfall succession, density, and stratigraphy as a function of elevation (Beniston et al., 2018).

The few studies analyzing past trends in extreme snowfall events indicate that extreme snow depths have decreased at all elevations, but primarily below 800 m (Blanchet et al., 2009; Marty and Blanchet 2012; Kunkel et al., 2016); however, there seems to be a less clear pattern for extreme snowfalls between 800 and 1,500 m (Marty and Blanchet, 2012). Due to warmer temperatures at low elevations, more rain events and a shorter snow cover duration are expected (Marty, 2008; Serquet et al., 2011).

Only few predictions of the future avalanche activity have been attempted so far since avalanches often occur at very local scales, making them difficult to relate to climate model outputs, even when using downscaling methods (Rousselot et al., 2012; Kotlarski et al., 2014). Castebrunet et al. (2014) developed a statistical model that relates past avalanche observations to snow and meteorological conditions to produce projections (under three greenhouse gas emissions scenarios) on annual and seasonal timescales of future natural avalanche activity in the French Alps. They predict a general decrease in mean (20–30%) and interannual avalanche activity, especially at lower elevations and in spring months. In contrast, an increase in avalanche activity is expected at high elevations in winter due to more favorable conditions for wet snow avalanches earlier in the winter season (Castebrunet et al., 2014), i.e. the already observed trend towards wetter snow avalanches is likely to continue (Sovilla et al., 2010; Ancey and Bain, 2015).

Forest cover changes and snow avalanches: Mountain forests serve a crucial role in avalanche control by preventing slab avalanche formation (Schneebeli and Bebi, 2004), and by reducing the runout distances of small to medium size avalanches that are released in forest gaps or slightly above the tree line (Teich et al., 2012a). Therefore, forest cover extent and forest structure in terms of crown closure, tree density, species composition and size and distribution of forest gaps directly influence the activity, i.e. frequency and magnitude of avalanches in forested terrain (Bebi et al., 2009; Teich et al., 2014).

The main protective effect of forest on avalanche formation is due to: 1) snow interception by tree crowns that reduces the amount of snow reaching the ground by up to 60% (for a dense evergreen coniferous canopy; Schmidt and Pomeroy, 1993) and creates a more heterogenous subcanopy snowpack when intercepted snow is falling or dripping down; 2) changes to the radiation and temperature regimes due to shading by the canopy, which reduces the formation of weak

snowpack layers; 3) the reduction of near-surface wind speeds, which decreases snow re-deposition and compaction; and 4) the direct support of the snowpack by stems, remnant stumps and dead wood (e.g. Schneebeli and Bebi, 2004). For previously released avalanches, the secondary protective effect of forests on avalanche runout becomes relevant, i.e. mass reduction by snow detrainment, deceleration and even stopping (Bartelt and Stöckli, 2001; Anderson and McClung, 2012; Feistl et al., 2014a). Within the first 100-200 m of the avalanche path, evergreen dense forests with a high tree density and with mean diameters smaller than 15 cm are able to significantly reduce runout distances of small to medium size avalanches (Teich et al., 2012a).

European mountain forests have changed considerably within the last decades, i.e. on average the extent of the forest cover has increased by 4% per decade over the past 25–115 years over the entire Alps (Bebi et al., 2017). This increase in forest area is mainly due to changes in land use (abandoned alpine pastures converting back to forest) as well as in climate conditions (Bebi et al., 2017). The effect of climate change on forest expansion at the upper tree line however, is not as important in contrast to the effect of changes in land use (Gehrig-Fasel et al., 2007), and other factors such as grazing, snow cover duration or competition by, e.g., dwarf-shrubs, limit its rapid expansion despite higher temperatures (e.g. Motta et al., 2006; Harsch et al., 2009; Barbeito et al., 2012).

In the Swiss Alps, e.g., the forest area above 1000 m asl has increased by 3.2% between the two Swiss National Forest Inventory periods of 1979-1985 and 1992-1997 (Bebi et al., 2009). This forest expansion has mostly occurred in potential avalanche release areas (slope angle $> 30°$) above 1400 m and thus led to a decrease in avalanche activity (Bebi et al., 2009). However, transitions from open forests to closed forests were less frequent on these steep slopes, which are often affected by regular avalanche disturbance (and other gravitational natural hazards) that maintain open forest structures and forest gaps (feedback effects; Zurbriggen et al., 2014). If these trends continue, we can expect further expansion in the area of avalanche protection forests in the Alps, but not necessarily stronger protective effects of forests growing on very steep slopes. Furthermore, although the above ground biomass is predicted to increase especially in higher elevations (~2200 m asl) and in less drought prone areas with mainly positive consequences for avalanche protection, the protective effect at intermediate elevations (~1600 m asl) may decrease due to changes in species composition (Elkin et al., 2013). That is, the main tree species of avalanche protection forests Norway spruce will be replaced in parts by more drought tolerant broadleaved trees that are also less susceptible to natural disturbances such as bark beetles and wind (Faccoli and Bernardinelli, 2014).

These shifts in species composition at higher elevations from evergreen conifer forests to more mixed forest stands may impact the protective effect of these forests considerably since crowns of broadleaved trees are bare in winter reducing snow interception, wind protection and shading effects (Huerta et al., 2019). Moreover, deciduous and mixed forest types may not only have a reduced protective effect against dry slab avalanche release and runout, but also increase the susceptibility of wet snow avalanche types (especially glide snow avalanches), which are predicted to increase in proportion compared to dry avalanche regimes (Castebrunet et al., 2014). Observations show that glide snow avalanches are more likely to release in broadleaved-dominated and especially beech forests, although the protective effect of the forest canopy on this type of avalanches is generally low and surface roughness is more important (Perzl and Walter, 2012; Bebi

et al., 2012). These forests usually have a smooth ground surface with less roughness elements and a slippery ground cover due to their persistent and poorly degradable litter, which allows an avalanche to glide directly on the ground. Glide snow avalanches are often small but can still be a threat to roads, railways and other infrastructure (Feistl et al., 2014b).

Warmer winter temperatures, decreasing snow depth, increasing forest cover and density in high altitudes in combination with ecological shifts and shifting forest disturbance regimes, will affect the future importance and protective capacity of avalanche protection forests. Simulation studies have shown that climate change may have, depending on the region, and climate and management scenario applied, both, positive and negative impacts on avalanche protection (e.g. Elkin et al., 2013; Maroschek at al., 2014). The key factors for the provision of avalanche protection were bark beetle disturbances, legacies of past land-use practices and the applied forest management strategies, but the effects on avalanche control are still highly uncertain. Even if the expected rise of tree line elevation may reduce both avalanche frequency and magnitude, present knowledge on avalanche–forest interactions is still incomplete (Bebi et al., 2009), and especially the effect of forest disturbances such as bark beetle outbreaks, wildfire and windthrow, and their cascading effects is currently understudied.

The predominance of Norway spruce in avalanche protection forests of the European Alps, which is susceptible to frequent epidemic and severe European spruce bark beetle (*Ips typographus*) outbreaks as predicted for the coming decades (Seidl et al., 2009), will be a major problem for future protection forest management. Following bark beetle-induced tree mortality, needles are shed from tree crowns reducing canopy interception and influencing other processes that provide protective effects against slab avalanche release (Winkler et al., 2014). However, a recent study has shown that it is not the effect of tree mortality per se that creates new avalanche release areas since standing dead spruce trees are still able to provide some avalanche protection, but that it's instead current post-infestation management that needs to be adapted especially in areas where bark beetle outbreaks have reached epidemic levels (Teich et al., 2019). In Norway spruce forests of the European Alps, reducing the spread of a European spruce bark beetle infestation within and into adjacent stands by salvage logging and sanitation felling can be critical to prevent the extent of an outbreak throughout an avalanche protection forest (Stadelmann et al., 2014). However, when bark beetle populations have reached epidemic levels, the removal of trees can lead to changes in forest density and create forest gaps over large extents, which could create new avalanche release areas. In such cases, it can be more appropriate to leave dead trees in place (Teich et al., 2019), and to prioritize strategies to increase resistance (decreased susceptibility) and resilience to subsequent bark beetle infestations, which may require manipulation of stand structure and species composition (e.g., Brang, 2001; Motta and Haudemand, 2000). Creating more structural and species diversity, i.e., uneven and multi-layered stands with a mosaic of tree sizes and age classes are not only ideal for long-term avalanche protection, but would also decrease the susceptibility to storm events (Wohlgemuth et al., 2017). Windstorms are currently the primary disturbance agent in the Alps and, again, post-disturbance management can have a significant effect on avalanche control. It was found that areas in avalanche protection forests that were disturbed by wind and not cleared after the event occurred, effectively prevented avalanche release for up to 20 years (Wohlgemuth et al., 2017). Furthermore, a high surface roughness (e.g. when downed woody debris is left on the forest floor) can also significantly shorten avalanche runout

distances (Feistl et al., 2014b). If current practices for post-disturbance forest management are continued, i.e. removing infested and downed trees and decreasing forest canopy cover and surface roughness, there might be problems with the allocation of monetary and operational resources to manage these forests.

The future management of mountain forests in the Alps has to take into account not only changes in climate and their effects on avalanche regimes and forest cover, and long-lasting effects of land-use history, but also the increasing influence of natural disturbances (Bebi et al., 2017). Where the protective function of forests against natural hazards is threatened by disturbances and other ecological processes, management should focus on increasing the resilience of mountain forests that allows forests to adapt to future environmental conditions (Seidl et al., 2014).

CC and FC in the PARs: Higher mean air temperatures in winter (DJF) as well as in summer (JJA) months are predicted for all PARs for the two climate change scenarios until the end of the 21st century (see section 3.1). The increases in winter temperatures will affect snow cover characteristics and most likely lead to a further increase in wet snow avalanche frequency, i.e. the trend towards earlier wet snow avalanche activity onset and the already observed shift from spring to winter months will continue (Pielmeier et al., 2013; Castebrunet et al., 2014). However, for the reference stations representative for the PARs Oberammergau (which is located at 835 m) as well as Val Ferret (1220 m), positive mean winter temperatures are already predicted for 2020. Hence, most of the winter precipitation may fall as rain instead of snow, which could lead to 1) reduced snow depths and duration and, therefore, a decrease in the avalanche activity, or 2) more rain on snow events, which can trigger avalanches (Conway and Raymond, 1993), and, therefore, increase (wet) snow avalanche activity. For the PARs Wipptal South and Vals/Gries, which are located at higher elevations (reference stations at 1330 m and 1445 m respectively) as well as for the PAR Kranjska Gora (846 m), winter mean air temperatures are predicted to be above freezing level around year 2070 under the “business as usual” emission scenario RCP8.5. However, generally increasing winter temperatures will also affect snow cover characteristics and winter precipitation and, therefore, avalanche activity in these PARs. That is, warmer air can hold more moisture, which in turn could lead to more extreme snow fall and avalanche events, which could be experienced in all PARs over the coming decades. A significant positive trend in the amount of winter precipitation was found for all PARs for the RCP8.5 scenario, but whether this precipitation falls as rain or snow, is dependent on the elevation or location of the respective region. Overall, the global effect on avalanche activity still remains unclear (Marty and Meister, 2012; Beniston et al., 2018).

The predicted increase in mean air temperatures will not only affect snow and avalanche regimes, but also forest cover extent and structure by, e.g. prolonging the growing season and, therefore, increasing the amount of forest biomass, which was modeled for all PARs with the forest growth simulator CALDIS (see section 3.2). An increase in biomass, i.e. forest density, is positive for forests’ protective effects to decrease avalanche release probability and to shorten runout distances (Teich et al., 2012c; Bebi et al., 2017). However, our simulation results do not provide insights into potential shifts in species composition, e.g. towards more mixed and broadleaves-dominated forests, which could reduce the capacity of these forests to protect against avalanches (Elkin et al., 2013). It is likely that the forests in PAR Kranjska Gora that are currently dominated by European beech will remain beech forests with negative implications for avalanche control. The low- and intermediate-elevation Norway spruce forests in the PAR Oberammergau may experience

enhanced tree mortality and a shift to more drought resistant broadleaved trees due to higher air temperatures, but also due to an increase in the frequency and magnitude of forest disturbances, which can severely damage the current monocultures (Seidl et al., 2014). This is true for spruce-dominated forests in all PARs since higher mean temperatures in the summer months combined with less precipitation (e.g., as predicted for the PAR Val Ferret for RCP8.5, Table 3) leads to more severe droughts, which decrease tree vitality and increase their susceptibility to pests, pathogens and windthrow. However, we did not take any forest management strategies into account, which have a considerable influence on the composition and structure and, therefore, the resistance, resilience and stability of future avalanche protection forests (Brang, 2001; Motta and Haudemand, 2000).

3.3.2 Rock fall scenarios

Since 1980, the frequency and magnitude of extreme rainfall events seems to increase in many parts of Austria (ÖKS15, 2016). The Alps already experience an increase in rock fall events due to air temperature, total rainfall and rainfall intensity (Ravanel and Deline, 2011; Gariano and Guzzetti, 2016). Changes in temperature, extreme precipitation, permafrost and snowmelt can be counted as triggering factors for the release of rock fall (Volkwein et al., 2011). As rainfall intensity and air temperature will increase in the study sites, the rock fall hazard will increase further (Casagli et al., 2017).

Forest stands, as rock fall influencing factors, must be considered separately for the release, transit and deposit zones. In the release areas forest might cause an increase of rock fall activity due to wedge effects of the roots, snow or wind effect on stem movement (Jaboyedoff et al., 2005, Jaboyedoff and Serron, 2005) (Figure 17). For the transit and the deposit zone forest stands decrease the runout of bouncing, falling and sliding rocks, if forest stands are at least >250 m long with no gaps of >40 m (Lingua et al., 2020).

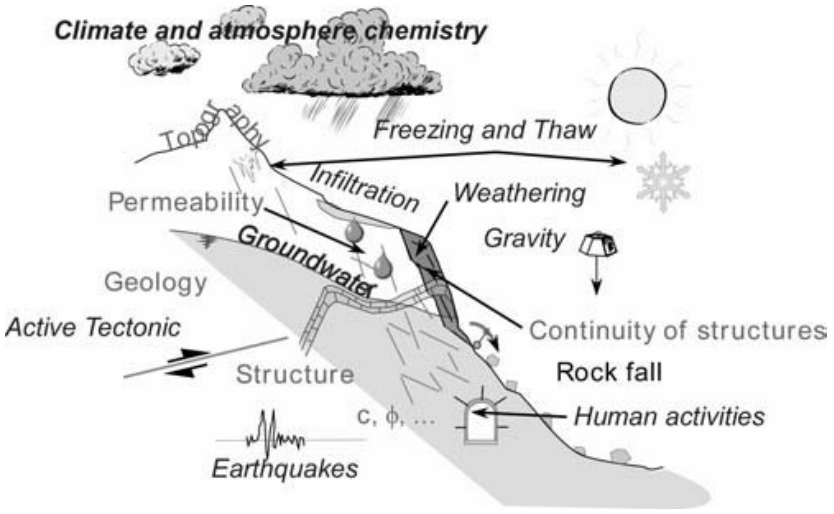

Figure 17 Concept of internal conditioning factors and external parameters that cause rock falls (Jaboyedoff and Serron, 2005)

Climate change and rock fall: Research has widely shown how gravitational hazards in mountains can be amplified in extreme weather situations (Gobiet et al., 2014; EEA1/2017, 2017). **For a comprehensive rock fall hazard assessment we need to consider the 1. Release probability, 2. Reach probability and 3. Rock fall intensity.** Climate change affects only the release probability of rock fall in the release area by e.g. influencing pore water pressures in the joint systems of the rock. Reach probability and rock fall intensity are determined by the process itself. Systematic statistical studies indicate that rock fall frequencies increase during periods of heavy rainfalls or snow melt (Sandersen et al., 1997; Delonca et al., 2014). The hydrostatic pore water pressure in the rock mass is decisively responsible for the trigger of bigger rock fall events and rock avalanches (Krähenbühl, 2004; Perret et al., 2006). Rainfall and snowmelt recharges groundwater, which increases slope damage driving it towards failure (Picarelli, 2016).

Periglacial processes (permafrost) is developed when mean temperatures in two or more years are below 0°C. In Austria, permafrost occurs usually above 2500 m (Ebohon and Schrott, 2008). During the summer months the surface or active layer of the permafrost melts and the thawing and refreezing processes exert stress on the rock masses. The longest possible duration of temperatures in the so-called frost cracking window between -3 and -8°C is considered to be particularly effective for the release of blocks (Krautblatter et al., 2013). Furthermore, a frozen discontinuity has a higher shear strength than the same joint without ice (Davies et al., 2001) .

Last but not least temperature change might influence rock fall activity also directly. In sun-exposed slopes, the temperatures in the rock and on the surface of the rock can exceed the air temperatures substantially. Especially in winter, sun-exposed rock walls can be subject to high-magnitude temperature changes that cause thermal stress on the rock (Hall and Andre, 2001). High-magnitude temperature variations have been shown to cause irreversible displacements causing cracking in discontinuities (Mulas et al., 2019).

Though climate parameters have a strong effect on the rock fall triggering probability, rock fall hazard depends on internal (disposition) and external factors that determine the probability of rock to release and to reach downward slope locations (Figure 17):

1. Release probability - The rock fall release area can be assessed with a rock slope stability analysis that takes into account: Geological Strength Index (GSI) as a rock quality rating system (or alternative methods), slope morphology (exposure, relief, slope angle, slope height, roughness etc.), bedrock types (lithologies), fracturing (joint sets, spacing, lengths), mechanical properties of the rock (friction angle, cohesion), frequency, structures, weathering, erosion, seismicity, microclimate and hydrogeology (Volkwein et al. 2011). In general, potential release areas have a mean slope inclination of >45° with a range between 32° and 50° depending on all the other parameters mentioned above (Gsteiger, 1993; Mölk and Rieder, 2017; ONR, 2017) (Figure 17).
2. Reach probability – is the probability that falling, bouncing rocks reach certain locations in their trajectories on the slope (Volkwein et al., 2011). Reach probability in the transit zone is given by the rock fall velocity, the slope angle, the rebound heights and the size of boulders and their mass. Rock fall velocities for big rock avalanches (Bergsturz, >1 Mio m^3) with a certain volume can reach up to 50 m/s, for rock fall and rock slides a maximum velocity of up to 40 m/s is possible (Dorren et al., 2007). Rock fall velocities on non-forested slopes range between 5 and 30 m/s (Dorren et al., 2005; Glover et al., 2012). α-angles of

rock fall trajectories where boulders still can bounce and roll and slide are given within a range between 51.2° and 28.5° with an approximate mean given in several publications of 32° (Toppe, 1987; Jaboyedoff et al., 2005; Colas et al., 2018). If the slope angle reaches about 25° blocks come to a halt (Dorren, 2008; Lingua et al., 2020). In experiments it has been shown that boulders with a length of 0.23-1.7 m can bounce with length of 2.2-33.6 m and a bounce height of 0.3-4.2 m (Rickli et al., 2004).

3. Rock fall intensity – is given by the runout length or α-angle, and the kinematic energy (Evans and Hungr, 1993). Kinematic energy (kJ) can be used to describe the impact of rocks hitting forest or infrastructure [E_{kin} [kJ] = (mass [kg] x velocity [m/s]^2 / 2) : 1000]. In experiments the impact energy of free falling rocks of sizes 800-4000 kg result in 20-600 kJ, rocks with 10000 kg can reach 3000 kJ (Rickli et al., 2004; Gerber, 2008; Volkwein et al., 2011).

The quantification of frequency is important for hazard assessment and dependent on statistical analysis of existing inventories of rock fall events. Existing inventories of rock fall events in Alpine countries are inhomogeneous, partly very incomplete or even non-existent and are handled differently from country to country (Volkwein et al., 2011). As frequency values are often unreliable, incomplete or not available at all, hazard assessment is done with heuristic ranking of selected instability indicators, deterministic or statistic methods (Poisel, 2017). The frequency of rock fall events in combination with their intensity define the hazard magnitude and thus the potential interaction with forests. Gaps in historical records can be accounted for with systematic studies of past climate change and rock fall events. Studies using geochronological methods such as dendrochronology, radiocarbon and cosmogenic nuclide dating have shown that rock slope failures since deglaciation occurred due to climatic triggering in addition to seismic activity (Hormes et al., 2008; Prager et al., 2008; Böhme et al., 2019). Since 2019 the Geological Survey of Austria systematically collects rock fall events in Austria and a clear dependence of rockfalls on intensive rain periods and snowmelt is reflected in this data set.

Forest cover changes and rock fall: Mountain forests with high basal area and high stem densities have been identified as a particularly effective measure against longer runout of rock fall by reducing kinematic energy and velocities of falling and bouncing blocks in the transit zone (e.g. Dorren and Berger 2006, Moos et al. 2017).

In order to assess the impact of future forest cover changes on rock fall probability we need to clearly differentiate the impact of trees on 1) the release areas, and 2) the transit zones until rock fall comes to a stop in the deposit zones, as forest cover changes in these two different areas imply a different impact.

In the release area trees can have a negative effect and result in an increase of rock fall probability with root pressure in joints and increased weathering effects (Jahn, 1988; Gerber, 2008). Also snow breakage and windthrow of trees in release areas might increase the rockfall frequency and therefore in instable areas forest has no protective effect or rather increase the rock fall probability (Jaboyedoff and Serron, 2005). It has been suggested to remove unstable trees in the top of release areas (Frehner et al., 2007). An efficient forest management needs to document the the development of tree growth also in higher altitudes, in order to act accordingly and remove trees on top of potential release areas with a slope inclination >45°.

The main protective effect of forest is cut down to the transit and deposit zone fo rock fall. Single trees might dissipate energy of a rockfall impact by local penetration of the rock into the tree stem,

deformation of the stem, rotation or translation of the root or rebound of the rock (Dorren et al., 2007). In real size rock experiments a Norway spruce tree absorbed 230 kJ rock impacts. In the transit and deposit zone rock velocity can be reduced by about 26% on forested slopes and rebound height of blocks was reduced by 33% (Dorren et al., 2005). This value translates to a reduction of the α-angle on forested slopes of about 6° (Oswald, 2020).

The simulation study from Moos et al. (2017) also indicates that rockfall intensity is reduced between 10 to 70% on forested slopes and rock fall frequency is reduced by 10 to 90%. A forest stand might be destroyed by a rock mass of approximately 10000 kg with a velocity of 20 m/s (Rickli et al., 2004). Therefore, forests offer protective effects against rock slides and rock fall up to a certain magnitude, while large magnitude rock fall events cannot be stopped (Jahn, 1988).

In a few studies the composition of forest has been investigated in order to quantify the highest protective effect against rock fall events: broadleaves-dominated forest with species that tolerate shade such as silver fir (*Albies alba*), European beech and Norway spruce, that reach higher stem densities and high basal areas have been proven to be very effective (Dupire et al., 2016) (Figure 18).

A forest that shows the highest effectiveness against rockfall is characterized by a high stem density, tall trees and strong hard wood trees. The high stem density increases energy dissipation of blocks and reduces velocity. Hard wood tree species can absorb a higher kinetic energy and are therefore more effective against large block volumes, and tall trees are advantageous for high jumping heights (Dorren et al., 2005; Berger and Dorren, 2006; Scheidl et al., in review) (Figure 18).

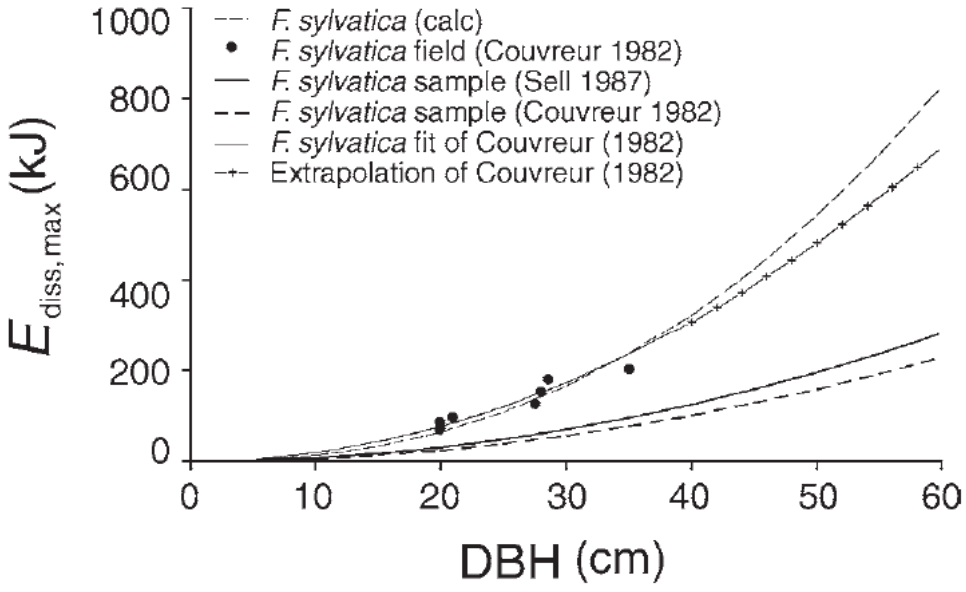

Figure 18 Energy dissipation (y-axis) during rockfall impact by broad-leaved and coniferous species indicates the importance of diameter at breast height (dbh) from field experiments (Dorren and Berger, 2006)

According to the FC modelling results an increase in stem volume and stem density/ha for each PAR can be expected if not counteracted by forest management. This would translate to an

improved effect of the forest against rockfall. In a recent publication, few main forest structure parameters are summarized as important for the reduction of runout length (Frehner et al., 2007; Lingua et al., 2020):

- dbh > 0.30 m
- Minimum forest length along the transit of > 250 m without gaps of > 40 m
- Rock fall reduction due to forest effect is mainly evident on slope inclinations between 30 and 25°
- > 350 stems/ha of trees with stem diameter at breast height (DBH) > 20 cm
- Conifers with a height (h) and diameter ratio h/dbh =< 65, Broadleaves with h/dbh =< 80

The optimal forest stand to withstand anticipated rockfall hazard in the Alpine Space is coppice forest with shrubs, high stand density and lower average tree height reducing the rockfall hazard by 20% (Scheidl et al., in review).

CC and FC in the PARs: The pure effect of CC will lead to an increase in rock fall in the release areas, especially in the PARs Vals/Gries, Oberammergau, Southern Wipptal and Kranjska Gora. In all PARs summer temperatures will increase and will cause higher thermal stress on sun-exposed rocks (Mulas et al., 2019), most likely causing an increase in irreversible displacements in discontinuities. In Val Ferret, Vals/Gries, Kranjska Gora and Southern Wipptal some potential release areas are situated in periglacial areas and higher temperatures will cause more permafrost to melt and cause higher instability in discontinuities that are now still filled with permafrost ice (Krautblatter et al., 2013; Draebing et al., 2017).

The projected higher temperatures are likely to result in increased disappearance of local glaciers and result in cascading rock slope failure effects such as the stress release due to glacier melting along valley sides, changes in slope hydrology and glacial rebound (Porter and Orombelli, 1981).

Winter precipitation is anticipated to slightly increase in all PARs and as temperatures are predicted to increase more precipitation will fall as rainfall. Especially in Vals/Gries, Oberammergau and Kranjska Gora also the extreme precipitation days may increase with 99th percentile almost two times as at present. If this materializes, an increase in rockfall frequency and magnitude is likely (Casagli et al., 2017).

In Val Ferret and in Kranjska Gora summer precipitation is projected to slightly decrease according to the downscaled simulations of this study. However, extreme precipitation in Kranjska Gora will increase and we still might predict a slight increase in rock fall activity during summer months in Kranjska Gora. In Val Ferret the rockfall activity during the summer months might just continue with similar frequency and magnitude as during the reference period. Though, as an increase in rockfall activity in all PARs is very likely, higher temperature might result in denser mixed forests with higher % of broadleaves. This tendency due to climate change should be supported with forest management in the transit zones in order to meet the challenges of increased rockfall activity.

3.3.3 Landslide scenarios

This section focuses on landslides of the slide-type movement (Cruden and Varnes, 1996; Hungr et al., 2013), which are well-known to be influenced by both, climatic changes (Crozier, 2010; Gariano and Guzzetti, 2016) and variations in forest cover and structure (Goetz et al., 2015; Schmaltz et al., 2019, 2017). Since global warming is frequently expected to lead to an increased occurrence of severe precipitation (e.g. Fowler and Hennessy, 1995), it is not surprising that an increase of rainfall-induced landslide activity represents a commonly expected impact of climate change (Crozier, 2010). Forest and land cover changes, which can be induced by climatic alterations, also have an impact on landslide processes, mainly because of the associated modifications in the hydrological (e.g. evapotranspiration, water extraction from soil via roots) and geomechanical effects on slope stability (e.g. root cohesion) (Marston, 2010; Papathoma-Köhle and Glade, 2013; Sidle and Ochiai, 2006).

Climate change and landslides: Scientific literature highlights that the topic of "landsliding and climate change" has increasingly been tackled since the release of the first Intergovernmental Panel on Climate Change (IPCC) report in 1990 (Figure 19).

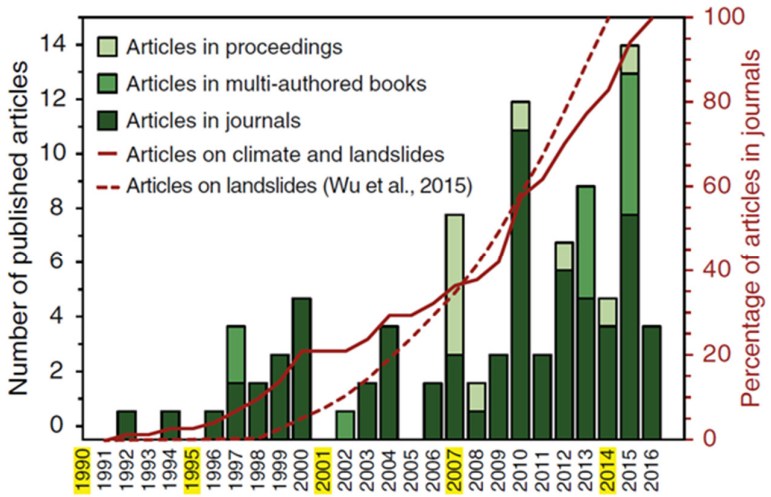

Figure 19 Number (bars) and percentage (solid line) of published scientific articles on climate and landslides between 1990 and 2016. Note that the release years of IPCC reports are highlighted in yellow (figure taken from Gariano and Guzzetti, 2016)

Despite the many published studies focusing on the topic of "landslides and climate" and albeit the warming of the global climate system is unequivocal, the specific effects of projected climate alterations on future landsliding is still under debate. Up to now, it is uncertain how the comparably well recognizable rising temperature trends (cf. section 3.1) and the more challenging to evaluate future precipitation patterns will affect the spatial and temporal distribution of upcoming slope instabilities or landslide magnitude-frequency relationships. Research that focused on the potential effects of changing precipitation and/or temperature patterns on specific landslide controlling factors, such as soil and rock weathering, hydromechanical pressure in discontinuities, snow melting, permafrost degradation and vegetation patterns, represents an important step towards a

more comprehensive understanding of the influence of climate change on landslide activity (Coe and Godt, 2012; Crozier, 2010; Sidle and Ochiai, 2006).

However, the elaboration of reliable statements for a defined area and period (e.g. "*climate change will induce a x-% increase in landslide frequency until 2050*") is anything than trivial, due to the manifold and complex interrelations between landslide controls, data limitations, complex scale (in)dependencies (e.g. climatic and landslide variables act on partially diverse scales), confounding effects (i.e. several landslide controls may change simultaneously; e.g. anthropogenic vs. climate influence) and the inherent uncertainties in climate projections, especially on extreme triggering events (Coe and Godt, 2012; Crozier, 2010; Gariano and Guzzetti, 2016; Stoffel et al., 2014; Stoffel and Huggel, 2012). The complexity involved might be a major reason why generally valid statements (e.g. "in places where rising temperatures will increase the frequency of heavy precipitation events, an initial rising number of landslides can be expected", "rising temperatures contribute to permafrost degradation and therefore to slope instability in high altitudes") become rarely tangible for an implementation into local risk reduction strategies. The following table (Table 4) summarizes the potential effects of climate change on slope stability.

Table 4 Potential climate change effects (first column), processes and conditions affected (second column) and potential slope stability responses (third column) (adapted from Crozier, 2010).

Climate change effects	Processes and conditions affected	Potential slope stability response
Increasing precipitation totals	Wetter antecedent conditions	▪ Less rainfall required to achieve critical water content ▪ Reduction in cohesion ▪ Reduction in soil capillary suction ▪ Softened layers may act as lubricants ▪ Higher water tables and reduction in shear strength ▪ Increase in the probability to reach critical pore pressures
	Increased weight (surcharge)	▪ Increased bulk density, leading to decrease in shear strength/stress ratio in cohesive material
	Higher water tables for longer periods	▪ More frequent attainment of critical water content during rainfall events
	Increased lubrication of contact surfaces between certain minerals	▪ Reduction in friction (certain minerals e.g. micas)
	Increase in river discharge	▪ Increase bank scour and removal of lateral and basal support from slopes

		▪ Higher lake levels, increase in bordering slope water tables
Increase in rainfall intensity	Infiltration more likely to exceed subsurface drainage rates and rapid build-up of perched water tables	▪ Landslide triggering by reduction in effective normal stress leading to reduction in shear strength ▪ Increase in cleft water pressures
	Increased throughflow	▪ Increase in seepage and drag forces, particle detachment and piping. ▪ Piping removes underlying structural support. Enhances drainage unless blockage occurs
Shift in rain bearing weather systems (e.g. cyclone tracks)	Areas previously unaffected, subject to high rainfall (and vice versa)	▪ Rapid adjustment of slopes to new climate regime (e.g. via increased/decreased landslide activity)
Increased variability in precipitation and temperature	More frequent wetting and drying cycles	▪ Increase fissuring, widening of joint systems ▪ Reduction in cohesion and rock mass joint friction
Increased temperature	Reduction in antecedent water conditions through evapotranspiration	▪ Lower antecedent water status—more rain required to trigger slides
	Reduction in interstitial ice and permafrost	▪ Reduction in cohesion in slope materials (e.g. debris and soil)
	Rapid snow melt—runoff and infiltration	▪ Build-up of porewater pressure and strength reduction
	Reduction in glacier volume	▪ Removal of lateral support to valley side slopes
Increased wind speed and duration	Enhanced evapotranspiration	▪ Reduction of soil moisture ▪ Enhanced drying and cracking

Forest/Land cover changes and landslides: Land cover changes, and particularly those associated with changes in forest cover and forest structure, are known to affect slope stability and the occurrence of landslide phenomena to a large extent (Glade, 2003; Malek et al., 2015; Reichenbach et al., 2014). Potential stabilizing hydrological and geomechanical effects of trees are commonly highlighted in the context of shallow landslide phenomena (Crozier, 1989; Marston,

2010; Montgomery et al., 2000; Papathoma-Köhle and Glade, 2013; Rickli and Graf, 2009; Schmaltz et al., 2019, 2017; Sidle and Ochiai, 2006). Multiple effects of forests on slope stability can be highlighted (Table 5).

Table 5 Relative influence of woody vegetation on slope stability (modified after Marston, 2010; based on Sidle and Ochiai, 2006) which can be used to deduce some influences of forest cover changes (e.g. deforestation or afforestation) on shallow landslide activity: ++ beneficial effect on stability, + marginally beneficial effect, - marginally adverse effect, - - adverse effect

Mechanism of wood vegetation		Influence on landslides
Hydrological effects	Interception of rainfall and snow by canopies, thus promoting evaporation and reducing water available for infiltration	++
	Root systems extract water from the soil leading to lower soil moisture levels	++
	Roots, stems, and organic litter increase ground surface roughness and soil infiltration capacities	-
	Depletion of soil moisture may cause desiccation cracks, resulting in higher infiltration capacity and short-circuiting of infiltrating water to deeper sliding surfaces	-
Mechanical effects	Individual strong woody roots anchor the soil mantle into the more stable substrate	++
	Strong roots tie across planes of weakness along the flanks of potential landslides	++
	Roots provide a membrane of reinforcement to the soil mantle, increasing shear strength	++
	Roots of woody vegetation anchor in firm strata providing support the upslope area through buttressing and arching	++
	Weight of trees increase the normal and downhill forces	+ -
	Wind transmits dynamic forces to the soil mantel via the tree bole	- -

For instance, woody vegetation intercepts rainfall and fosters evapotranspiration. The roots of trees can extract water from the soil and enhance shear strength. These processes clearly increase the stability of a slope. On the other hand, dependent on the position of the trees on the slope, tree weight can add to the normal and downhill forces resulting in decreased slope stability. The soil structure can be disturbed by dead roots leading to an increased water percolation under forest and a higher infiltration capacity that diminishes overall slope stability. In some cases, the destabilizing effects of forest may even offset stabilizing effects like root cohesion (Crozier, 2010; Marston, 2010; Papathoma-Köhle and Glade, 2013; Stangl et al., 2009). However, particularly for shallow landslides located on gently inclined slopes, woody vegetation is usually considered to stabilize a hillslope. Changes in the general land cover from forests to non-forests are often associated with an increased shallow landslide activity (Goetz et al., 2015; Reichenbach et al., 2014; Schmaltz et al., 2019; Sidle and Ochiai, 2006). In this context, also potential lag times have to be taken into account, such as the tree-species dependent time span before the roots of newly planted trees stabilizes the soil or the time span before the roots of logged trees lose their strength (Sidle and Ochiai, 2006).

CC and FC in the PARs: The elaborated climate change scenarios (see section 3.1) revealed that all PARs will experience increasing temperatures in the future, particularly when considering long-term developments and the "business as usual" emission scenario (RCP8.5). An interpretation of the projected temperature trends might lead to the conclusion that more precipitation might be required on vegetated slopes in order to reach critical landslide conditions, because a rise in temperature increases evapotranspiration and reduces antecedent soil moisture conditions (Comegna et al., 2013; Crozier, 2010; Gariano and Guzzetti, 2016). However, temperature increase is also expected to modify properties of the water cycle and sediment availability, which in turn can increase landslide activity. For instance, the projected warmer climate is likely to foster rapid snowmelt that enhances surface runoff, water infiltration and the subsequent build-up of critical pore water pressures. It is likely that rising temperatures will cause more common rain-on-snow events in the PARs that can lead to an increased frequency of critical soil moisture and slope instability conditions (Gariano and Guzzetti, 2016).

The projected temperature trends might especially be of relevance for areas surrounded by high altitude glacial and/or periglacial areas in the PARs Vals/Gries (altitude up to 3,100 m. a.s.l), Wipptal South (up to 3,500 m. a.s.l.), Val Ferret (up to 4,200 m. a.s.l.) and Kranjska Gora (up to 2,860 m a.s.l.). In those high Alpine areas, projected reduction in snowpack and duration will likely influence landslide activity and the seasonality of landslide events (Stoffel et al., 2014). The temperature driven reduction in interstitial ice and permafrost degradation can increase the availability of sediments while simultaneously reducing shear strength in soils and rocks. Permafrost degradation is of particular relevance for rock fall processes, but does also influence landslides of the slide-type movement. It is expected that PAR areas currently underlain by permafrost will become less stable at progressively higher elevations due to the ongoing rising temperatures (Stoffel and Huggel, 2012).

High altitude slopes that are laterally stabilized by glacier ice will loose their support due to a further ongoing glacier retreat (Stoffel and Huggel, 2012). Additionally, climate warming will further decrease the hydrological "buffering function" of glaciers (i.e. glaciers buffer extreme

meteorological conditions) and lead to changes in the water regime that co-determine slope stability (Crozier, 2010).

The elaborated precipitation scenarios - which have to be interpreted with caution (see section 3.1) - indicate a trend of slightly wetter conditions in the PARs. This trend was observed to be more pronounced for future autumn and winter seasons. The projected increasing precipitation totals are expected to rather affect deep seated slope movements, as a consequence of their dependency on long duration precipitation trends (e.g. seasonal precipitation) and associated ground water conditions (Crozier, 2010; Sidle and Ochiai, 2006). A tendency of higher water tables as a consequence of an increasing amount of precipitation may contribute to decreasing shear strength, soil suction and cohesion in soil material and an increasing loading (i.e. weight of water) (Gariano and Guzzetti, 2016; Sidle and Ochiai, 2006). In contrast to deep seated landslides, the occurrence of shallow first-time landslides is known to be controlled by rainfall peaks (i.e. intense and short duration events) (Crozier, 2010; Gariano and Guzzetti, 2016; Sidle and Ochiai, 2006). The analysis of the selected climate model data (see section 3.1 and D.T1.1.6) indicated that the return time of extreme precipitation events might decrease in the PARs Kranjska Gora, Vals/Gries, Oberammergau and Wipptal South, in the likely case that greenhouse gas concentrations continue to rise (RCP8.5). Thus, there is "*high confidence that changes in heavy precipitation will affect landslides*" (IPCC special report as cited in Gariano and Guzzetti, 2016) while an increasing frequency of extreme rainfall might go hand in hand with a growing shallow landslide activity (Stoffel et al., 2014). Critical shallow landslide conditions are likely to be reached more frequently in the future in case the elaborated higher frequency of extreme rainfall events actually materializes in the PARs.

The projected temperature increase in the PARs has the potential to induce more abundant vegetation at higher altitudes which may partly offset previously described destabilizing climate effects (Crozier, 2010; Stoffel and Huggel, 2012). The elaboration of the "pure" climate effect on forest growth suggests an increase in forest within the PARs when neglecting changes in the forest management practice. Denser (woody) vegetation in an area, also because of rising temperatures, goes hand in hand with an increased interception and evaporation, a reduction of water infiltration and an increase in geomechanical stabilizing effects (i.e. root cohesion) (Glade, 2003; Sidle and Ochiai, 2006). How land use and agricultural and forestry practices will change in response to the projected warming is considered crucial for future landslide activities (Gariano and Guzzetti, 2016). Climate change is likely to be accompanied by an adaptation of vegetation species and changes in vegetation management practices, both with potential implications on slope stability (see Table x) (Sidle and Bogaard, 2016). In should be noted that in cases where humans influence a landscape to a large extent, such as in the PARs, the relative effect of climate change on landslide activity and the frequency of landslide occurrence becomes less important (Gariano and Guzzetti, 2016). Finally, it is emphasized that the establishment of links from projected climate changes in the PARs to alterations in vegetation/forest patterns and finally to the expected natural hazard situation is partly hampered by challenging to grasp feedback loops and complex process interactions (Sidle and Ochiai, 2006). For instance, an increasing amount of precipitation may facilitate slope instability due to associated hydrological effects. However, increasing precipitation totals may simultaneously enhance the growth of vegetation species that increase slope stability (Sidle and Ochiai, 2006).

4 Discussion

The analyses presented in this report mainly focused on potential effects of climate change on forests and gravity-driven natural hazards in Alpine terrain. Mountain geosystems, such as the Alps, commonly exhibit a higher susceptibility to dynamic stressors (e.g. changes in temperature or land cover) than many others landscapes and are particularly prone to climate induced changes. Climate warming has already caused a variety of impacts on the mountain environments and is expected to further influence social and natural systems in the future (Beniston, 2003; Schneiderbauer et al., 2013; Slaymaker et al., 2009; Terzi et al., 2019). Well-known consequences of rising temperatures, such as permafrost degradation, increase of extreme precipitation events, glacier retreat and associated changes in the water cycle and sediment transport, have recently gained increasing attention not only by scientists, but also by decision makers and local people (Einhorn et al., 2015; Keiler et al., 2010).

During the last decade, an increasing number of scientists and institutions highlighted the demand to account for changing environmental conditions in natural hazard modelling. However, insufficient data support, complex process interactions and associated uncertainties might be major reasons why an explicit consideration of climate change and/or forest change scenarios is still rare when assessing areas susceptible to gravity-driven hazards, critical threshold conditions (e.g. for early warning), or when estimating future environmental hazards and risks (Gallina et al., 2016; Gariano and Guzzetti, 2016; Reichenbach et al., 2014; Beniston et al., 2018; Schmaltz et al., 2019). In general, observed and projected climate changes are expected to alter many environmental variables (see e.g. IPCC, 2014) that will in turn influence the frequency, magnitude and location of gravity-driven natural hazards, such as landslides, rock falls, debris flows and avalanches (Einhorn et al., 2015; Gallina et al., 2016; Keiler et al., 2010; Rubel et al., 2017). Keiler and Fuchs (2016) highlight that an increasing activity of several natural hazards can be expected for the Alpine Space. Considering also growing population pressures and strong changes in the exposure of elements at risk, it is anticipated that negative natural hazard impacts (e.g. damage to infrastructure) will become more prevalent and economically damaging in the future (Keiler and Fuchs, 2016; Slaymaker et al., 2009). However, reliable site-specific elaborations of how projected climate fluctuations may influence the response of specific hillslopes and the associated natural hazard or risk situation are not yet available (Alvioli et al., 2018).

The findings related to this report provide quantitative evidence that the PARs will experience a further rise in (mean) temperatures in the future with several implications for forests (see section 3.2) and natural hazard processes (see section 3.3). In analogy to other climate change studies focusing on Alpine terrain, the conducted analyses did not reveal straightforward and certain precipitation trends (i.e. increasing or decreasing amount of precipitation). However, an increase in the frequency of heavy precipitation events represents a commonly expected consequence of climate warming, since increasing temperatures are known to enhance (saturation specific) humidity and thus also the potential to increase precipitation intensities. However, researchers frequently highlight that the development of reliable local extreme precipitation scenarios for mountain terrain is riddled by uncertainties and subject to considerable spatial and temporal variability (Brönnimann et al., 2018; Einhorn et al., 2015; Isotta et al., 2014).

It is emphasized that the impacts of climate change on mountain environments are sometimes co-determined and in other cases even driven by human impact and socio-economic developments. Deciphering the "real" contribution of climate warming on forest development and natural hazards can represent a ticklish problem, especially in intensively managed areas. From a short-term perspective, it is fair to assume that the influence of human activities on natural hazards and their controlling factors (e.g. land use changes) might regularly exceed the impact of climate change in the Alpine Space (Goudie, 2013; Slaymaker et al., 2009). We underline that an increasing frequency of documented natural hazard events should not be automatically attributed to climate change alone. Alterations in land management practices (e.g. changing land use practices and/or forest management), changes in the documentation of hazard events (e.g. more complete documentation of recent events, increasing number of studies) and changes in the exposure or vulnerability of elements at risk (e.g. denser infrastructure) are likely to contribute to an increasing number of registered natural hazard events (Guzzetti et al., 2012; Steger et al., 2017; Wood et al., 2015). In order to understand potential upcoming losses and risks due to mountain natural hazards, it is vital to additionally consider the spatio-temporal development in exposure and vulnerability (Keiler and Fuchs, 2016). In this context, widespread mono-disciplinary Natural Science research (e.g. on climate change and its impact) should be complemented by Social Science perspectives in order to account for both, "natural" changes (e.g. climate and vegetation changes) and socio-economic developments (e.g. changes in exposure and vulnerability) (Goudie, 2013; Keiler and Fuchs, 2016; Slaymaker et al., 2009; Sperotto et al., 2017).

In a nutshell, the conducted analysis and the literature reviews indicate that the following changes can be expected in the upcoming decades in the PARs:

Climate change: A considerable increase in mean temperatures can be expected. In most PARs, a trend of increasing mean precipitation and an increasing frequency of intense precipitation might materialize (however, high uncertainty in the models).

Forest change: The "direct" effect of climate change on forest growth and structure is expected to be less relevant than the actual implementation of forest management strategies and the manifestation of climate-affected biotic stressors (pests, pathogens).

Natural hazard change: The impact of projected climate and forest changes on gravity-driven natural hazards are manifold (e.g. changes in water cycle, vegetation effects, feedback loops) and no generic conclusion can be drawn (see section 3.3). Changes in the exposure and vulnerability of elements at risks (e.g. people, infrastructure) and the influence of humans on process controlling factors (e.g. vegetation via land management) are expected to exceed the "pure" impact of climate on the natural hazard risk situation. This also implies that damage caused by future natural hazards is not at the mercy of (locally) difficult to influence climatic patterns but can be guided by actions and decisions at PAR level. In this context, forest management and spatial planning will play a major role.

5 References

Alvioli, M., Melillo, M., Guzzetti, F., Rossi, M., Palazzi, E., von Hardenberg, J., Brunetti, M.T., Peruccacci, S., 2018. Implications of climate change on landslide hazard in Central Italy. Science of The Total Environment 630, 1528–1543. https://doi.org/10.1016/j.scitotenv.2018.02.315

Ancey, C., Bain, V., 2015. Dynamics of glide avalanches and snow gliding. Rev., Geophys. 53, 745–784.

Anderson, G., McClung, D., 2012. Snow avalanche penetration into mature forest from timber-harvested terrain. Canadian Geotechnical Journal 49(4), 477-484.

Barbeito, I., Dawes, M., Rixen, C., Senn, J., Bebi, P., 2012. Factors driving survival and growth at treeline: a 30-year experiment of 92,000 trees. Ecology 93, 389-401.

Bartelt, P., Bühler, Y., Buser, O., Christen, M., Meier, L., 2012. Modeling mass-dependent flow regime transitions to predict the stopping and depositional behavior of snow avalanches. J. Geophys. Res., 117, F01015. https://doi.org/10.1029/2010JF001957.

Bartelt, P., Stöckli, V., 2001. The influence of tree and branch fracture, overturning and debris entrainment on snow avalanche flow. Annals of Glaciology 32, 209-216.

Bebi, P., Kulakowski, D., Rixen, C., 2009. Snow avalanche disturbances in forest ecosystems—State of research and implications for management. For. Ecol. Manage. 257, 1883–1892. https://doi.org/10.1016/j.foreco.2009.01.050.

Bebi, P., Seidl, R., Motta, R., Fuhr, M., Firm, D., Krumm, F., Conedera, M., Ginzler, C., Wohlgemuth, T., Kulakowski, D., 2017. Changes of forest cover and disturbance regimes in the mountain forests of the Alps. For. Ecol. Manage. 388, 43–56. https://doi.org/10.1016/j.foreco.2016.10.028.

Bebi, P., Teich, M., Schwaab, J., Krumm, F., Walz, A., Gret-Regamey, A., 2012. Entwicklung und Leistungen von Schutzwäldern unter dem Einfluss des Klimawandels. Schlussbericht im Rahmen des Forschungsprogramms „Wald und Klimawandel“. Eidg. Forschungsanstalt für Wald, Schnee und Landschaft WSL, Bern, Bundesamt für Umwelt.

Bellaire, S., Jamieson, B., Thumlert, S., Goodrich, J., Statham, G., 2016. Analysis of long-term weather, snow and avalanche data at Glacier National Park, BC, Canada. Cold Regions Science and Technology 121, 118-125.

Beniston, M., 2003. Climatic change in mountain regions: a review of possible impacts. Climatic Change 59, 5–31.

Beniston, M., Farinotti, D., Stoffel, M., Andreassen, L.M., Coppola, E., Eckert, N., Fantini, A., Giacona, F., Hauck, C., Huss, M., Huwald, H., Lehning, M., López-Moreno, J.-I, Magnusson, J., Marty, C., Morán-Tejéda, E., Morin, S., Naaim, M., Provenzale, A., Rabatel, A., Six, D., Stötter, J., Strasser, U., Terzago, S., Vincent, C., 2018. The European mountain cryosphere: a review of its current state, trends, and future challenges. Cryosphere 12(2), 759-794.

Berger, F., Dorren, L., 2006. Objective Comparison of Rockfall Models using Real Size Experimental Data. Disaster Mitigation of Debris Flows, Slope Failures and Landslides, 245-252.

Berger, F., Dorren, L., Kleemayr, K., Maier, B., Planinsek, S., Bigot, C., Bourrier, F., Jancke, O., Toe, D., Cerbu, G., 2013. Eco-Engineering and Protection Forests Against Rockfalls and Snow Avalanches. Management Strategies to Adapt Alpine Space Forests to Climate Change Risks. https://doi.org/10.5772/56275

Blanchet, J., Marty, C., Lehning, M., 2009. Extreme value statistics of snowfall in the Swiss Alpine region. Water Resour. Res. 45, 1–12. https://doi.org/10.1029/2009WR007916.

Böhme, M., Hermanns, R., Gosse, J., Hilger, P., Eiken, T., Lauknes, T., Dehls, J., 2019. Comparison of monitoring data with paleo–slip rates: Cosmogenic nuclide dating detects acceleration of a rockslide. Geology, 47(4), 339-342.

Brang, P., 2001. Resistance and elasticity: promising concepts for the management of protection forests in the European Alps. For. Ecol. Manage. 145, 107–119. https://doi.org/10.1016/S0378-1127(00)00578-8.

Brönnimann, S., Rajczak, J., Fischer, E.M., Raible, C.C., Rohrer, M., Schär, C., 2018. Changing seasonality of moderate and extreme precipitation events in the Alps. Natural Hazards and Earth System Sciences 18, 2047–2056. https://doi.org/10.5194/nhess-18-2047-2018

Casagli, N., Guzzetti, F., Jaboyedoff, M., Nadim, F., Petley, D., 2017. Hydrological Risk: Landslide. In: K. Poljanšek, M. Marin Ferrer, T. De Groeve, I. Clark (Eds.), Science for disaster risk management 2017: knowing better and losing less. . Disaster Risk Management Knowledge Centre, Publications Office of the European Union, Luxembourg, pp. 209-218.

Castebrunet, H., Eckert, N., Giraud, G., 2012. Snow and weather climatic control on snow avalanche occurrence fluctuations over 50 yr in the French Alps. Clim Past 8, 855–875. doi:10.5194/cp-8-855-2012.

Castebrunet, H., Eckert, N., Giraud, G., Durand, Y., Morin, S., 2014. Projected changes of snow conditions and avalanche activity in a warming climate: a case study in the French Alps over the 2020–2050 and 2070–2100 periods. Cryosph Discuss 8, 581–640. doi:10.5194/tcd-8-581-2014.

Coe, J.A., Godt, J.W., 2012. Review of approaches for assessing the impact of climate change on landslide hazards. Presented at the Landslides and Engineered Slopes: Protecting Society through Improved Understanding - Proceedings of the 11th International and 2nd North American Symposium on Landslides and Engineered Slopes, 2012, pp. 371–377.

Colas, B., Berger, F., Toe, D., 2018. Run-out of rockfall: towards objective assistance in determining the angles of the energy line method., 4th Rock Slope Stability Symposium, Chambery.

Comegna, L., Picarelli, L., Bucchignani, E., Mercogliano, P., 2013. Potential effects of incoming climate changes on the behaviour of slow active landslides in clay. Landslides 10, 373–391. https://doi.org/10.1007/s10346-012-0339-3

Conway, H., & Raymond, C. F. (1993). Snow stability during rain. Journal of Glaciology, 39(133), 635-642.

Corona, C., Lopez Saez, J., Stoffel, M., Bonnefoy, M., Richard, D., Astrade, L., Berger, F., 2012. How much of the real avalanche activity can be captured with tree rings? An evaluation of classic dendrogeomorphic approaches and comparison with historical archives. Cold Regions Science and Technology 74, 31-42. doi:10.1016/j.coldregions.2012.01.003.

Crozier, M.J., 1989. Landslides: causes, consequences & environment. Routledge, London; New York.

Crozier, M.J., 2010. Deciphering the effect of climate change on landslide activity: A review. Geomorphology 124, 260–267. https://doi.org/10.1016/j.geomorph.2010.04.009

Cruden, D.M., Varnes, D.J., 1996. Landslide Types and Processes, TRB Special Report. National Academy Press, Washington.

Cutter, S.L., 1996. Vulnerability to environmental hazards. Progress in Human Geography 20, 529–539. https://doi.org/10.1177/030913259602000407

Davies, M., Hamza, O., Harris, C., 2001. The effect of rise in mean annual air temperature on the stability of rock slopes containing ice-filled discontinuities. Permafrost and Periglacial Processes 12, 137-144.

Delonca, A., Gunzburger, Y., Verdel, T., 2014. Statistical correlation between meteorological and rockfall databases. Natural Hazards and Earth System Sciences, 14(8), 1953-1964.

Dorren, L.K., Berger, F., le Hir, C., Mermin, E., Tardif, P., 2005. Mechanisms, effects and management implications of rockfall in forests. Forest Ecology and Management, 215(1-3), 183-195.

Dorren, L.K.A., 2008. Rockfall and protection forests - models, experiments and reality. Habilitation, Universität für Bodenkultur, Wien.

Dorren, L.K.A., Berger, F., 2006. Stem breakage of trees and energy dissipation at rockfall impacts. Tree Physiology, 26, 63-71.

Dorren, L.K.A., F., B., Jonsson, M., Krautblatter, M., Mölk, M., Stoffel, M., Wehrli, A., 2007. State of the art in rockfall - forest interactions. . Schweizerische Zeitschrift für Forstwesen, 158, 158-141.

Draebing, D., Krautblatter, M., Hoffmann, T.J.G.R.L., 2017. Thermo-cryogenic controls of fracture kinematics in permafrost rockwalls. 44(8), 3535-3544.

Dupire, S., Bourrier, F., Monnet, J.-M., Bigot, S., Borgniet, L., Berger, F., Curt, T., 2016. The protective effect of forests against rockfalls across the French Alps: Influence of forest diversity. Forest Ecology and Management, 382, 269-279.

Ebohon, B., Schrott, L., 2008. Modelling mountain permafrost distribution: A new permafrost map of Austria. In: D.L. Kane, K.M. Hinkel (Eds.), Proceedings of the 9th International Conference on Permafrost, USPA. , University of Alaska, Fairbanks, pp. 397-402.

EEA1/2017, 2017. Climate change, impacts and vulnerability in Europe 2016. An indicator-based report., European Environment Agency, Luxembourg.

Eckert, N., Baya, H., and Deschatres, M., 2010. Assessing the response of snow avalanche runout elevations to climate fluctuations using hierarchical modeling: application to 61 winters of data in France. J. Climate, 23, 3157–3180. https://doi.org/10.1175/2010JCLI3312.1.

Eckert, N., Keylock, C. J., Castebrunet, H., Lavigne, A., and Naaim, M., 2013. Temporal trends in avalanche activity in the French Alps and subregions: from occurrences and runout elevations to unsteady return periods, J. Glaciol. 59, 93–114. https://doi.org/10.3189/2013JoG12J091.

Einhorn, B., Eckert, N., Chaix, C., Ravanel, L., Deline, P., Gardent, M., Boudières, V., Richard, D., Vengeon, J.-M., Giraud, G., Schoeneich, P., 2015. Climate change and natural hazards in the Alps. Observed and potential impacts on physical and socio-economic systems. Journal of Alpine Research | Revue de géographie alpine. https://doi.org/10.4000/rga.2878

Elkin, C., Gutiérrez, A.G., Leuzinger, S., Manusch, C., Temperli, C., Rasche, L., Bugmann, H., 2013. A 2°C warmer world is not safe for ecosystem services in the European Alps. Global Change Biology 19(6), 1827-1840.

Evans, S., Hungr, O., 1993. The assessment of rockfall hazard at the base of talus slopes. Canadian geotechnical journal, 30(4), 620-636.

Faccoli, M., Bernardinelli, I., 2014. Composition and Elevation of Spruce Forests Affect Susceptibility to Bark Beetle Attacks: Implications for Forest Management. Forests 5, 88–102. https://doi.org/10.3390/f5010088.

Feigenwinter, I., Kotlarski, S., Casanueva, A., Fischer, A.M., Schwierz, C., Liniger, M.A., 2018. Exploring quantile mapping as a tool to produce user-tailored climate scenarios for Switzerland, Technical Report MeteoSwiss, 270, 44 pp.

Feistl, T., Bebi, P., Dreier, L., Hanewinkel, M., Bartelt, P., 2014b. Quantification of basal friction for technical and silvicultural glide-snow avalanche mitigation measures. Natural Hazards and Earth System Sciences 14(11), 2921.

Feistl, T., Bebi, P., Teich, M., Bühler, Y., Christen, M., Thuro, K., Bartelt, P., 2014a. Observations and modeling of the braking effect of forests on small and medium avalanches. Journal of Glaciology 60(219), 124-138.

Fowler, A.M., Hennessy, K.J., 1995. Potential impacts of global warming on the frequency and magnitude of heavy precipitation. Natural Hazards 11, 283–303.

Frehner, M., Wasser, B., Schwitter, R., 2007. Sustainability and Success Monitoring in Protection Forests: Guidelines for Silvicultural Interventions in Forests with Protective Functions. Federal Office for the Environment FOEN.

Gallina, V., Torresan, S., Critto, A., Sperotto, A., Glade, T., Marcomini, A., 2016. A review of multi-risk methodologies for natural hazards: Consequences and challenges for a climate change impact assessment. Journal of Environmental Management 168, 123–132. https://doi.org/10.1016/j.jenvman.2015.11.011

Gariano, S.L., Guzzetti, F., 2016. Landslides in a changing climate. Earth-Science Reviews 162, 227–252. https://doi.org/10.1016/j.earscirev.2016.08.011

Gehrig-Fasel, J., Guisan, A., Zimmermann, N., 2007. Tree line shifts in the Swiss Alps. Climate change or land abandonment? Journal of Vegetation Science 19, 571-582.

Gerber, W., 2008. Waldwirkung und Steinschlag., Proceedings 14. Arbeitstagung Schweizerischen Gebrigswaldpflegegruppe & FAN, Grafenort/Engelberg, pp. 1-15.

Glade, T., 2003. Landslide occurrence as a response to land use change: a review of evidence from New Zealand. Catena 51, 297–314.

Glade, T., Anderson, M., Crozier, M.J. (Eds.), 2005. Landslide hazard and risk: Issues, Concepts and Approach. John Wiley, Chichester.

Glover, J., denk, M., Bourrier, F., Volkwein, A., Gerber, W., 2012. Measuring the kinetic energy dissipation effects of rock fall attenuating systems with video analysis., 12th Congress INTERPRAEVENT, Grenoble, pp. 151-161.

Gobiet, A., Kotlarski, S., Beniston, M., Heinrich, G., Rajczak, J., Stoffel, M., 2014. 21st century climate change in the European Alps — A review. Science of The Total Environment 493(1), 1138–1151.

Goetz, Guthrie, R.H., Brenning, A., 2015. Forest harvesting is associated with increased landslide activity during an extreme rainstorm on Vancouver Island, Canada. Natural Hazards and Earth System Science 15, 1311–1330. https://doi.org/10.5194/nhess-15-1311-2015

Goudie, A.S., 2013. The Human Impact on the Natural Environment: Past, Present, and Future. John Wiley & Sons.

Gsteiger, P., 1993. Steinschlagschutzwald. ein beitrag zur abgrenzung, beurteilung und bewirtschaftung. Schweiz. Z. Forstwes, 144(2), 115-132.

Gudmundsson, L., Bremnes, J.B., Haugen, J.E., Engen-Skaugen, T., 2012. Technical Note: Downscaling RCM precipitation to the station scale using statistical transformations – a comparison of methods. Hydrology and Earth System Sciences, 16, 3383-3390. https://doi.org/10.5194/hess-16-3383-2012

Guzzetti, F., Mondini, A.C., Cardinali, M., Fiorucci, F., Santangelo, M., Chang, K.-T., 2012. Landslide inventory maps: New tools for an old problem. Earth-Science Reviews 112, 42–66. https://doi.org/10.1016/j.earscirev.2012.02.001

Hall, K., André, M.F., 2001. New insights into rock weathering from high-frequency rock temperature data: an Antarctic study of weathering by thermal stress. Geomorphology, 41, 23-35.

Harsch, M.A., Hulme, P.E., McGlone, M.S., Duncan, R.P., 2009. Are treeline advancing? A global meta analysis of treeline responses to global warming. Ecology letters 12, 1040-1049.

Hormes, A., Ivy-Ochs, S., Kubik, P.W., Ferreli, L., Michetti, A.M., 2008. ^{10}Be exposure ages of a rock avalanche and a late glacial moraine in Alta Valtellina, Italian Alps. Quaternary International, 190, 136-145.

Huerta, M.L., Molotch, N.P., and McPhee, J., 2019. Snowfall interception in a deciduous Nothofagus forest and implications for spatial snowpack distribution. Hydrol. Process. 1-17. https://doi.org/10.1002/hyp.13439.

Hungr, O., Leroueil, S., Picarelli, L., 2013. The Varnes classification of landslide types, an update. Landslides 11, 167–194. https://doi.org/10.1007/s10346-013-0436-y

IPCC, 2014. Climate Change 2014: Synthesis Report. Contribution of Working Groups I, II and III to the Fifth Assessment Report of the Intergovernmental Panel on Climate Change, Geneva, Switzerland 151 pp. URL https://www.ipcc.ch/report/ar5/syr/ (accessed 11.25.19).

Isotta, F.A., Begert, M., Frei, C., 2019. Long-term consistent monthly temperature and precipitation grid data sets for Switzerland over the past 150 years. Journal of Geophysical Research: Atmospheres 124, 3783– 3799. https://doi.org/10.1029/2018JD029910

Isotta, F.A., Frei, C., Weilguni, V., Perčec Tadić, M., Lassègues, P., Rudolf, B., Pavan, V., Cacciamani, C., Antolini, G., Ratto, S.M., Munari, M., Micheletti, S., Bonati, V., Lussana, C., Ronchi, C., Panettieri, E., Marigo, G., Vertačnik, G., 2014. The climate of daily precipitation in the Alps: development and analysis of a high-resolution grid dataset from pan-Alpine rain-gauge data: CLIMATE OF DAILY PRECIPITATION IN THE ALPS. Int. J. Climatol. 34, 1657–1675. https://doi.org/10.1002/joc.3794

Jaboyedoff, M., Dudt, J.-P., Labiouse, V., 2005. An attempt to refine rockfall hazard zoning based on the kinetic energy, frequency and fragmentation degree. Natural Hazards and Earth System Science, 5(5), 621-632.

Jaboyedoff, M., Serron, M.-H., 2005. Hazard assessment within an Integrated Risk Assessment Process for Landslides (IRAPL).

Jacob, D., Petersen, J., Eggert, B., Alias, A., Christensen, O.B., Bouwer, L.M., Braun, A., Colette, A., Déqué, M., Georgievski, G., et al., 2014. EURO-CORDEX: new high-resolution climate change projections for European impact research. Regional Environmental Change 14(2), 563–578. https://doi.org/10.1007/s10113-013-0499-2

Jahn, J., 1988. Entwaldung und Steinschlag., Proceedings Interpraevent, Graz, pp. 185-198.

Jomelli, V., Delval, C., Grancher, D., Escande, S., Brunstein, D., Hetu, B., Filion, L., Pech, P., 2007. Probabilistic analysis of recent snow avalanche activity and weather in the French Alps. Cold Regions Science and Technology 47 (1–2), 180–192.

Keiler, M., Fuchs, S., 2016. Vulnerability and Exposure to Geomorphic Hazards: Some Insights from the European Alps, in: Meadows, M.E., Lin, J.-C. (Eds.), Geomorphology and Society, Advances in Geographical and Environmental Sciences. Springer Japan, Tokyo, pp. 165–180. https://doi.org/10.1007/978-4-431-56000-5_10

Keiler, M., Knight, J., Harrison, S., 2010. Climate change and geomorphological hazards in the eastern European Alps. Phil. Trans. R. Soc. A 368, 2461–2479. https://doi.org/10.1098/rsta.2010.0047

Kendall, M.G., 1975. Rank Correlation Methods. Griffin, London.

Kindermann, G., 2010. Eine klimasensitive Weiterentwicklung des Kreisflächenzuwachsmodells aus PROGNAUS. Centralblatt für das gesamte Forstwesen 127, 147–178.

Kotlarski, S., Keuler, K., Christensen, O. B., Colette, A., Déqué, M., Gobiet, A., Goergen, K., Jacob, D., Lüthi, D., van Meijgaard, E., Nikulin, G., Schär, C., Teichmann, C., Vautard, R., Warrach-Sagi, K., Wulfmeyer, V., 2014. Regional climate modeling on European scales: a joint standard evaluation of the EURO-CORDEX RCM ensemble. Geosci. Model Dev. 7, 1297–1333., https://doi.org/10.5194/gmd-7-1297-2014.

Krautblatter, M., Funk, D., Günzel, F.K., 2013. Why permafrost rocks become unstable: a rock-ice mechanical model in time and space. Earth Surface Processes and Landforms, 38, 876-887.

Krähenbühl, R., 2004. Temperatur und Kluftwasser als Ursachen von Felssturz. Bulletin für Angewandte Geologie, 9, 19-35.

Kunkel, K.E., Robinson, D.A., Champion, S., Yin, X., Estilow, T., Frankson, R.M., 2016. Trends and extremes in Northern Hemisphere snow characteristics. Current Climate Change Reports 2, 65–73. https://doi.org/10.1007/s40641-016-0036-8.

Laternser, M., Schneebeli, M., 2002. Temporal trend and spatial distribution of avalanche activity during the last 50 years in Switzerland. Natural Hazards 27(3), 201-230.

Ledermann, T., Kindermann, G., Gschwantner, T., 2017. Austria, in: Barreiro, S., Schelhaas, M.-J., McRoberts, R.E., Kändler, G. (Eds.), Forest Inventory-Based Projection Systems for Wood and Biomass Availability. Springer International Publishing, Cham, pp. 79–95. https://doi.org/10.1007/978-3-319-56201-8_6

Lingua, E., Bettella, F., Pividori, M., Marzano, R., Garbarino, M., Piras, M., Kobal, M., Berger, F., 2020. The Protective Role of Forests to Reduce Rockfall Risks and Impacts in the Alps Under a Climate Change Perspective, Climate Change, Hazards and Adaptation Options. Springer, pp. 333-347.

Maraun, D, Wetterhall, F., Ireson, A.M., Chandler, R.E., Kendon, E. J., Widmann, M., Brienen, S., Rust, H.W., Sauter, V., Themeßl, M., Venema, V.K.C., Chun, K. P., Goodess, C. M., Jones, R. G., Onof, C., Vrac, M., Thiele-Eich, I., 2010. Precipitation downscaling under climate

change: Recent developments to bridge the gap between dynamical models and the end user. Reviews of Geophysics 48, RG3003. https://doi.org/10.1029/2009RG000314

Marston, R.A., 2010. Geomorphology and vegetation on hillslopes: Interactions, dependencies, and feedback loops. Geomorphology 116, 206–217. https://doi.org/10.1016/j.geomorph.2009.09.028

Marty, C., 2008. Regime shift of snow days in Switzerland. Geophys. Res. Lett. 35, L12501. https://doi.org/10.1029/2008GL033998.

Marty, C., Blanchet, J., 2012. Long-term changes in annual maximum snow depth and snowfall in Switzerland based on extreme value statistics. Climatic Change 111, 705–721.

Marty, C., Meister, R., 2012. Long-term snow and weather observations at Weissfluhjoch and its relation to other high-altitude observatories in the Alps. Theor. Appl. Climatol. 110, 573–583. http://dx.doi.org/10.1007/s00704-012-0584-3.

McClung, D.M., 2003. Magnitude and Frequency of Avalanches in Relation to Terrain and Forest Cover. Arctic, Antarctic, and Alpine Research 35, 82–90. https://doi.org/10.1657/1523-0430(2003)035[0082:MAFOAI]2.0.CO;2

Mölk, M., Rieder, B., 2017. Rockfall hazard zones in Austria. Experience, problems and solutions in the development of a standardised procedure. Geomechanics and Tunnelling, 10(1), 24-33.

Motta, R., Haudemand, J.-C., 2000. Protective Forests and Silvicultural Stability. Mt. Res. Dev. 20, 180–187. https://doi.org/10.1659/0276-4741(2000) 020[0180:PFASS]2.0. CO;2.

Motta, R., Morales, M.S., Nola, P., 2006. Human land-use, forest dynamics and tree growth at the treeline in the Western Italian Alps. Ann. For. Sci. 63, 739-747.

Montgomery, D.R., Schmidt, K.M., Greenberg, H.M., Dietrich, W.E., 2000. Forest clearing and regional landsliding. Geology 28, 311–314. https://doi.org/10.1130/0091-7613(2000)28<311:FCARL>2.0.CO;2

Moos, C., Dorren, L., Stoffel, M., 2017. Quantifying the effect of forests on frequency and intensity of rockfalls. Natural Hazards and Earth System Sciences 17, 291–304. https://doi.org/10.5194/nhess-17-291-2017

Mulas, M., Marnas, M., Ciccarese, G., Corsini, A., 2019. Sinusoidal wave fit indexing of irreversible displacements for crackmeters monitoring of rockfall areas: test at Pietra di Bismantova (Northern Apennines, Italy). Landslides. https://doi.org/10.1007/s10346-019-01248-x

Murphy, J., Sexton, D., Barnett, D., Jones, G.S., Webb, M.J., Collins, M., Stainforth, D.A., 2004. Quantification of modelling uncertainties in a large ensemble of climate change simulations. Nature 430, 768–772. https://doi.org/10.1038/nature02771

Nikulin, G., Kjellstrom, E., Hansson, U., Strandberg, G., Ullerstig, A., 2011. Evaluation and future projections of temperature, precipitation and wind extremes over Europe in an ensemble of regional climate simulations. Tellus Series A - Dynamic Meteorology and Oceanography 63(1), 41–55. https://doi.org/10.1111/j.1600-0870.2010.00466.x

ÖKS15, 2016. Klimaszenarien für Österreich. Daten - Methoden - Klimaanalyse.

ONR, 2017. ONR 24810. Technical protection against rockfall - Terms and definitions, effects of actions, design, monitoring and maintenance., pp. 118.

Oswald, V., 2020. Auswirkungen des Schutzwaldes auf Steinschlagmodellierungen in Vals. Sensitivitätsanalyse in Rockyfor3D und RAMMS: ROCKFALL. Master thesis, Universität Innsbruck, Innsbruck, 122 pp.

Papathoma-Köhle, M., Glade, T., 2013. The role of vegetation cover change for landslide hazard and risk, in: In: G. Renaud, Karen Sudmeier-Rieux and Marisol Estrella (Eds): The Role of Ecosystems in Disaster Risk Reduction. UNU-Press, Tokyo.

Perret, S., Stoffel, M., Kienholz, H., 2006. Spatial and temporal rockfall activity in a forest stand in the Swiss Prealps - a dendrogeomorphological case study. Geomorphology, 74, 219-231.

Perzl, F., Walter, D., 2012. Die Lawinen-Schutzwirkung des Waldes im Klimawandel - Literaturüberblick über gegenwärtige Klimatrends in den Alpen, mögliche Auswirkungen der Klimaveränderung auf die Schneedeckenparameter, die Lawinenaktivität und die Lawinen-Schutzwirkung des Waldes. Bericht im Rahmen des Interreg-Alpine-Space-Projektes MANFRED. https://bfw.ac.at/cms_stamm/600/PDF/MANFRED_CC_Avalanche_Forest_DE_3.pdf.

Picarelli, L., 2016. Groundwater in slopes. In: J.J. Clague, D. Stead (Eds.), Landslides: Types, Mechanisms and Modelling, pp. 235-251.

Pielmeier, C., Techel, F., Marty, C., Stucki, T., 2013. Wet snow avalanche activity in the Swiss Alps – trend analysis for mid-winter season. International Snow Science Workshop, Grenoble, France, 07–11 October 2013, 1240–1246.

Poisel, R., 2017. Felsstürze - Ablösemechanismen. In: R. Poisel, A. Preh (Eds.), Tagungsband - Gefahren durch Steinfall und Felssturz. Berichte der Geologischen Bundesanstalt. Geologische Bundesanstalt, Wlen, pp. 49-58.

Pomeroy, J.W., Schmidt, R.A., 1993. The use of fractal geometry in modelling intercepted snow accumulation and sublimation. Proc. Eastern Snow Conference 50, 1-10.

Porter, S.C., Orombelli, G., 1981. Alpine Rockfall Hazards: recognition and dating of rockfall deposits in the western Italian Alps lead to an understanding of the potential hazards of giant rockfalls in mountainous regions. American Scientist, 69(1), 67-75.

Prager, C., Zangerl, C., Patzelt, G., Brandner, R.J.N.H., Sciences, E.S., 2008. Age distribution of fossil landslides in the Tyrol (Austria) and its surrounding areas. 8(2), 377-407.

Rajczak, J., Schär, C., 2017. Projections of future precipitation extremes over Europe: A multimodel assessment of climate simulations. Journal of Geophysical Research: Atmospheres 122, 10773–10800. https://doi.org/10.1002/2017JD027176

Ravanel, L., Deline, P., 2011. Climate influence on rockfalls in high-Alpine steep rockwalls: The north side of the Aiguilles de Chamonix (Mont Blanc massif) since the end of the 'Little Ice Age'. The Holocene, 21(2), 357-365.

Reichenbach, P., Busca, C., Mondini, A.C., Rossi, M., 2014. The Influence of Land Use Change on Landslide Susceptibility Zonation: The Briga Catchment Test Site (Messina, Italy). Environmental Management 54, 1372–1384. https://doi.org/10.1007/s00267-014-0357-0

Reynolds, A., Richards, G., Iglesia, B., Rayward-Smith, V., 2006. Clustering Rules: A Comparison of Partitioning and Hierarchical Clustering Algorithms. Journal of Mathematical Modelling and Algorithms 5, 475-504. https://doi.org/10.1007/s10852-005-9022-1

Rickli, C., Graf, F., 2009. Effects of forests on shallow landslides–case studies in Switzerland. Forest Snow and Landscape Research 82, 33–44.

Rickli, C., Graf, F., Gerber, W., Frei, M., Böll, A., 2004. Der Wald und seine Bedeutung bei Naturgefahren geologischen Ursprungs, Forum für Wissen, pp. 27-34.

Rickli, C., Zürcher, K., Frey, W., Lüscher, P., 2002. Wirkungen des Waldes auf oberflächennahe Rutschprozesse. Schweizerische Zeitschrift für Forstwesen 153(11), 437–445.

Rousselot, M., Durand, Y., Giraud, G., Mérindol, L., Dombrowski-Etchevers, I., Déqué, M., Castebrunet, H., 2012. Statistical adaptation of ALADIN RCM outputs over the French Alps – application to future climate and snow cover. The Cryosphere 6, 785– 805. https://doi.org/10.5194/tc-6-785-2012.

Rubel, F., Brugger, K., Haslinger, K., Auer, I., 2017. The climate of the European Alps: Shift of very high resolution Köppen-Geiger climate zones 1800–2100. metz 26, 115–125. https://doi.org/10.1127/metz/2016/0816

Sandersen, F., Bakkehøi, S., Hestnes, E., Lied, K., 1997. The influence of meteorological factors on the initiation of debris flows, rockfalls, rockslides and rockmass stability. Publikasjon-Norges Geotekniske Institutt, 201, 97-114.

Scheidl, C., Heiser, M., Vospernik, S., Lauss, E., Perzl, F., Kofler, A., Kleemayr, K., Bettella, F., Lingua, E., Garbarino, M., Skudnik, M., Trappmann, D., Berger, F., in review. Assessing the protective effect of mountain forests against rockfall on an alpine transregional scale.

Schläppy, R., Jomelli, V., Eckert, N., Stoffel, M., Grancher, D., Brunstein, D., Corona, C., Deschatres, M., 2016. Can we infer avalanche–climate relations using tree-ring data? Case studies from the French Alps. Reg. Environ. Change 16, 629–642.

Schmaltz, E.M., Steger, S., Glade, T., 2017. The influence of forest cover on landslide occurrence explored with spatio-temporal information. Geomorphology 290, 250–264. https://doi.org/10.1016/j.geomorph.2017.04.024

Schmaltz, E.M., Van Beek, L.P.H., Bogaard, T.A., Kraushaar, S., Steger, S., Glade, T., 2019. Strategies to improve the explanatory power of a dynamic slope stability model by enhancing land cover parameterisation and model complexity. Earth Surface Processes and Landforms 44, 1259–1273. https://doi.org/10.1002/esp.4570

Schmidli, J., Frei, C., 2005. Trends of heavy precipitation and wet and dry spells in Switzerland during the 20th century. International Journal of Climatology 25, 753–771. https://doi.org/10.1002/joc.1179

Schmidli, J., Goodess, C.M., Frei, C., Haylock, M.R., Hundecha, Y., Ribalaygua, J., Schmith, T., 2007. Statistical and dynamical downscaling of precipitation: An evaluation and comparison of scenarios for the European Alps. Journal of Geophysical Research 112, D04105. https://doi.org/10.1029/2005JD007026

Schneebeli, M., Bebi, P., 2004. Snow and avalanche control. In Burley, J., Evans, J., and Youngquist, J.A. (eds.), Encyclopedia of Forest Sciences. Elsevier, 397-402.

Schneebeli, M., Laternser, M., Ammann, W., 1997. Destructive snow avalanches and climate change in the Swiss Alps. Eclogae Geologicae Helvetiae 90 (3), 457–461.

Schneiderbauer, S., Zebisch, M., Kass, S., Pedoth, L., 2013. Assessment of vulnerability to natural hazards and climate change in mountain environments. Measuring Vulnerability to Natural Hazards: towards Disaster Resilient Societies 2.

Schweizer, J., Jamieson, J. B., Schneebeli, M., 2003. Snow avalanche formation. Rev. Geophys. 41, 1016. https://doi.org/10.1029/2002RG000123.

Seidl, R., Schelhaas, M.-J., Lindner, M., Lexer, M.J., 2009. Modelling bark beetle disturbances in a large scale forest scenario model to assess climate change impacts and evaluate adaptive management strategies. Reg. Environ. Chang. 9 101–119. https://doi.org/10.1007/s10113-008-0068-2.

Seidl, R., Schelhaas, M.-J., Rammer, W., Verkerk, P.J., 2014. Increasing forest disturbances in Europe and their impact on carbon storage. Nat. Clim. Chang. 4, 806–810. https://doi.org/10.1038/nclimate2318.

Serquet, G., Marty, C., Dulex, J.-P., Rebetez, M., 2011. Seasonal trends and temperature dependence of the snowfall/precipitation-day ratio in Switzerland. Geophys. Res. Lett. 38, 14–18. https://doi.org/10.1029/2011GL046976.

Sidle, R.C., Bogaard, T.A., 2016. Dynamic earth system and ecological controls of rainfall-initiated landslides. Earth-Science Reviews 159, 275–291. doi.org/10.1016/j.earscirev.2016.05.013

Sidle, R.C., Ochiai, H., 2006. Landslides: processes, prediction, and land use. American Geophysical Union.

Slaymaker, O., Spencer, T., Embleton-Hamann, C. (Eds.), 2009. Geomorphology and global environmental change. Cambridge University Press, Cambridge ; New York.

Sovilla, B., Kern, M., Schaer, M., 2010. Slow drag in wet snow avalanche flow. J. Glaciol. 56, 58-592.

Sperotto, A., Molina, J.-L., Torresan, S., Critto, A., Marcomini, A., 2017. Reviewing Bayesian Networks potentials for climate change impacts assessment and management: A multi-risk perspective. Journal of Environmental Management 202, 320–331. https://doi.org/10.1016/j.jenvman.2017.07.044

Stadelmann, G., Bugmann, H., Wermelinger, B., Bigler, C., 2014. Spatial interactions between storm damage and subsequent infestations by the European spruce bark beetle. For. Ecol. Manage. 318, 167–174. https://doi.org/10.1016/j.foreco.2014.01. 022.

Stangl, R., Hochbichler, E., Bellos, P.N., Florineth, F., 2009. Allometric estimation of the above-ground biomass components of Alnus incana (L.) Moench used for landslide stabilisation at Bad Goisern (Austria). Plant and Soil 324, 115–129. https://doi.org/10.1007/s11104-008-9888-6

Steger, S., 2017. Spatial analysis and statistical modelling of landslide susceptibility - pitfalls and solutions. Dissertation thesis. University of Vienna, Austria.

Steger, S., Brenning, A., Bell, R., Glade, T., 2017. The influence of systematically incomplete shallow landslide inventories on statistical susceptibility models and suggestions for improvements. Landslides 1–15. https://doi.org/10.1007/s10346-017-0820-0

Stoffel, M., Corona, C., 2014. Dendroecological dating of geomorphic disturbance in trees. Tree Ring Res 70, 3–20. doi:10.3959/1536-1098-70.1.3.

Stoffel, M., Huggel, C., 2012. Effects of climate change on mass movements in mountain environments. Progress in Physical Geography: Earth and Environment 36, 421–439. https://doi.org/10.1177/0309133312441010

Stoffel, M., Tiranti, D., Huggel, C., 2014. Climate change impacts on mass movements — Case studies from the European Alps. Science of The Total Environment 493, 1255–1266. https://doi.org/10.1016/j.scitotenv.2014.02.102

Tebaldi, C., Reto, K., 2007. The use of the multi-model ensemble in probabilistic climate projections. Philosophical Transactions of the Royal Society A: Mathematical, Physical and Engineering Sciences, 365. http://doi.org/10.1098/rsta.2007.2076

Teich, M., Bartelt, P., Grêt-Regamey, A., Bebi, P., 2012a. Snow avalanches in forested terrain: influence of forest parameters, topography, and avalanche characteristics on runout distance. Arctic, Antarctic, and Alpine Research 44(4), 509-519.

Teich, M., Fischer, J.-T., Feistl, T., Bebi, P., Christen, M., Grêt-Regamey, A., 2014. Computational snow avalanche simulation in forested terrain. Natural Hazards and Earth System Sciences 14(8), 2233-2248.

Teich, M., Giunta, A.D., Hagenmuller, P., Bebi, P., Schneebeli, M., Jenkins, M.J., 2019. Effects of bark beetle attacks on forest snowpack and avalanche formation–Implications for protection forest management. Forest ecology and management 438, 186-203.

Teich, M., Marty, C., Gollut, C., Grêt-Regamey, A., Bebi, P., 2012b. Snow and weather conditions associated with avalanche releases in forests: rare situations with decreasing trends during the last 41 years. Cold Reg. Sci. Technol. 83–84, 77–88. https://doi.org/10.1016/j.coldregions.2012.06.007.

Teich, M., Zurbriggen, N., Bartelt, P., Grêt-Regamey, A., Marty, C., Ulrich, M., Bebi, P., 2012c. Potential impacts of climate change on snow avalanches starting in forested terrain. Proceedings, 2012 International Snow Science Workshop, Anchorage, Alaska, 244-251.

Terzi, S., Torresan, S., Schneiderbauer, S., Critto, A., Zebisch, M., Marcomini, A., 2019. Multi-risk assessment in mountain regions: A review of modelling approaches for climate change adaptation. Journal of Environmental Management 232, 759–771. https://doi.org/10.1016/j.jenvman.2018.11.100

Theil, H., 1950. A rank-invariant method of linear and polynomial regression analysis. I. Proceedings of the Koninklijke Nederlandse Akademie van Wetenschappen A53: 386–392.

Themeßl, M., Gobiet, A., Heinrich, G., 2012. Empirical-statistical downscaling and error correction of regional climate models and its impact on the climate change signal. Climatic Change, 112, 449-468. https://doi.org/10.1007/s10584-011-0224-4

Toppe, R., 1987. Terrain models: a tool for natural hazard mapping. IAHS, Publication, 162.

Volkwein, A., Schellenberg, K., Labiouse, V., Agliardi, F., Berger, F., Bourrier, F., Dorren, L.K., Gerber, W., Jaboyedoff, M., 2011. Rockfall characterisation and structural protection-a review. Natural Hazards and Earth System Sciences, 11, p. 2617-p. 2651.

Wilcke, R.A.I., Bärring, L., 2016. Selecting regional climate scenarios for impact modelling studies, Environmental Modelling & Software 78, 191-201. https://doi.org/10.1016/j.envsoft.2016.01.002

Winkler, R., Boon, S., Zimonick, B., Spittlehouse, D., 2014. Snow accumulation and ablation response to changes in forest structure and snow surface albedo after attack by mountain pine beetle. Hydrological Processes 28(2), 197-209. https://doi.org/10.1002/hyp.9574

Wohlgemuth, T., Schwitter, R., Bebi, P., Sutter, F., Brang, P., 2017. Post-windthrow management in protection forests of the Swiss Alps. Eur. J. For. Res. 136, 1029–1040. https://doi.org/10.1007/s10342-017-1031-x.

Wood, J.L., Harrison, S., Reinhardt, L., 2015. Landslide inventories for climate impacts research in the European Alps. Geomorphology 228, 398–408. https://doi.org/10.1016/j.geomorph.2014.09.005

Zhang, R., Corte-Real, J., Moreira, M., Kilsby, C., Burton, A., J. Fowler, H.J., Blenkinsop, S., Birkinshaw, S., Forsythe, N., Nunes, J.P., Sampaio, E., 2019. Downscaling climate change of mean climatology and extremes of precipitation and temperature: Application to a Mediterranean climate basin. International Journal of Climatology 39, 4985– 5005. https://doi.org/10.1002/joc.6122

Zimmermann, M., 1997. Murganggefahr und Klimaänderung - ein GIS-basierter Ansatz. vdf Hochschulverlag AG.

Zurbriggen, N., Nabel, J. E., Teich, M., Bebi, P., Lischke, H., 2014. Explicit avalanche-forest feedback simulations improve the performance of a coupled avalanche-forest model. Ecological Complexity 17, 56-66.

Appendix A: Instructions for collecting forest and site parameters

Please provide data records for forest and site parameters for no more than 15-20 areas of interest. We will focus on maximum three main forest types in each PAR such as subalpine spruce, spruce-fir and/or spruce-fir-beech forests (or other main forest types in your PAR), and on forests with a protective function or with functions that are particularly of interest in your PAR.

Goal: Since in GreenRisk4ALPs, we decided to not use the forest development projections (future climate change driven forest scenarios) for detailed hazard modeling but rather as basis for discussions, we will focus those projections on protection forests with a direct object protection function including "hot-spot/cold-spot" areas (or on forests with other functions that are particularly of interest in your PAR).

In General: When designing your field work, keep in mind that the spatial arrangement and resolution of your sampling points to gather the data required for projecting the forest's development under climate change with CALDIS depends on the goal and further use of the results. In general, forest development projections are made for the observation unit; the **observation unit can be a point** (e.g. collected by sample plots and/or angle count samples) **or a stand** (e.g. averaged for stand-scale from point observations or estimated). Once you've decided, what areas you are considering as important/of interest and would like to have projections for, please provide forest and site parameters that represent the present forest (e.g. at two to three different elevations, if the forest stand is covering a slope).

Important: All parameters can also be estimated from nearby forest inventory points or from other data sources (but: as more accurate the input data, as more accurate the results); however, please make sure that the provided data represents the forest of interest and not only one inventory point. For example, if the area/stand of interest is very inhomogeneous in space (e.g. some parts are very dense, others are sparsely covered by trees), it should be split up in more or less homogenous sub-stands as representative mean values are typically not able to describe the heterogeneity in space. However, multi-storied stands do not need to be split up in separate sub-stands (i.e. parameters for each layer need to be submitted with the same stand and sampling point ID. An example is provided in the Excel-template.)

When you submit your data, please also provide a documentation of how this data was collected/gathered, e.g. via angle count samples, other sampling plot methods, estimates/model output based on forest inventory points, or other data sources since this will be part of the deliverable D.T1.1.3 "Report on 'New assessment methods for protection forests in the AS".

An Excel-file is provided to fill in your data.

Basic information:

- ID (each record of forest and site parameters should have one unique ID that links forest, site and other parameters - starting with the two character ISO 3166 country code [https://en.wikipedia.org/wiki/List_of_ISO_3166_country_codes], and followed by, e.g., a two digit stand ID, and, if sample plot data is provided, a three digit sample ID, e.g. AT01001, AT01002, AT02001, etc.)

- sampling date, if possible
- stand size (ha) (if the record is representing a forest stand)

For each ID/record, the following **forest parameters** need to be provided:

- Tree species (Species code following EN 13556 [https://de.wikipedia.org/wiki/DIN_EN_13556])
- Diameter at breast height (dbh) (cm)
- Tree height (m)
- Crown height (height up to the beginning of the living crown) (m)
- Number of stems per ha

If you submit data collected by sample plots/angle count samples, forest parameters need to be provided per tree [single parameters can also be estimated]. If you submit stand-based estimates, forest parameters need to be submitted per unique type. For example, for a two-layer single species stand you have to submit at least two lines of data, one for each layer. An example is provided in the Excel-template.

The **site parameters** are:

- Slope angle (°)
- Exposition (°)
- Relief: position of the stand on a slope/in the landscape in 8 classes:

1 upper slope/convex slope
2 middle slope
3 lower slope/concave slope
4 trench
5 valley bottom
6 flat
7 depression
8 stream

- Soil type (based on expert opinion/according to the Austrian National Forest Inventory ANFI) → please provide any information on soil type that we can match it to the ANFI specifications
- Vegetation type (based on expert opinion/according to the ANFI) → please provide any information on vegetation type that we can match it to the ANFI specifications
- Elevation (m)
- Position (Lat, Lon)
- Water balance/hydrological regime (estimated in 5 classes):

1 dry
2 moderately fresh
3 fresh
4 very fresh
5 wet

- Soil depth (2 classes; in most cases >30 cm):

1, 0-30 cm
2, >30 cm

- Growing region (based on expert opinion/according to the ANFI) → please provide any information on yield or site class that we can match it to the ANFI specifications

Optional/additional data:

- Site index per tree species (dominant tree height at age 100)

Forest management/harvesting scenarios:
Information on planned/future forest management (thinning, harvesting) are necessary for predictions > 20 years into the future. These can be derived from past management strategies in the form of targeted tree height, targeted dbh, targeted stand density for harvesting decisions, mean harvest volume in percent, etc. The goal is to project the probability that a tree gets harvested based on the available input information.

ID	Sampling date (DD.MM.YY)	Slope (°)	Exposition (°)	Relief[1]	Soil type	Vegetation type	Main tree species[2]	Mean dbh[3] (cm)	Mean height (m)	Stems/ha	Elevation (m)	Latitude	Longtitude	Water balance[1]	Soil depth[1]	Growth region
PAR1 Val Ferret																
IT01001	17.07.19	34	307	2	Cambisols	Subalpine spruce forest	BTXX, LADC, PCAB	22	12	734	1474	45,82072	6,97132	3	2	Northern Graie Alps
IT01002	17.07.19	36	295	2	Cambisols	Subalpine spruce forest	LADC, PCAB	22	18	982	1492	45,82178	6,97205	3	2	Northern Graie Alps
IT01003	17.07.19	49	320	2	Cambisols	Subalpine spruce forest	LADC, PCAB	21	15	627	1538	45,8246	6,97748	3	2	Northern Graie Alps
IT01004	17.07.19	50	316	2	Cambisols	Subalpine spruce forest	LADC, PCAB	22	16	892	1501	45,82414	6,97652	3	2	Northern Graie Alps
IT01005	17.07.19	43	312	2	Cambisols	Subalpine spruce forest	LADC, PCAB	26	13	919	1501	45,82332	6,97532	3	2	Northern Graie Alps
IT02001	18.07.19	5	143	6	Cambisols	Subalpine larch forest	LADC	25	14	1278	1649	45,84305	7,009	2	2	Northern Graie Alps
IT02002	18.07.19	8	178	3	Cambisols	Subalpine larch forest	LADC	21	15	1221	1663	45,84391	7,00835	2	2	Northern Graie Alps
IT02003	18.07.19	14	212	3	Cambisols	Subalpine larch forest	LADC	17	11	1376	1695	45,84478	7,00814	2	2	Northern Graie Alps
IT02004	18.07.19	15	144	3	Cambisols	Subalpine larch forest	LADC	26	20	363	1704	45,84566	7,00927	2	2	Northern Graie Alps
IT02005	18.07.19	15	127	3	Cambisols	Subalpine larch forest	LADC	40	18	395	1689	45,84607	7,00994	2	2	Northern Graie Alps
IT03001	18.07.19	9	91	3	Cambisols	Subalpine larch forest	LADC, PCAB	23	16	1031	1655	45,84188	7,0027	2	2	Northern Graie Alps
IT03002	18.07.19	8	105	2	Cambisols	Subalpine larch forest	LADC, PCAB	38	16	514	1685	45,84252	7,00264	2	2	Northern Graie Alps
IT03003	18.07.19	24	145	2	Cambisols	Subalpine larch forest	LADC	35	22	628	1720	45,84299	7,00223	2	2	Northern Graie Alps
IT03004	18.07.19	26	184	2	Cambisols	Subalpine larch forest	LADC	42	17	532	1767	45,8432	7,00062	2	2	Northern Graie Alps
IT04001	18.07.19	17	111	6	Cambisols	Subalpine larch forest	LADC	67	27	200	1777	45,84229	6,99794	2	2	Northern Graie Alps
IT04002	18.07.19	21	146	1	Cambisols	Subalpine larch forest	PCAB	40	19	409	1735	45,84102	6,99789	2	2	Northern Graie Alps
IT04003	18.07.19	14	149	2	Cambisols	Subalpine larch forest	PCAB	51	23	394	1687	45,84068	6,99888	2	2	Northern Graie Alps
IT05		21	160	2	Cambisols	Subalpine larch forest	LADC, PCAB	35	18	1329	1641	45,83548	6,98125	2	2	Northern Graie Alps
IT06		35	283	2	Cambisols	Subalpine larch forest	LADC, PCAB	29	17	1250	1953	45,83705	7,01365	3	2	Northern Graie Alps
PAR2 Kranjska Gora																
SI01	05.09.19	40	180	1	Dystric cambisol	Subalpine beech forest	FASY, PCAB	23	17	100	1000	46,5176	13,726	3	2	Karawanks
SI02	05.09.19	32	270	1	Dystric cambisol	Alpine beech forest	FASY	28	19	83	1300	46,5144	13,7574	2	2	Karawanks
SI03	05.09.19	28	45	1	Rendzina on carbonate gravel	Subalpine spruce forest	FASY, PCAB	32	26	35	900	46,4834	13,7212	2	1	Julian Alps
SI04	06.09.19	18	0	1	Dystric cambisol	Subalpine beech forest	FASY	32	24	25	900	46,4906	13,7158	3	1	Julian Alps
SI05	06.09.19	40	315	1	Dystric cambisol	Subalpine beech forest	FASY, PCAB	28	20	80	900	46,4887	13,7106	2	2	Julian Alps
SI06	06.09.19	34	180	1	Rendzina on carbonate rock	Secondary spruce forest	PCAB	52	33	43	900	46,4979	13,7208	3	2	Karawanks
SI07	10.09.19	26	180	1	Rendzina on carbonate rock	Secondary spruce forest	FASY, PCAB	29	17	50	1000	46,4977	13,7314	3	2	Karawanks
SI08	10.09.19	35	135	4	Dystric cambisol	Secondary spruce forest	PCAB	39	25	35	1100	46,5017	13,7678	3	2	Karawanks
SI09	13.09.19	36	90	1	Dystric cambisol	Alpine beech forest	PCAB, FASY, ABAL	34	21	53	1200	46,4763	13,7164	2	2	Julian Alps
SI10	13.09.19	40	45	1	Rendzina on carbonate gravel	Secondary spruce forest	FASY	34	22	25	1000	46,4799	13,7317	3	2	Julian Alps
SI11	13.09.19	37	0	2	Rendzina on carbonate gravel	Secondary spruce forest	FASY, PCAB	24	20	30	900	46,4819	13,7734	2	2	Julian Alps
SI12	13.09.19	26	180	1	Dystric cambisol	Subalpine beech forest	FASY, PCAB	28	17	55	1100	46,4964	13,7888	1	1	Karawanks
SI13	16.09.19	16	180	2	Rendzina on carbonate gravel	Mixed conifer forest	PNSY, PCAB	27	18	58	800	46,4805	13,8715	2	1	Karawanks
SI14	16.09.19	26	45	3	Rendzina on carbonate gravel	Alpine beech forest	FASY	31	22	50	1100	46,3972	13,8356	2	1	Julian Alps
PAR3 Oberammergau																
DE4	06.08.19	34	170	3	Pararenzina	tiefmontan bis subalpiner Bergmischwald und Fichtenwald	FXEX, FASY	38	23	436	900	47,57589	11,03112	2	1	Mittlere Bayerische Kalkalpen
DE5	06.08.19	16	170	3	Braunerde	see above	FASY, PCAB	46	30	293	850	47,57622	11,0622	1	2	Mittlere Bayerische Kalkalpen
DE6	07.08.19	12	260	2	Pseudogley-Braunerde	see above	PCAB	53	33	167	1100	47,6204	11,07008	1	2	Oberbayerische Flysch-Voralpen
DE7	07.08.19	17	160	2	Pseudogley-Braunerde	see above	PCAB	52	31	288	1300	47,61973	11,08366	2	2	Oberbayerische Flysch-Voralpen
DE8	07.08.19	27	260	2	Pseudogley-Braunerde	see above	PCAB	47	28	545	1100	47,61222	11,08332	2	2	Oberbayerische Flysch-Voralpen
DE9	07.08.19	35	260	2	Braunerde	see above	PCAB	54	30	452	1400	47,61187	11,09544	1	1	Oberbayerische Flysch-Voralpen
DE10	06.08.19	27	120	2	Braunerde	see above	PCAB	25	17	1590	1400	47,61339	11,10858	1	1	Oberbayerische Flysch-Voralpen
DE11	06.08.19	25	230	3	Pseudogley-Braunerde	see above	PCAB	33	26	777	900	47,60222	11,08333	1	2	Oberbayerische Flysch-Voralpen
DE12	07.08.19	23	230	2	Pseudogley-Braunerde	see above	PCAB	28	23	1333	1100	47,60208	11,09578	1	2	Oberbayerische Flysch-Voralpen
DE13	06.08.19	30	230	2	Pseudogley-Braunerde	see above	PCAB	56	33	235	1200	47,60394	11,11386	2	2	Mittlere Bayerische Kalkalpen
DE14	06.08.19	22	20	2	Rendzina	see above	PCAB	45	34	222	1000	47,59665	11,10209	1	1	Mittlere Bayerische Kalkalpen
DE15	05.08.19	24	300	2	Rendzina	see above	PCAB	30	25	977	1100	47,59778	11,11028	1	1	Mittlere Bayerische Kalkalpen
DE16	05.08.19	10	300	2	Rendzina	see above	PCAB	57	29	207	1300	47,59176	11,10748	1	2	Mittlere Bayerische Kalkalpen
DE17	05.08.19	27	250	2	Rendzina	see above	PCAB	50	21	240	1400	47,58951	11,1011	2	1	Mittlere Bayerische Kalkalpen
DE18	05.08.19	33	20	2	Rendzina	see above	PCAB	49	28	469	1300	47,58843	11,11427	1	2	Mittlere Bayerische Kalkalpen
DE19	05.08.19	27	115	2	Podsol-Braunerde	see above	FASY, ABAL	27	14	385	1100	47,57555	11,09689	3	2	Mittlere Bayerische Kalkalpen
DE20	05.08.19	28	250	3	Braunerde	see above	PCAB	42	30	276	1000	47,57419	11,10637	1	2	Mittlere Bayerische Kalkalpen
PAR5 Southern Wipptal																
IT_5A	19.08.19	60	45	2	hoher Skelettgehalt, schluffig-lehmig		PCAB	31	23		1483	47,003166	11,509714	3	2	Randliche Innenalpen
IT_5B	19.08.19	65	260	2	Kalk Braunlehm, Kalkmoder		PCAB	31	19		1463	46,958103	11,465544	3	2	Randliche Innenalpen
IT_5C	19.08.20	55	80	2	podsolierte oder basenarme Braunerden		PCAB	54	41		1487	46,96203	11,335393	2	1	Zentrale Innenalpen
IT_5D	19.08.19	70	65	2	podsolierte oder basenarme Braunerden		PCAB	34	25		1538	46,942268	11,393295	2	1	Zentrale Innenalpen

IT_5E	19.08.20	68	220	2	Rendzina-Pararendzina, Kalk-Braunerde, hoher Skelettgehalt		PCAB	35	26		1118	46,930862	11,451287	1	1	Randliche Innenalpen
IT_5F	19.08.19	64	285	2	podsolierte oder basenarme Braunerden		PCAB	60	34		1348	46,946765	11,388278	2	1	Südliche Zwischenalpen
IT_5G	08.06.19	60	20	2	Braunlehm-Rendzina, Pararemdzina		PCAB, LADC	45	27		1250	46,93584	11,39826	2	1	Randliche Innenalpen
IT_5H	19.08.20	50	300	2	frische Kalkbraunerde, verbraunte Pararendzina		LADC, PCAB	29	27		1557	46,91675	11,528264	3	2	Randliche Innenalpen
IT_5I	19.08.20	45	55	2	Braunlehm-Rendzina, Pararemdzina		PCAB, LADC	45	27		1473	46,951259	11,554769	2	1	Randliche Innenalpen
IT_5J	19.08.20	55	135	2	Semipodsole oder podsolige, basenarme Braunerden		PCAB, LADC	50	26		1821	46,984764	11,647815	1	1	Südliche Zwischenalpen
PAR6 Vals/Gries																
AT200	31.08.19	38	230	2	Hangschutt silikatisch-karbonatreich	Montaner warmer Karbonat-Fichtenwald	LADC	38	22	305	1367	47,05147	11,52343	2	2	Subkontinentale Innenalpen - Westteil
AT201	31.08.19	31	196	3	Hangschutt silikatisch-karbonatreich	Frischer Karbonat-Fichten-Tannenwald	PCAB	13	12	3619	1331	47,0428	11,55643	3	1	Subkontinentale Innenalpen - Westteil
AT202	31.08.19	39	206	2	Silikatgesteine kalkarm	Warmer basischer (Lärchen-)Fichtenwald	PCAB	20	15	900	1413	47,04353	11,55785	2	1	Subkontinentale Innenalpen - Westteil
AT203	01.09.19	36	8	2	Hangschutt silikatisch-karbonatreich	Subalpiner basischer Lärchen-Fichtenwald	PCAB	19	13	568	1609	47,0364	11,55153	3	2	Subkontinentale Innenalpen - Westteil
AT204	01.09.19	40	200	3	Kies/Schotter silikatisch-karbonatreich	Montaner warmer Karbonat-Fichtenwald	LADC	59	30	196	1309	47,04649	11,53317	1	2	Subkontinentale Innenalpen - Westteil
AT205	03.09.19	40	201	2	Silikatgesteine kalkarm	Montaner warmer Karbonat-Fichtenwald	PCAB, LADC, PNNN	27	16	652	1627	47,02988	11,50232	2	1	Subkontinentale Innenalpen - Westteil
AT206	03.09.19	36	255	1	Silikatgesteine kalkreich	Subalpiner trockener Karbonat-(Lärchen-)Fichtenwald	LADC, PCAB	15	8	618	1902	47,05609	11,52995	2	2	Subkontinentale Innenalpen - Westteil

[1]See Appendix B for definition of classes

[2]Species code following EN 13556 (https://de.wikipedia.org/wiki/DIN_EN_13556)

[3]dbh = diameter at breast height

Appendix C: CALDIS results for single stands

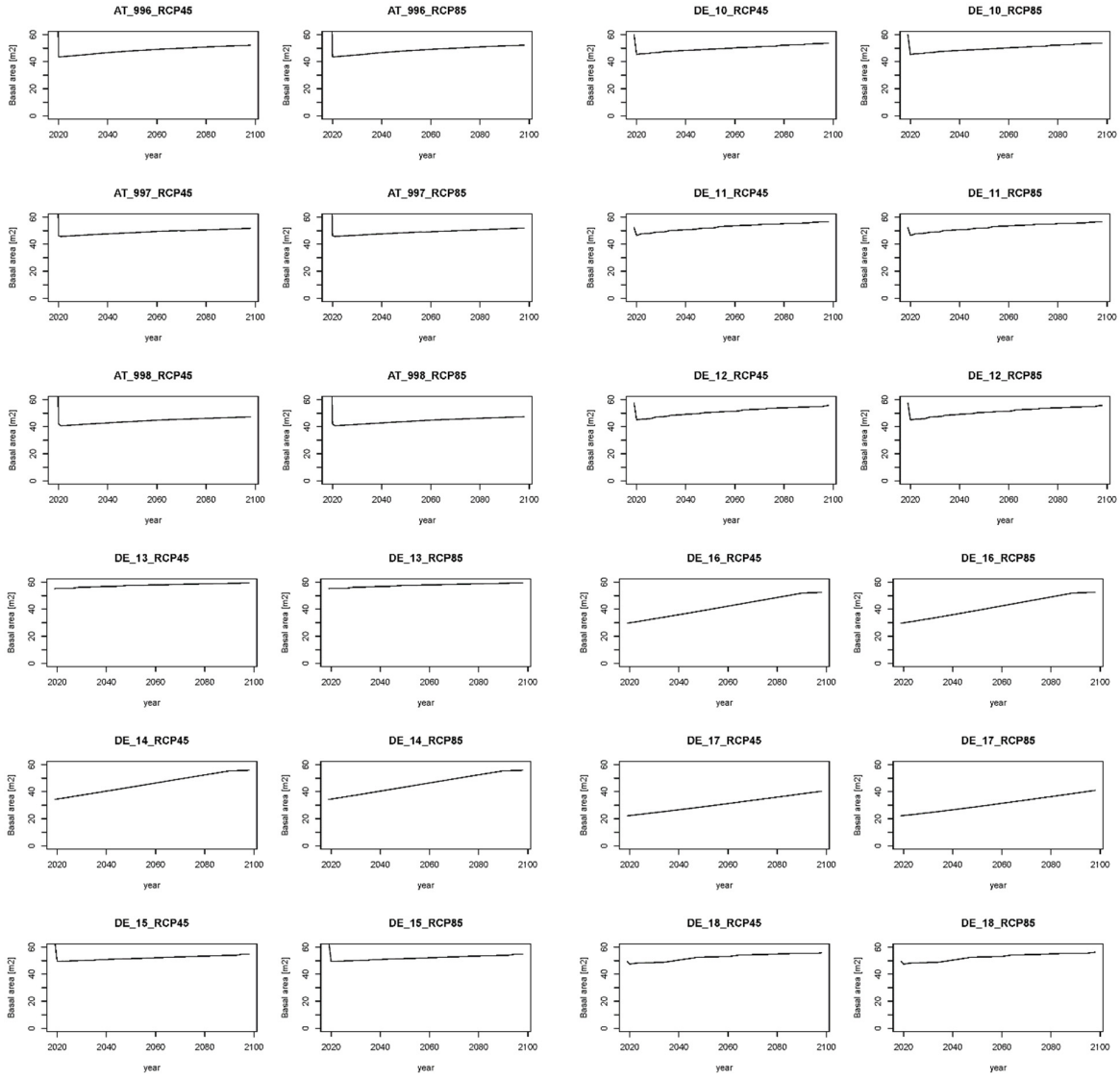

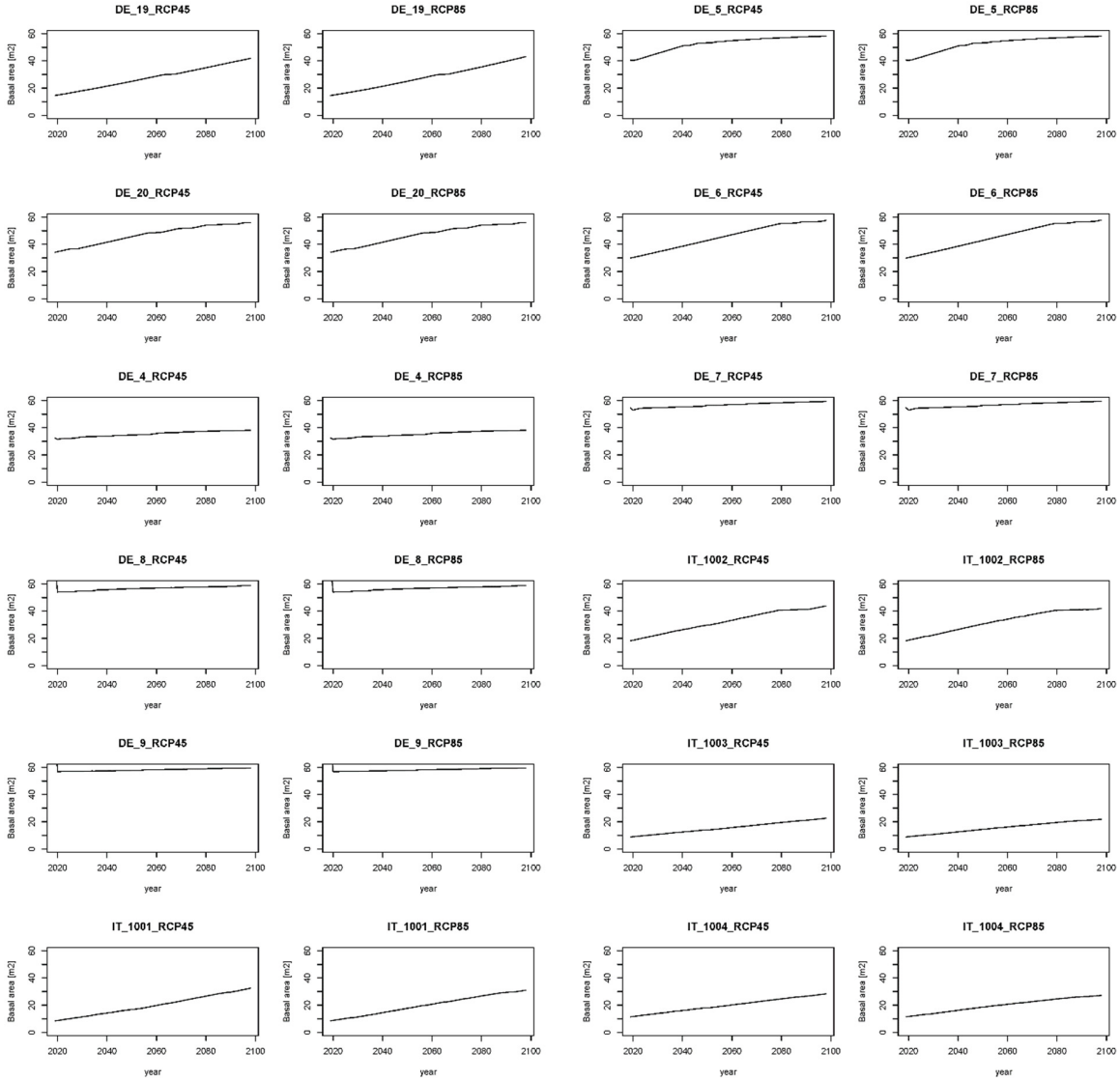
DE_19_RCP45
DE_19_RCP85
DE_5_RCP45
DE_5_RCP85
DE_20_RCP45
DE_20_RCP85
DE_6_RCP45
DE_6_RCP85
DE_4_RCP45
DE_4_RCP85
DE_7_RCP45
DE_7_RCP85
DE_8_RCP45
DE_8_RCP85
IT_1002_RCP45
IT_1002_RCP85
DE_9_RCP45
DE_9_RCP85
IT_1003_RCP45
IT_1003_RCP85
IT_1001_RCP45
IT_1001_RCP85
IT_1004_RCP45
IT_1004_RCP85
Basal area [m2]
year
0
20
40
60
2020
2040
2060
2080
2100

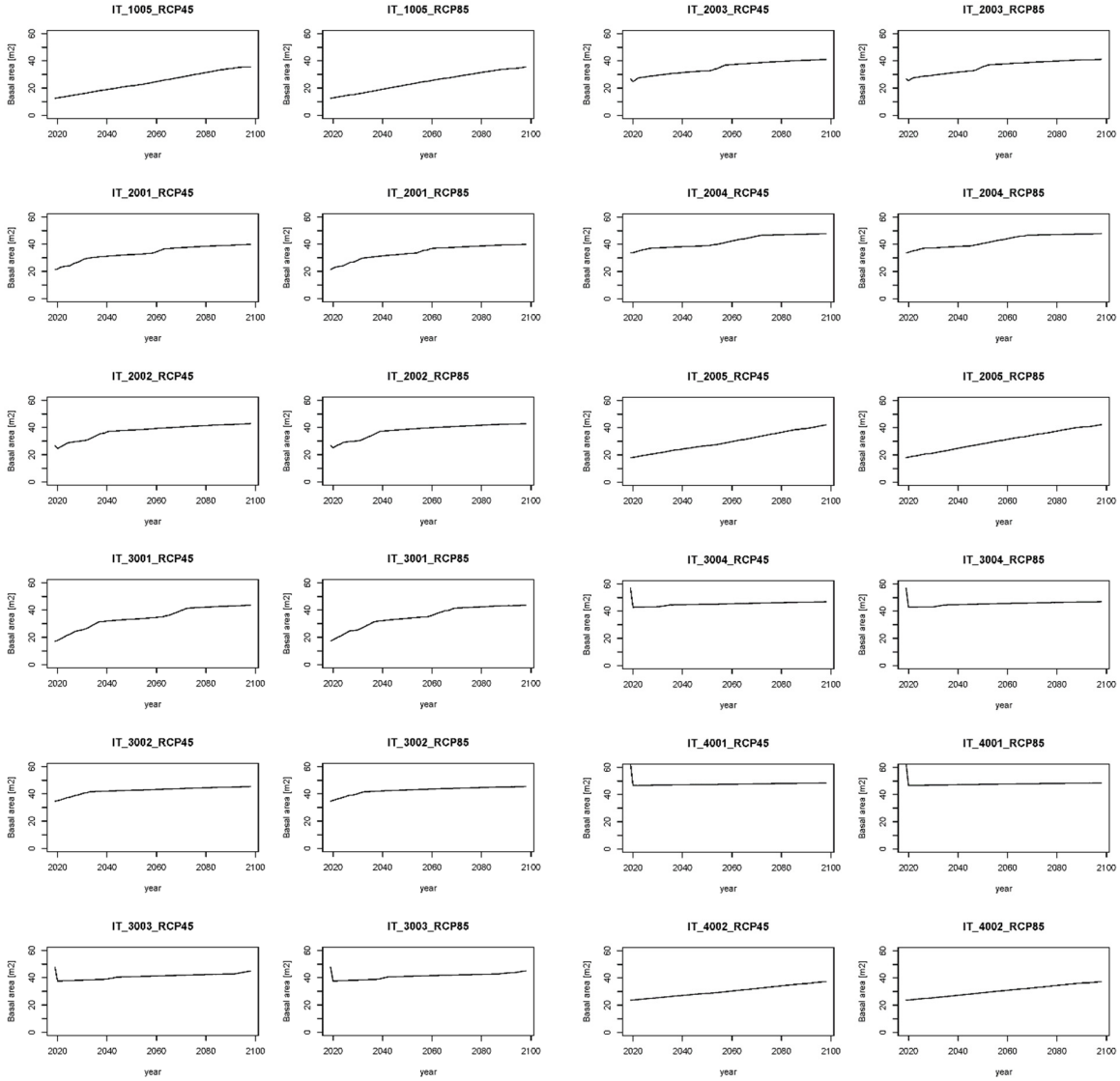
IT_1005_RCP45
IT_1005_RCP85
IT_2003_RCP45
IT_2003_RCP85
IT_2001_RCP45
IT_2001_RCP85
IT_2004_RCP45
IT_2004_RCP85
IT_2002_RCP45
IT_2002_RCP85
IT_2005_RCP45
IT_2005_RCP85
IT_3001_RCP45
IT_3001_RCP85
IT_3004_RCP45
IT_3004_RCP85
IT_3002_RCP45
IT_3002_RCP85
IT_4001_RCP45
IT_4001_RCP85
IT_3003_RCP45
IT_3003_RCP85
IT_4002_RCP45
IT_4002_RCP85
Basal area [m2]
year
0
20
40
60
2020
2040
2060
2080
2100

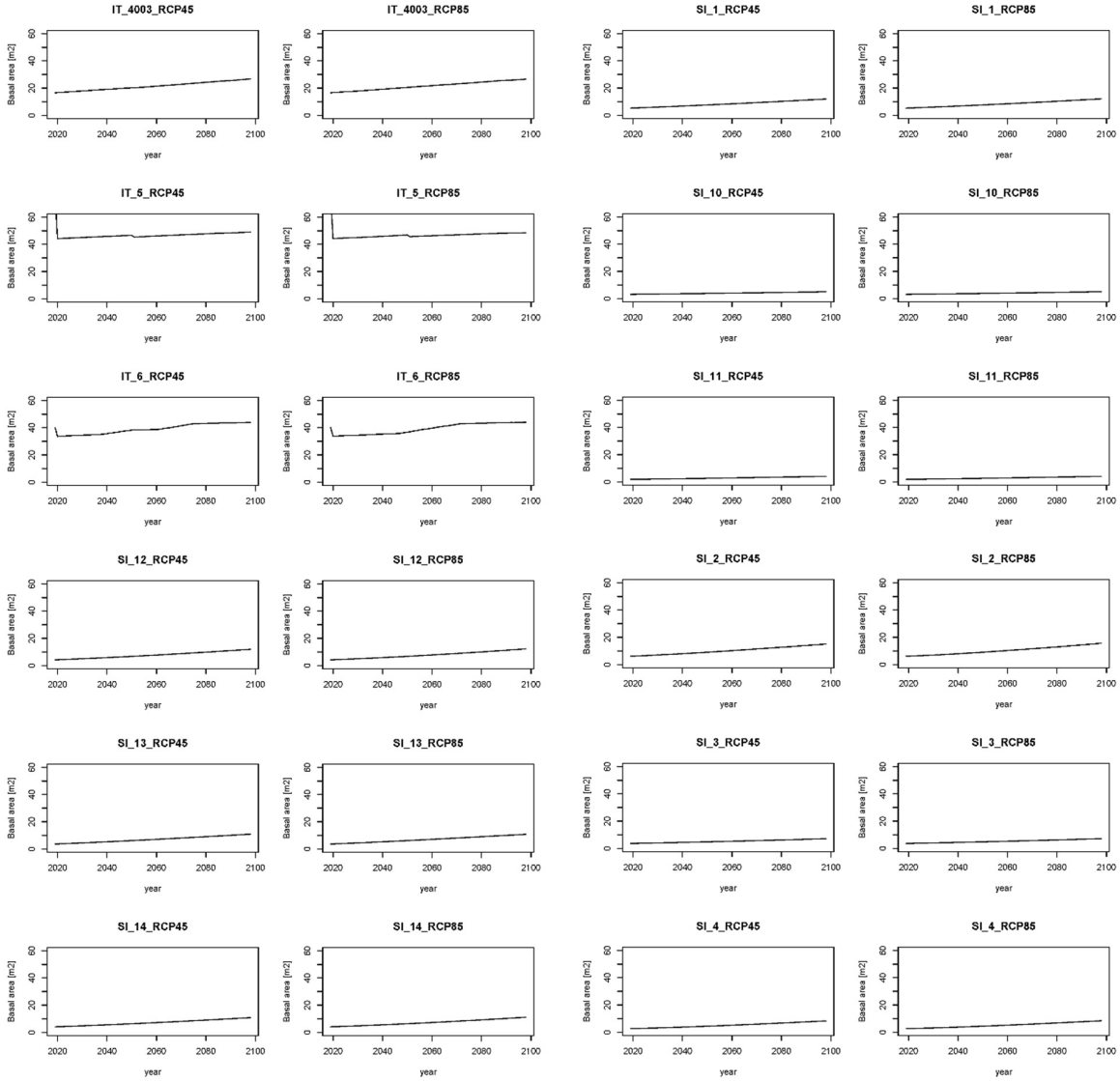
IT_4003_RCP45
IT_4003_RCP85
SI_1_RCP45
SI_1_RCP85
IT_5_RCP45
IT_5_RCP85
SI_10_RCP45
SI_10_RCP85
IT_6_RCP45
IT_6_RCP85
SI_11_RCP45
SI_11_RCP85
SI_12_RCP45
SI_12_RCP85
SI_2_RCP45
SI_2_RCP85
SI_13_RCP45
SI_13_RCP85
SI_3_RCP45
SI_3_RCP85
SI_14_RCP45
SI_14_RCP85
SI_4_RCP45
SI_4_RCP85
Basal area [m2]
year
0
20
40
60
2020
2040
2060
2080
2100

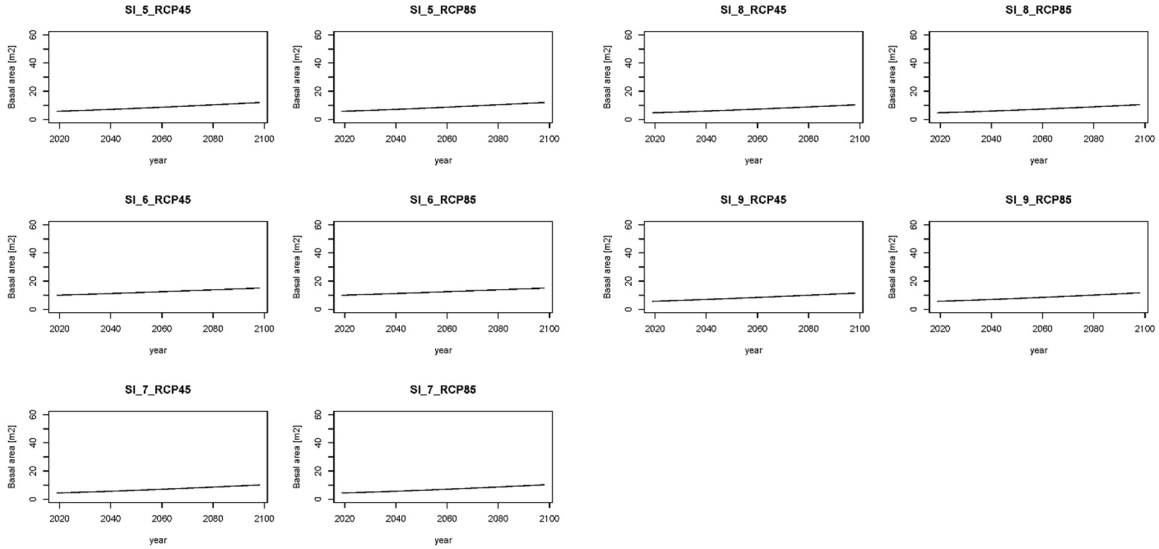
SI_5_RCP45
SI_5_RCP85
SI_8_RCP45
SI_8_RCP85
SI_6_RCP45
SI_6_RCP85
SI_9_RCP45
SI_9_RCP85
SI_7_RCP45
SI_7_RCP85
Basal area [m2]
year

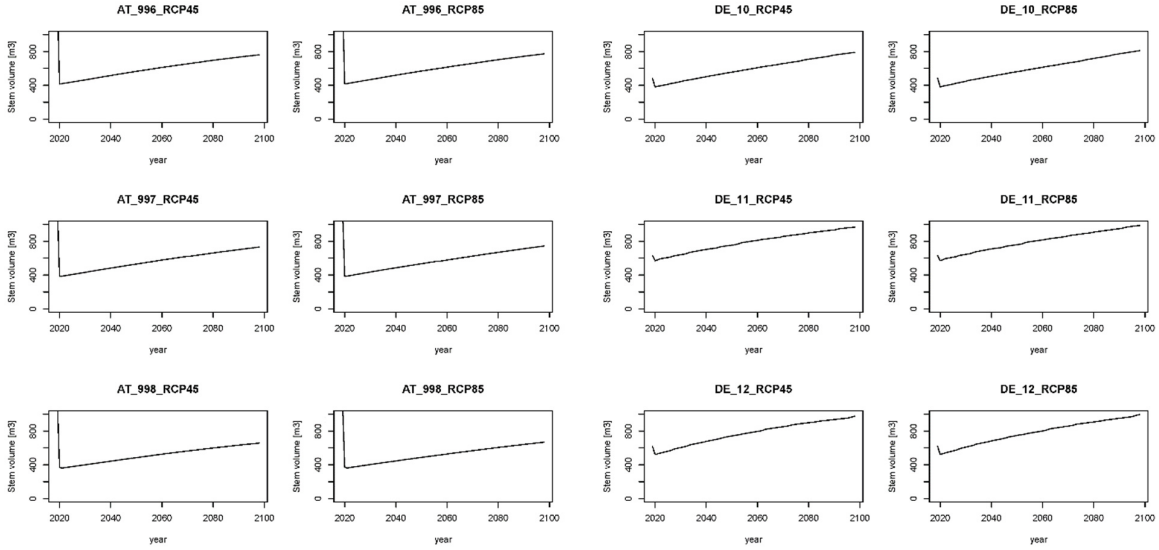
AT_996_RCP45
AT_996_RCP85
DE_10_RCP45
DE_10_RCP85
AT_997_RCP45
AT_997_RCP85
DE_11_RCP45
DE_11_RCP85
AT_998_RCP45
AT_998_RCP85
DE_12_RCP45
DE_12_RCP85
Stem volume [m3]
year

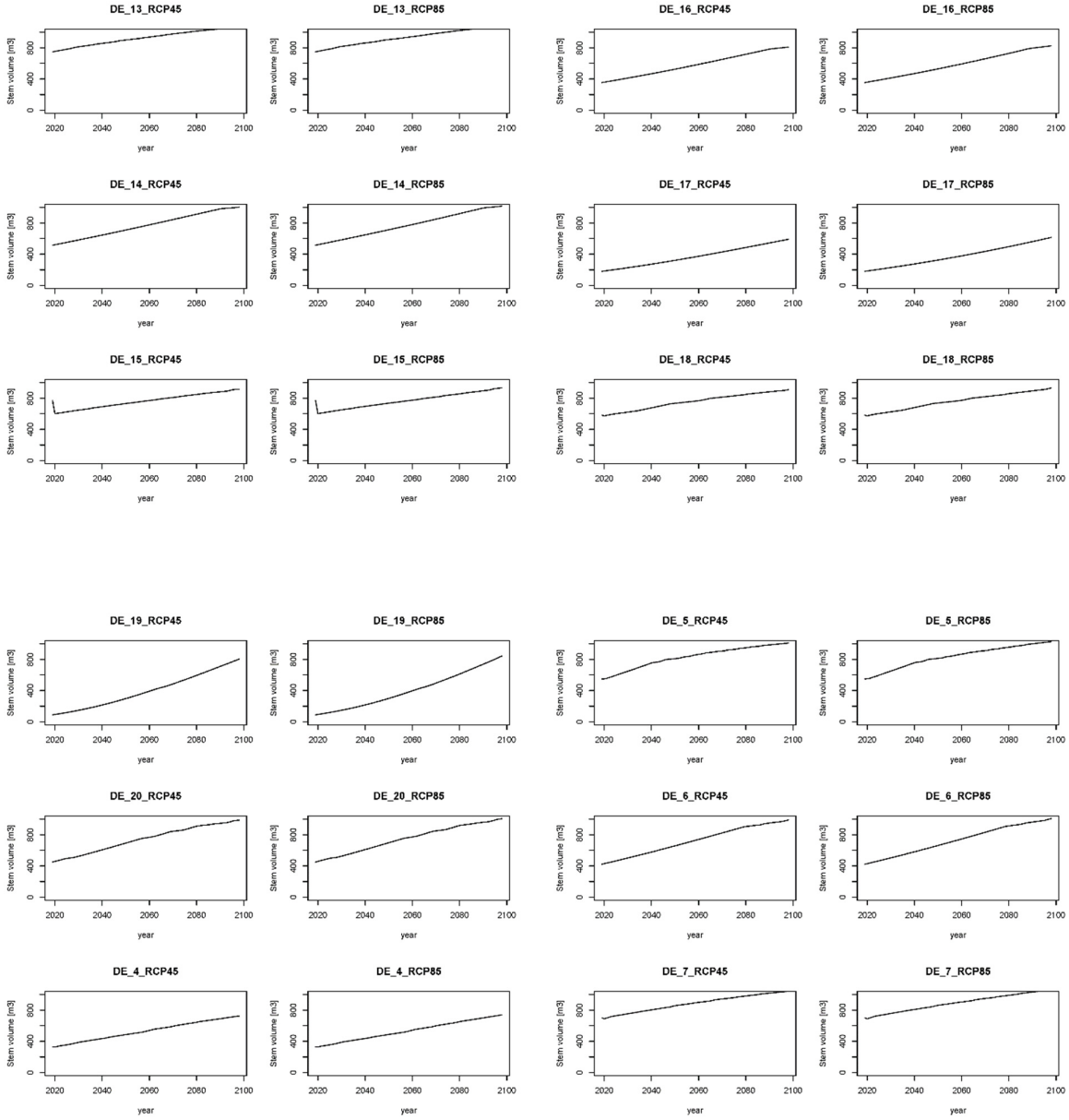
DE_13_RCP45
DE_13_RCP85
DE_16_RCP45
DE_16_RCP85
DE_14_RCP45
DE_14_RCP85
DE_17_RCP45
DE_17_RCP85
DE_15_RCP45
DE_15_RCP85
DE_18_RCP45
DE_18_RCP85
DE_19_RCP45
DE_19_RCP85
DE_5_RCP45
DE_5_RCP85
DE_20_RCP45
DE_20_RCP85
DE_6_RCP45
DE_6_RCP85
DE_4_RCP45
DE_4_RCP85
DE_7_RCP45
DE_7_RCP85
Stem volume [m3]
year
0
400
800
2020
2040
2060
2080
2100

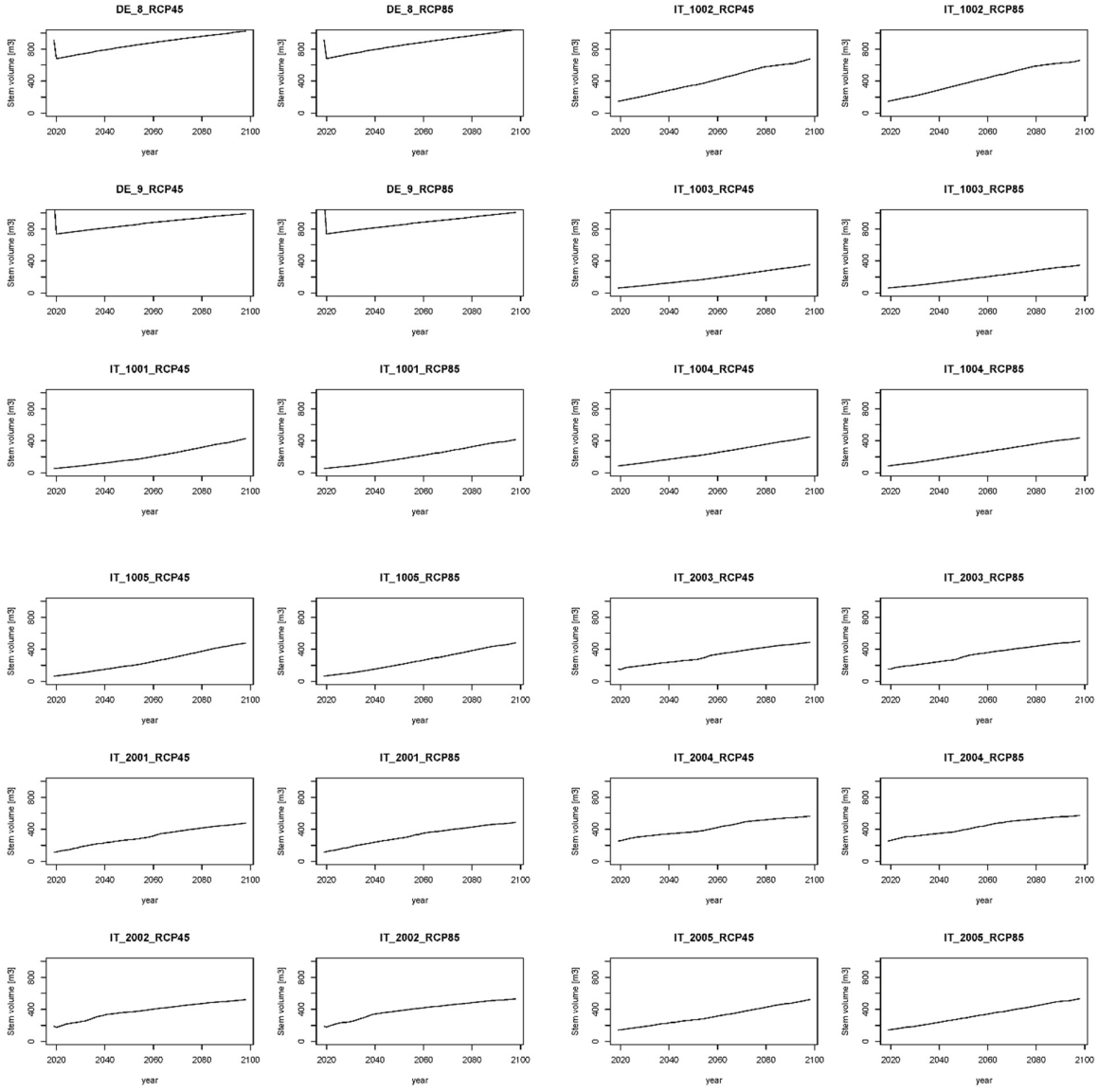
DE_8_RCP45
DE_8_RCP85
IT_1002_RCP45
IT_1002_RCP85
DE_9_RCP45
DE_9_RCP85
IT_1003_RCP45
IT_1003_RCP85
IT_1001_RCP45
IT_1001_RCP85
IT_1004_RCP45
IT_1004_RCP85
IT_1005_RCP45
IT_1005_RCP85
IT_2003_RCP45
IT_2003_RCP85
IT_2001_RCP45
IT_2001_RCP85
IT_2004_RCP45
IT_2004_RCP85
IT_2002_RCP45
IT_2002_RCP85
IT_2005_RCP45
IT_2005_RCP85
Stem volume [m3]
year
0
400
800
2020
2040
2060
2080
2100

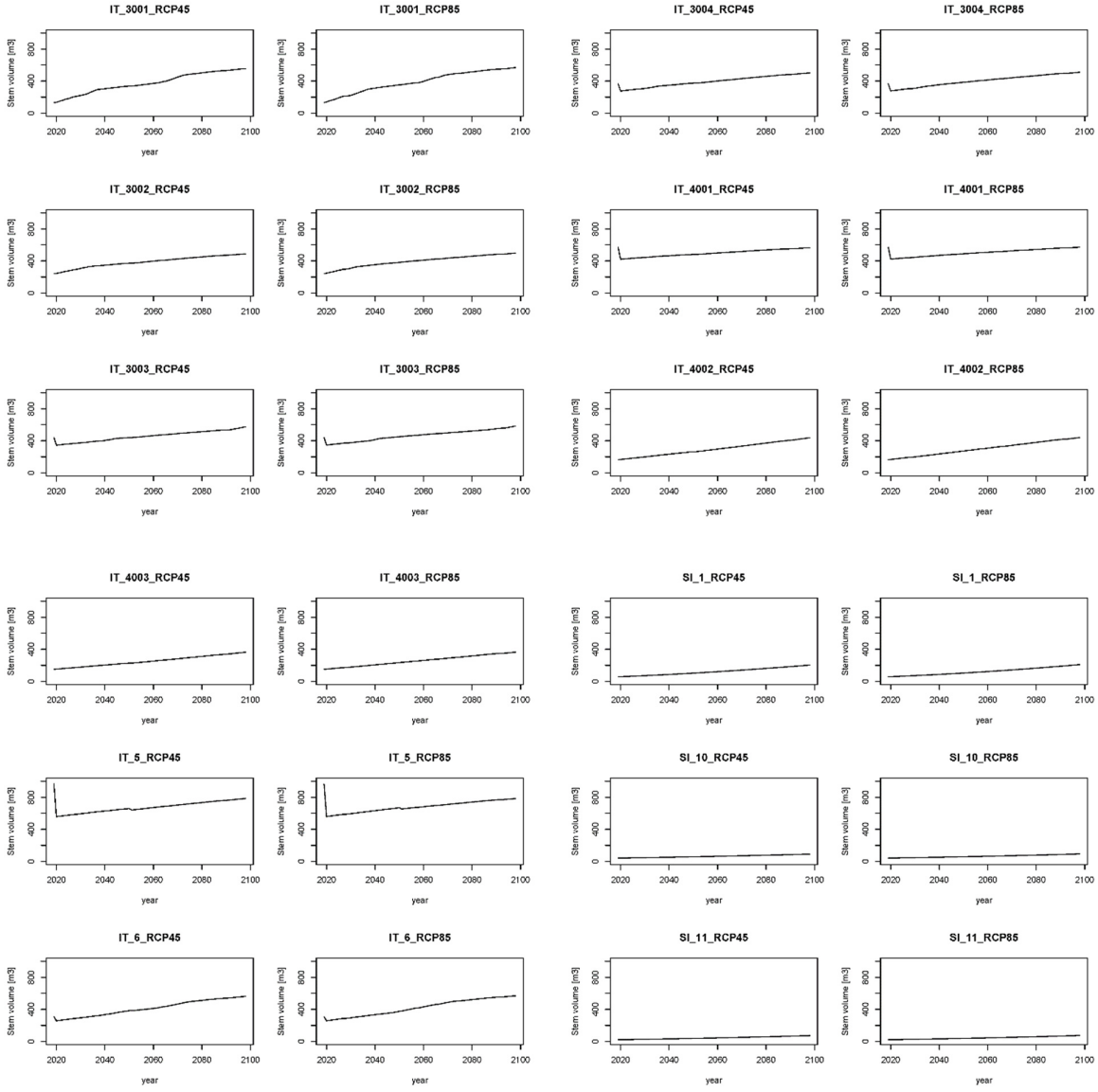
IT_3001_RCP45
IT_3001_RCP85
IT_3004_RCP45
IT_3004_RCP85
IT_3002_RCP45
IT_3002_RCP85
IT_4001_RCP45
IT_4001_RCP85
IT_3003_RCP45
IT_3003_RCP85
IT_4002_RCP45
IT_4002_RCP85
IT_4003_RCP45
IT_4003_RCP85
SI_1_RCP45
SI_1_RCP85
IT_5_RCP45
IT_5_RCP85
SI_10_RCP45
SI_10_RCP85
IT_6_RCP45
IT_6_RCP85
SI_11_RCP45
SI_11_RCP85
Stem volume [m3]
year

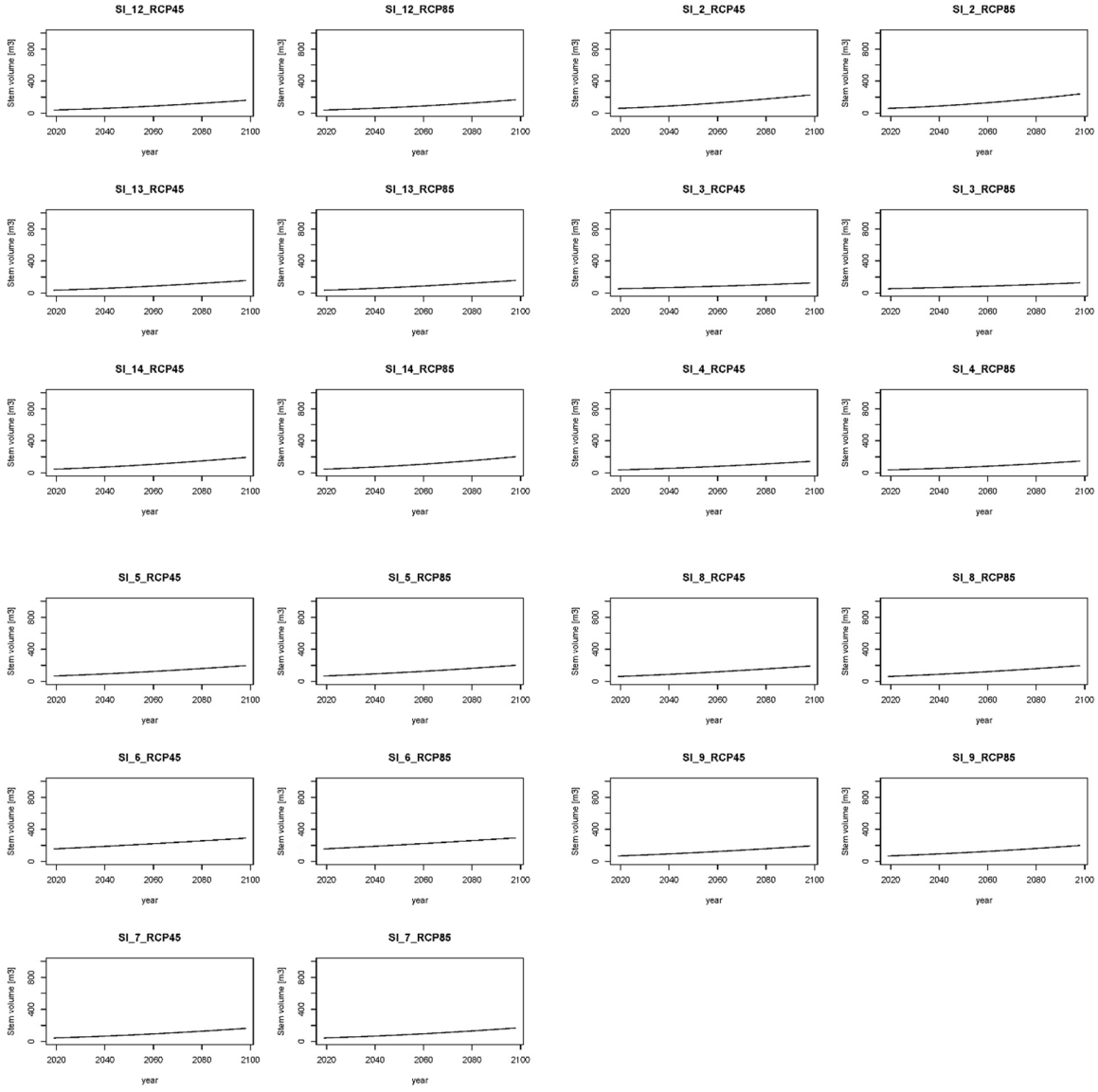
SI_12_RCP45
SI_12_RCP85
SI_2_RCP45
SI_2_RCP85
SI_13_RCP45
SI_13_RCP85
SI_3_RCP45
SI_3_RCP85
SI_14_RCP45
SI_14_RCP85
SI_4_RCP45
SI_4_RCP85
SI_5_RCP45
SI_5_RCP85
SI_8_RCP45
SI_8_RCP85
SI_6_RCP45
SI_6_RCP85
SI_9_RCP45
SI_9_RCP85
SI_7_RCP45
SI_7_RCP85
Stem volume [m3]
0
400
800
2020
2040
2060
2080
2100
year